Michigan (One Point) Cone Test for Evaluating the Density of Open-Graded Drainage Course (OGDC) Materials

Final Report

Report Number: SPR-1769

Michigan Department of Transportation

Office of Research Administration

885 Ricks Road

Lansing, MI 38909

By

Surya S.C. Congress, Bora Cetin, Peyman Parastegari

Michigan State University

220 Trowbridge Rd

East Lansing, MI 48823

May 15, 2026

TECHNICAL REPORT DOCUMENTATION PAGE

1. Report No.	2. Government Accession No.	3. Recipient's Catalog No.
SPR-1769	N/A	Kenneth Koepke

4. Title and Subtitle	5. Report Date
Michigan (One Point) Cone Test for Evaluating the Density of Open-Graded Drainage Course (OGDC) Materials	May 15, 2026
	6. Performing Organization Code N/A

7. Author(s)	8. Performing Organization Report No.
Surya S.C. Congress, Bora Cetin, Peyman Parastegari	**N/A**

9. Performing Organization Name and Address	10. Work Unit No.
Michigan State University Civil and Environmental Engineering Michigan State University 220 Trowbridge Rd East Lansing, MI 48823	N/A
	11. Contract or Grant No. 2024-0433

12. Sponsoring Agency Name and Address	13. Type of Report and Period Covered
Michigan Department of Transportation (MDOT) Research Administration 8885 Ricks Road P.O. Box 33049 Lansing, Michigan 48909	Final Report
	14. Sponsoring Agency Code N/A

15. Supplementary Notes
N/A

16. Abstract

Pavement infrastructure is a significant public investment (over $60 billion annually in the U.S.), yet 39% of major roads are in poor condition, resulting in costly repairs and user expenses. Maximizing pavement longevity is critical to address a projected $684 billion funding gap in road maintenance, and improving compaction quality in pavement base layers has been identified as a high-return strategy to extend service life. This study investigates compaction of open-graded drainage course (OGDC) aggregates, which form the permeable base layers crucial to pavement stability and drainage, using the One-Point M-Cone Test (M-Cone). This collaborative study with the Michigan Department of Transportation (MDOT) compared M-Cone results with those from standard laboratory compaction methods across multiple OGDC aggregate sources. Statistical analyses were applied to evaluate the influence of different operators and material sources on the M-Cone outcomes within the controlled laboratory conditions of this study. The results showed that the M-Cone test can achieve maximum dry density (MDD) values comparable to those obtained with the Modified Proctor test, except for aggregates with a high water-absorption tendency. Statistical tests indicated no significant operator variability in M-Cone testing within the controlled laboratory conditions evaluated. Sieve analyses of particle size distributions before and after compaction confirmed that all methods produced some fine particles from aggregate breakage. Overall, the one-point M-Cone test, conducted by trained operators in a laboratory setting, is a reliable indicator of compaction.

17. Key Words	18. Distribution Statement		
Pavement, Drainage, Open-Graded, Density, Michigan Cone, Modified Proctor, Gyratory, Operator Variability, Statistical Analyses	No restrictions. This document is also available to the public through the Michigan Department of Transportation.		
19. Security Classif. (of this report)	**20. Security Classif. (of this page)**	**21. No. of Pages**	**22. Price**
Unclassified	Unclassified	142	$125,972

Form DOT F 1700.7 (8-72) Reproduction of completed page authorized

ACKNOWLEDGEMENTS

The authors would like to thank the Michigan Department of Transportation (MDOT) for its financial support and the research advisory provided by Arthur Koziarski, Kenneth Koepke, Lindsey Renner, John Watson, Justin Foster, Eric Mueller, and Mary Hoffmeyer, who also offered cooperation and valuable suggestions, data, and feedback on the results, and coordinated the meetings. We also thank Ambikesh Dwivedi, Nathan Hicks, Lewis Thiedeman, and Raja Jaladurgam for their assistance with the project activities.

DISCLAIMER

This publication is disseminated in the interest of information exchange. The Michigan Department of Transportation (hereinafter referred to as MDOT) expressly disclaims any liability, of any kind, or for any reason, that might otherwise arise out of any use of this publication or the information or data provided in the publication. MDOT further disclaims any responsibility for typographical errors or accuracy of the information provided or contained within this information. MDOT makes no warranties or representations whatsoever regarding the quality, content, completeness, suitability, adequacy, sequence, accuracy, or timeliness of the information and data provided, or that the contents represent standards, specifications, or regulations.

This material is based upon work supported by the Federal Highway Administration under SPR-1769. Any opinions, findings, and conclusions or recommendations expressed in this publication are those of the author(s) and do not necessarily reflect the views of the Federal Highway Administration.

TABLE OF CONTENTS

ACKNOWLEDGEMENTS iv

ABBREVIATIONS AND ACRONYMS USED IN THE REPORT xiv

EXECUTIVE SUMMARY 1

1 INTRODUCTION 2

1.1 Statement of Problem 2

1.2 Background and Significance of Work 2

1.3 Research Objectives 3

1.4 Report Organization 4

2 LITERATURE REVIEW 5

2.1 Pavement Construction and Performance 5

2.2 Open-Graded Drainage Course (OGDC) 6

2.3 Density Testing Methods 7

2.3.1 Laboratory Tests 7

2.3.2 Field Tests 12

2.4 Instrumentation for Density Measurements 15

2.5 Sieve Analysis Types 17

2.5.1 Dry Sieve Analysis 17

2.5.2 Wet Sieve Analysis 18

2.6 Statistical Analysis 19

2.6.1 T-Test 19

2.6.2 Two-Way ANOVA 21

2.7 Department of Transportation (DOT) Procedures for Density Testing 22
2.7.1 California 25
2.7.2 Illinois 25
2.7.3 Ohio 26
2.7.4 Florida 26
2.7.5 Texas 27
2.7.6 Michigan 27
3 METHODOLOGY 30
3.1 Research Design 30
3.1.1 M-Cone 31
3.1.2 Modified Proctor 31
3.1.3 Vibratory Table 31
3.1.4 Superpave Gyratory Compactor (SGC) 32
3.1.5 Specific Gravity and Absorption 33
3.1.6 Sieve Analyses: Before and After Testing 33
3.1.7 Field Validation 34
3.1.8 Operator Variation: Statistical Analysis 34
3.2 Materials/Instrumentation 35
3.2.1 Sources 35
3.3 Testing Procedures 39
3.3.1 Sieve Analysis 39

3.3.2 M-Cone Test 47
3.3.3 Modified Proctor Compaction Test 53
3.3.4 Vibratory Table Method 56
3.3.5 OGDC Soil Compaction Using the Superpave Gyratory Compactor 59
3.3.6 In-Place Density and Water Content Measurement by Nuclear Gauge 62
4 RESULTS 67
4.1 Specific Gravity and Water Absorption 67
4.2 Density Results 70
4.2.1 M-Cone 70
4.2.2 Modified Proctor 80
4.2.3 Gyratory 86
4.2.4 Vibratory 90
4.2.5 Nuclear Gauge 94
4.3 Sieve Analysis 98
4.4 Energy Values 102
4.5 Statistical Analysis 107
4.5.1 T-Test 107
4.5.2 ANOVA 110
5 DISCUSSION 120
5.1 Operator Variability in the M-Cone Test 120
5.2 Comparison of MDD Results: M-Cone vs. Modified Proctor 122

5.3 Particle Crushing During Compaction....128

6 CONCLUSIONS....129

7 RECOMMENDATIONS....131

REFERENCES....132

APPENDIX- A....137

List of Tables

Table 1. Summary of State DOT Procedures and Applicability of OGDC Material 23

Table 2. Details of OGDC Materials Used in this Study.....37

Table 3. Summary of Specific Gravity and Water Absorption Test Results.....68

Table 4. Details of M-Cone Testing 71

Table 5. M-Cone Test Results from Various Sources 73

Table 6. Summary of Statistical Results from One-Point M-Cone Test.....79

Table 7. Modified Proctor Test Results from Various Sources.....81

Table 8. Summary of Statistical Results from Modified Proctor Test.....85

Table 9. Gyratory Test Results from Various Sources 87

Table 10. Summary of Statistical Results from Gyratory Compaction Test 89

Table 11. Vibratory Table Test Results from Various Sources. 91

Table 12. Summary of Statistical Results from Vibratory Table Test.....93

Table 13. Summary of Nuclear Gauge Information and Test Results.....95

Table 14. Dry Density Results for Four Laboratory Compaction Methods 96

Table 15. Comparison of Dry and Wet Percent Passing No. 200 for Representative Specimens by Source and Method 99

Table 16. Impact Energy and Compaction Results from Various Sources.....103

Table 17. Paired T-Test Results for Maximum Dry Density and Optimum Moisture Content Analysis.....109

Table 18. Two-Way ANOVA Condition and Conclusion.....115

Table 19. ANOVA Test Results for MDD 117

Table 20. ANOVA Test Results for OMC.....117

Table 21. ANOVA Test Results for Energy 118

Table 22. A Comparison of Density, Moisture Content and Effective Moisture Content of Various OGDC Sources for Different Tests 124

List of Figures

Figure 1. M-Cone Test Apparatus Comprising of M-Cone, Pounding Block, and Cone Stopper, and Chart for Interpreting Maximum Dry Density Values From M-Cone Testing.....28

Figure 2. Wet Sieve Analysis Gradation Curves of Each OGDC Source Before Testing.....44

Figure 3. M-Cone Test (a) Apparatus Comprising Of M-Cone, Pounding Block, and Cone Stopper, (b) Chart for Interpreting Maximum Dry Density Values From M-Cone Testing....48

Figure 4. Speedy Test Apparatus for In-situ Determination of Moisture Content 50

Figure 5. Accelerometer Embedded Underneath the Base Plate of M-Cone 52

Figure 6. Modified Proctor Apparatus.....54

Figure 7. Vibratory Table Apparatus.....57

Figure 8. Superpave Gyratory Compactor Apparatus.....60

Figure 9. Troxler 3440 Nuclear Density Gauge Setup 63

Figure 10. Box Plot of the Percentage Difference in Wet Sieve Analysis Results Between the After-Compaction and Before-Compaction Tests using M-Cone Test for All Sources.....102

Figure 1A. Modified Proctor Test: Maximum Dry Unit Weight-Optimum Moisture Content Plot for Lafarge.....137

Figure 2A. Modified Proctor Test: Maximum Dry Unit Weight-Optimum Moisture Content Plot for Port Inland.....138

Figure 3A. Modified Proctor Test: Maximum Dry Unit Weight-Optimum Moisture Content Plot for Great Lake.....138

Figure 4A. Modified Proctor Test: Maximum Dry Unit Weight-Optimum Moisture Content Plot for Stone Co.....139

Figure 5A. Modified Proctor Test: Maximum Dry Unit Weight-Optimum Moisture Content Plot for Calcite.....139

Figure 6A. Modified Proctor Test: Maximum Dry Unit Weight-Optimum Moisture Content Plot for StGrLa2024.....140

Figure 7A. Modified Proctor Test: Maximum Dry Unit Weight-Optimum Moisture Content Plot for SylMe2025.....140

Figure 8A. Modified Proctor Test: Maximum Dry Unit Weight-Optimum Moisture Content Plot for SylMe2025_2.....141

Figure 9A. Modified Proctor Test: Maximum Dry Unit Weight-Optimum Moisture Content Plot for Slag 141

Figure 10A. Modified Proctor Test: Maximum Dry Unit Weight-Optimum Moisture Content Plot for I-275.....142

ABBREVIATIONS AND ACRONYMS USED IN THE REPORT

Technical Terms

ALARA: As Low As Reasonably Achievable

ANOVA: Analysis of Variance

Caltrans: California Department of Transportation

CBR: California Bearing Ratio

CCC: Continuous Compaction Control

CCV: Compaction Control Value

CMV: Compaction Meter Value

DCP: Dynamic Cone Penetrometer

DCPI: Dynamic Cone Penetration Index

DOT: Department of Transportation

FDOT: Florida Department of Transportation

FHWA: Federal Highway Administration

GAB: Graded Aggregate Base

IC: Intelligent Compaction

ICMV: Intelligent Compaction Measurement Value

IDOT: Illinois Department of Transportation

JRCP: Jointed Reinforced Concrete Pavement

LBR: Limerock Bearing Ratio

LWD: Light Weight Deflectometer

M-Cone: One – Point Michigan Cone

MDD: Maximum Dry Density

MDOT: Michigan Department of Transportation

ODOT: Ohio Department of Transportation

OGDC: Open-Graded Drainage Course

OMC: Optimum Moisture Content

QC: Quality Control

RAP: Reclaimed Asphalt Pavement

RMV: Resonance Meter Value

SD: Standard Deviation

SGC: Superpave Gyratory Compactor

SHA: State Highway Administration

SHRP: Strategic Highway Research Program

SSA / SSB / SSAB / SSE / SST: Sum of Squares components in ANOVA

SSG: Soil Stiffness Gauge

t-test: The paired t-test

TxDOT: Texas Department of Transportation

UCS: Unconfined Compressive Strength

UGB: Unbound Granular Base

USACE: United States Army Corps of Engineers

EXECUTIVE SUMMARY

The resiliency of modern road networks depends heavily on the durability of their foundation layers, particularly as maintenance costs continue to climb globally. This research focuses on optimizing the longevity of pavement systems by evaluating the density testing for Open-Graded Drainage Course (OGDC) materials. These specific aggregate layers are vital because they must remain porous enough to facilitate water drainage while providing a rigid enough base to support heavy traffic. In coordination with the Michigan Department of Transportation (MDOT), this study evaluates the reliability of the One-Point M-Cone Test (M-Cone) for determining the density of these permeable bases. To ensure a rigorous evaluation, the M-Cone was benchmarked against established laboratory procedures, including the Modified Proctor, Vibratory, and Gyratory compaction methods, across a diverse range of OGDC materials sourced from MDOT-approved vendors. A distinctive feature of this study was the integration of accelerometer technology directly onto the M-Cone apparatus. By recording vibration and impact data during testing, researchers were able to perform high-resolution statistical analyses that go beyond traditional visual or manual observations. This sensor-based approach provided empirical data to compare the energy and consistency of the M-Cone operated in laboratory conditions by different operators on various OGDC material sources.

A central concern in any manual field test is whether results vary depending on who performs the task. The statistical findings from this study indicate that the M-Cone procedure produced consistent results between two trained operators under the controlled laboratory conditions evaluated. While M-Cone generally matched the density results of the Modified Proctor test, it was observed that material-specific properties, specifically aggregate water absorption characteristics, can influence the results, highlighting the need for source-specific awareness during quality control. The study also addressed the physical integrity of the aggregates through detailed gradation assessments. By analyzing the breakdown of aggregates during compaction, it was observed that the M-Cone causes the least particle breakage among the established density tests. Ultimately, the research demonstrates that the M-Cone test, when conducted by trained operators under controlled laboratory conditions, is a repeatable method for evaluating compaction of OGDC materials for the sources considered in this study. Implementing this standardized testing approach enables the construction of roads that drain water effectively without compromising structural support, thereby reducing the financial burden of frequent road repairs.

1 INTRODUCTION

1.1 Statement of Problem

Millions of tons of aggregate materials are used annually in the construction of highway base/subbase layers due to their satisfactory mechanical properties. The highway base/subbase layer is a critical component of pavement structures. There are two primary functions of highway base/subbase layers: (1) acting as a foundation to provide adequate mechanical support to the asphalt or concrete layer to prevent fatigue and occurrence of rutting failures, and (2) providing adequate drainage to move the excessive infiltrated water out and away from the pavement structure. While most aggregates provide good bearing capacity, most base/subbase materials lack long-term drainage performance. Thus, to overcome drainage-related problems in pavement systems, departments of transportation (DOTs) began using Open-Graded Drainage Course (OGDC) materials, which are coarse, free-draining aggregate layers with minimal fines designed to facilitate rapid drainage while providing structural support within the pavement system.

The Michigan Department of Transportation (MDOT) also began using OGDC in pavement foundation systems, which has drawn attention to the current practice of using One-Point M-Cone tests in field applications to determine the maximum density of such materials (e.g., soils). MDOT is interested in investigating whether the current field tests, including the M-Cone test, correlate with other industry-standard tests on OGDC materials. Studies from the 1960's, 70's, and early 2000's indicated that, for many applications, M-Cone Maximum density values exceed those obtained with other acceptable testing methods. MDOT would like to explore whether M-Cone testing practices, as written, are an effective means of determining the maximum density of OGDC, or whether modifications to this current process are more appropriate.

1.2 Background and Significance of Work

Optimal compaction of pavement foundation layers, including base, subbase, and subgrade layers during road construction, is very important for maximizing the service life of roads and minimizing the thickness of pavement layers. Proper compaction enhances the engineering properties (shear strength, stiffness) of pavement foundation materials. Good compaction

yields high-quality, long-lasting roadways, while poor or uneven compaction can lead to failures such as settlement, cracks, and rutting.

The moisture level during compaction is the most influential parameter on the density and, consequently, on the stiffness and strength of pavement foundation materials. It is well known that the maximum dry density (γ_{dmax}) of soils and geomaterials is achieved when they are compacted at optimum moisture (w_{optm}) content. Part of the challenge is transferring the optimal compaction and moisture content data from laboratory testing to the field. Many state departments of transportation (DOTs) and their contractors have used nuclear density gauges to determine the in-situ density of the compacted soil. In addition to the nuclear density gauge test, MDOT has been using the Michigan (one-point) cone test to determine γ_{dmax} of granular soils for decades. However, given the use of OGDC materials for pavement construction, it is necessary to determine whether the M-Cone test is a viable method for testing them and to correlate it with other industry-standard tests. Further, it is necessary to determine whether any modification to the test procedure may be required to ensure this method can be reliably used for OGDC materials.

1.3 Research Objectives

The specific objectives of this study are summarized as follows.

- Study available literature to determine what other studies found when comparing the M-Cone to other practical methods.
- Evaluate the available industry-accepted methods for determining maximum density for OGDC while being considerate of the moisture necessary to achieve this maximum density.
- Perform a side-by-side comparison of widely accepted maximum density determination methods on OGDC. The number of samples and correlations must be sufficient to write and adapt policy from, so a strong correlation across many different samples is preferred.
- Provide a recommendation and a Word document format that proposes the necessary updates to the Density Testing and Inspection Manual.

1.4 Report Organization

The report is organized as follows. The first section covers the introduction, problem statement, background, and research objectives. The second section covers the literature review on density testing methods, sieve analysis, statistical analysis, and DOT practices. The third section covers the research methodology involving the research design, materials, instrumentation, and testing procedures. The subsequent sections provide the testing results and the discussion. Finally, the salient findings from the study are provided in the conclusions section, along with a section dedicated to recommendations for the OGDC material testing.

2 LITERATURE REVIEW

2.1 Pavement Construction and Performance

Pavement construction represents one of the most significant infrastructure investments in the United States, with recent federal-aid highway funding exceeding $60 billion annually (FHWA 2025). Even with these investments, 39% of major U.S. roads are still in poor condition, costing the average driver over $1,400 each year in additional vehicle operating costs and delays (ACSE 2025). Improving and sustaining pavement performance is critical to address the projected $684 billion road funding gap over the next decade (ACSE 2025). Research shows that the quality of the pavement foundation, particularly subgrade stability and proper compaction, is a decisive factor in long-term performance, as inadequate compaction accelerates deterioration through settlement, fatigue cracking, and moisture-induced damage, thus increasing rehabilitation needs (Schaefer et al. 2008).

Flexible pavements are constructed as layered systems comprising the subgrade, subbase, base course, and asphalt surface, which act together to distribute traffic loads to the underlying soils. The stiffness and load-spreading capacity of each layer are governed by in-place density and uniformity (Linden et al. 1989). Performance studies indicate that variability in compaction can reduce service life by 40–50 % compared with pavements meeting specified density targets (Linden et al. 1989). Economic analyses show that modest improvements in compaction deliver disproportionately large life-cycle cost savings. A National Center for Asphalt Technology (NCAT) case study found that increasing asphalt overlay density increased the projected service life by 11%, resulting in significant deferred reconstruction costs. However, the performance gains from higher surface density depend on the support condition of the base/subgrade. NCAT advises agencies to evaluate the underlying base when targeting higher in-place density; weak or unsupportive layers can make even minimal density requirements difficult to achieve, and defects in the underlying layers can minimize any long-term performance gain. In practice, the density achieved in an overlay also depends on the underlying pavement layers, as the penetration of compaction energy and resulting mat density are influenced by the support beneath (Tran et al. 2016).

The compaction quality of subgrade and base courses is equally critical. Uniform compaction minimizes differential settlement and reduces risks of reflective cracking, pumping, and other structural distress. The United States Federal Highway Administration (FHWA) research

demonstrates that non-uniform compaction creates localized weak zones that concentrate strain and accelerate deterioration (Nieves 2013). For open-graded drainage course (OGDC) layers, MDOT specifies placement and compaction methods that avoid aggregate segregation and preserve gradation. In Michigan, the granular layers are placed in horizontal lifts (up to 18 in. for granular soils, in accordance with the 2020 MDOT Standard Specifications for Construction, Section 301), compacted uniformly to meet the specified density, and verified by in-place measurements using the nuclear density gauge with minimum frequencies (e.g., subbase and aggregate base: 1 test per 500 ft for a 24-ft width). MDOT requires each lift to meet compaction specifications before the next is placed (MDOT 2024).

Life-cycle cost modeling confirms that inadequate initial compaction leads to early distress in the pavement's service life and increases overall maintenance costs. A 1989 report by the Transportation Research Board (TRB) found that delaying the onset of critical distress by just one year can reduce cumulative maintenance expenditures by 15–20% at the network level (Markow 1989). SHRP-H-358 report similarly found that achieving the specified density during construction will help delay the need for high-cost rehabilitation during its service life, making compaction quality control a high-return-on-investment (Smith et al. 1993). Zaltuom (2018) reported that a 1% increase in in-place air voids can approximately double the pavement permeability, accelerate moisture infiltration, and reduce service life by 35% (Zaltuom 2018). The subsequent sections discuss the open-graded drainage course (OGDC) material, which contributes to the drainage in the pavement layers in Michigan.

2.2 Open-Graded Drainage Course (OGDC)

An open-graded drainage course (OGDC) is a layer of coarse aggregate placed beneath the pavement to support construction while helping water drain away quickly. By limiting the amount of fine material, the mix leaves open spaces between the stones, creating channels that allow the water to pass freely to subsurface drains and prevent it from pooling within the pavement structure. The primary function of OGDC is to intercept and remove infiltrated water, reducing the risk of base erosion, pumping, and frost heave. Field studies have demonstrated that even relatively thin OGDC layers provide rapid drainage, preserve the modulus of subgrade reaction, and reduce seasonal performance variability (Hansen Will et al. 2009; Novak 1983).

OGDC's low fines content and high permeability reduce frost susceptibility. By preventing water retention in the base, OGDC limits frost heave potential in cold climates, improving ride quality and reducing seasonal maintenance demands (Hansen Will et al. 2009). Stabilized OGDC, typically coated with asphalt or cement (also called treated OGDC), not only maintains permeability but also enhances load transfer. Long-term performance evaluations conducted by MDOT showed that jointed reinforced concrete pavements (JRCP) with treated OGDC exhibited excellent load transfer effectiveness (greater than 85%), minimal structural distress, and projected service lives exceeding those of untreated alternatives (Hansen et al. 2009).

While OGDC materials provide significant drainage and performance benefits, their open gradation also introduces challenges in achieving consistent compaction. The open gradation of OGDC increases variability in achievable density. M-Cone Test trials conducted in past studies indicated higher standard deviations in density values for OGDC (4.1–6.1 pcf) compared to dense-graded materials (1.5–2.2 pcf) (Krueger 2011). The long-term benefits of OGDC depend on sustained drainage performance. Field evaluations documented that inadequate drainage led to base erosion, joint settlement (0.10–0.2 in.), and reduced load transfer capacity (Hansen Will et al. 2009). MDOT began using OGDC as a standard base in 1984 and widely implemented stabilized OGDC in Portland Cement Concrete (PCC) reconstruction projects from 1990 to 1995, often using recycled concrete pavement as aggregate. These stabilized systems, incorporating asphalt or cement coatings, prevented calcium carbonate leaching that could clog drains, maintained permeability, and provided durable base support. In total, 13 JRCP projects covering 115 lane-miles were constructed with treated OGDC during this period, with performance data showing minimal cracking, faulting, or spalling over more than a decade of service (Baladi 1998; Hansen Will et al. 2009). The subsequent section discusses the practices adopted by other DOTs across the US.

2.3 Density Testing Methods

2.3.1 Laboratory Tests

Standard Proctor: Compaction of the pavement base layer is a key factor in pavement performance, as it directly affects the pavement's stability and durability. Proper compaction quality control is essential for achieving good engineering performance (Choi et al. 2018). In practice, compaction quality is typically assessed by the density-based relative compaction, defined as the ratio of the field dry density to the maximum dry density obtained from a

laboratory Standard Proctor test (Choi et al. 2018). The Proctor compaction tests, including the Standard and Modified Proctor methods, remain among the most widely used laboratory procedures for determining a soil's maximum dry density and optimum moisture content (Fattah et al. 2019). However, conventional impact compaction tests have limitations when applied to coarse-grained and open-graded materials. These materials often exhibit weak or poorly defined moisture–density relationships, and their large particle sizes may not be fully compatible with standard mold dimensions. Despite these limitations, the Modified Proctor test remains a widely accepted reference method for determining maximum dry density and is commonly used as a benchmark for compaction evaluation. Differences observed between compaction methods are generally attributed to variations in compaction mechanisms, moisture conditions, and material characteristics (Drnevich et al. 2007).

Modified Proctor: The Modified Proctor compaction test (AASHTO-T180 2004) is a standard laboratory method for determining the optimum moisture content (OMC) and maximum dry density (MDD) of a soil or aggregate by compacting it with a higher energy input than the Standard Proctor test. It remains one of the most common lab procedures for characterizing compaction behavior of pavement base and subbase materials. Fattah et al. (2019) reported that the Proctor impact test (including the Modified Proctor) is widely used to find the MDD and OMC of soils; however, a key shortcoming is that it uses impact blows in a rigid mold, which may not accurately simulate modern field compaction methods (Fattah et al. 2019).

For OGDC materials, the concept of optimum moisture content is less clear or relevant. In a typical dense-graded soil, adding a moderate amount of water lubricates particles. Water helps achieve a higher density up to an optimum point, beyond which excess water replaces the soil, reducing dry density. A previous study points out that in free-draining aggregates, the maximum density is typically obtained when compacting in either a dry or partially saturated condition. These inherent characteristics limit the usefulness of a traditional Proctor moisture-density curve for OGDC (Choi et al. 2020).

Another practical limitation is the size of aggregate particles in OGDC. The Modified Proctor test has mold size restrictions, and material with very large particles (up to 50 mm or more in open-graded bases) cannot be tested without adjusting the gradation. While the Modified Proctor applies a higher compaction effort and can provide a useful reference estimate of achievable density, its applicability to open-graded materials is limited due to differences in

compaction behavior and material characteristics. In some cases, vibratory-based laboratory compaction methods have been shown to produce densities comparable to those obtained from the Modified Proctor test for coarse granular materials (Choi et al. 2020). This indicates that the Modified Proctor test can provide a reasonable reference estimate of achievable density for such materials. In summary, the Modified Proctor remains a valuable reference test; it is relatively simple and widely used for characterizing compaction behavior, but its direct applicability to open-graded drainage materials is limited by the test's inherent assumptions (e.g., a distinct OMC) and physical constraints, including mold size and impact-based compaction.

Despite the above limitations, the Modified Proctor test does offer some advantages and consistent roles in the context of drainage materials. It provides a standardized index of compaction potential that engineers are familiar with and can serve as a starting point for specifying a compaction requirement (e.g., field compaction of the open-graded base to at least 95% of the Modified Proctor density). In cases where the OGDC contains a small percentage of fines (e.g., a few percent passing the No. 200 sieve to improve stability), the Modified Proctor can still show a modest density gain with a small moisture addition, allowing you to set a practical field moisture target (Aydilek et al. 2015). For instance, when compacted, several graded aggregate base materials with varying fine contents were tested using both the Modified Proctor (impact) and a vibratory compaction method. They found that vibratory compaction produced only slightly higher maximum dry densities (often at slightly lower optimum moisture content) than the Modified Proctor results.

In one aggregate sample with relatively low fines, the vibratory method yielded a maximum dry unit weight of about 2–3 pcf higher than the Modified Proctor value (with the OMC shifting from ~5.3% to ~4.8%). This indicates that the Modified Proctor test can reasonably achieve densities comparable to those of field-realistic methods for coarse aggregates (Aydilek et al. 2015). In practice, the Modified Proctor MDD provides a baseline for quality control (QC). In practice, contractors often specify compaction as a percentage of the Modified Proctor maximum dry density to ensure the layer's stability and permeability. Accordingly, for coarse OGDC within mold-size limits, the higher-energy Modified Proctor is a reasonable index of near-maximum achievable density, with slightly higher $\gamma_{d(max)}$ from vibratory compaction methods (Choi et al. 2020).

That said, the relevance of the Modified Proctor test for OGDC is mainly as a reference point, rather than a definitive measure of field compaction quality. Researchers are increasingly recommending alternative compaction assessments for open-graded bases. For example, modulus-based approaches (e.g., lightweight deflectometer (LWD) and soil stiffness gauge (SSG)) are proposed to overcome challenges in density measurement and directly verify the layer's stiffness and stability (Choi et al. 2020). Overall, the Modified Proctor test provides a convenient measure of compaction characteristics (maximum density and nominal optimum moisture) for drainage materials. Still, it has notable limitations in applicability to highly open-graded aggregates. Its advantages lie in its familiarity and the relatively high compaction effort, yet issues with oversized particles, non-representative OMC targets for free-draining OGDC, and differences in compaction mechanism limit its relevance. The literature thus suggests that engineers should use Modified Proctor results for OGDC with caution and consider them alongside other indicators of compaction suited to free-draining aggregate behavior (Aydilek et al. 2015; Choi et al. 2020; Fattah et al. 2019).

Vibratory Table: The vibratory table compaction test is used to determine the maximum dry density (maximum index density) of OGDC materials. This laboratory method, standardized in ASTM-D4253 2016, involves placing the aggregate in a mold and applying controlled vertical vibration, often with a surcharge weight on top to densify the material. The vibratory compaction procedure is far more effective for coarse aggregates, consistently yielding higher achievable densities than the Proctor hammer method and better simulating field compaction by vibratory rollers (Nazzal 2014). Notably, while ASTM provides a standard for this vibratory table, there is no direct AASHTO equivalent for such a test (Nazzal 2014). Nevertheless, the method has been widely adopted for characterizing open-graded aggregates. For instance, the Federal Highway Administration's (FHWA's) recent study on open-graded aggregate backfills required participating laboratories to use the ASTM D4253 vibratory table (Method 1A) to determine each sample's maximum dry unit weight (Nicks et al. 2023).

In some cases, agencies supplement density-based acceptance criteria with performance-based measures (e.g., stiffness or deflection) for open-graded materials, particularly where density measurements are less reliable. However, density-based approaches continue to be used in practice, often in combination with these alternative measures. As a result, compaction is frequently specified such that the base is compacted until no further movement is observed under the compactor (i.e., compaction to refusal), along with a qualitative visual inspection to

ensure stability (Nicks 2018), because obtaining reliable in-situ density readings in coarse, open-graded material is difficult. Moreover, research has shown that the performance of open-graded aggregate bases improves significantly with greater compaction (i.e., higher relative density). Laboratory testing demonstrates that increasing the relative density of an open-graded aggregate from a very loose state (around 30% of its maximum density) to a dense state (around 95% of its maximum) can substantially increase the material's shear strength and stiffness, contributing to better load support and stability in service (Chen et al. 2022; Nicks Jennifer 2018).

Gyratory compaction: Several studies have demonstrated that gyratory compaction can achieve compaction outcomes comparable to, or superior to, those of traditional methods for base/subbase materials. Fattah et al. (2019) reported compacting a granular subbase with a Superpave Gyratory Compactor (SGC). They found it capable of achieving higher densities than those obtained with the Standard and Modified Proctor methods, even at moisture contents below the optimum. The method also reaches dry density levels similar to those achieved by modern heavy compaction equipment in the field. In that study, SGC specimens continued to gain density with additional gyrations (up to 500), with about 90% of total compaction achieved within the first 50 gyrations. This highlights the SGC's efficiency in rapidly densifying aggregate through its continuous kneading action (Fattah et al. 2019).

Not only does the gyratory method better mimic field loading, but it can also produce internal aggregate structures and strengths more representative of field-compacted layers. Ping et al. (2003) reported that for granular soils (fine sands and silty sands), gyratory compaction is the most suitable technique to simulate field compaction, yielding specimen internal structures closer to those produced by actual field compaction and traffic loading. Moreover, gyratory-compacted specimens have shown dry densities and strength properties closer to field measurements than those produced by laboratory vibratory compaction (Ping et al. 2003). In other words, SGC samples tend to replicate particle orientation and interlock achieved under a roller's kneading action better than static or vibratory methods. Past research by the U.S. Army Corps of Engineers (USACE) also confirmed that SGC can attain moisture–density relationships comparable to Proctor compaction, but with the notable advantage of higher achievable densities at lower water contents. Overall, the literature demonstrates that the SGC is an effective laboratory tool for compacting unbound drainage materials, often yielding

densities and structures that reflect heavier field compaction than those achieved with traditional lab methods (Ping et al. 2003).

The aggregate size distribution (gradation) is a dominant factor in compaction behavior. Open-graded materials with minimal fines compact differently from well-graded materials. In a comprehensive study using an orthogonal test design, it was found that gradation had the greatest influence on gyratory compaction, followed sequentially by vertical pressure and moisture content. Coarse permeable gradations inherently achieve lower dry densities. Adding finer particles can increase density by filling voids, but excessive fines may reduce permeability. Thus, gradation must be optimized to balance density and drainage (Xiao et al. 2021).

Recent research has examined the mesoscale behavior of particles during gyratory compaction, especially for open-graded aggregates. SmartRock sensors, which are instrumented aggregate particles, were introduced into laboratory gyratory specimens to track real-time particle motion (acceleration and rotation) during compaction. By embedding four SmartRock sensors at different locations in a permeable aggregate base specimen, they captured how individual particles move and reorient under the SGC's action (Xiao et al. 2021). The data showed that while the initial compaction stage was similar across different gradations and conditions, the intermediate stage and the gyration count required to reach a stable condition varied significantly with material properties and test parameters. Coarser or drier specimens often required more gyrations to stabilize fully, indicating that aggregate properties and SGC settings chiefly affect the intermediate compaction phase (Xiao et al. 2021).

2.3.2 Field Tests

Nuclear gauge: As an in-situ field test, the nuclear density gauge provides direct measurements of density and moisture in OGDC layers and has been shown to effectively assess compaction on active projects. For example, a reconstruction project on I-94 in Michigan placed a 270 mm thick OGDC base (over a geotextile separator) beneath new concrete pavement. Nuclear gauge tests on this OGDC after placement, compaction, and trimming showed mean dry densities of 19–20 kN/m³, with very low in-situ moisture content (about 1–2% by weight). The dry density was fairly uniform (coefficient of variation ~3–5%), indicating consistent compaction of the open-graded aggregate (Li et al. 2018). Another study in Indiana obtained similar results, where an open-graded #53 stone was evaluated as a drainage layer. Nuclear gauge measurements

confirmed that the compaction procedure used (initial static rolling, followed by vibratory passes and a static finish) achieved adequate relative compaction in the coarse aggregate layer, while still yielding high post-compaction permeability suitable for drainage. Notably, nearly half of the nuclear gauge tests in the section on natural subgrade fell below the 95% compaction criterion, while in the section with a stabilized subgrade, less than ~6% of points fell below 95% (Garzon-Sabogal et al. 2024). These outcomes underscore that achieving uniform compaction in OGDC is possible, but it may require favorable conditions and effective construction control.

Recent research has also validated the accuracy and limitations of nuclear gauges when used on unconventional drainage materials. The research evaluated the performance of atomic gauges on unbound base mixes containing 30% reclaimed asphalt pavement (RAP), as using recycled asphalt in base layers can affect both density and moisture readings. It found that the nuclear device accurately measured the wet density of RAP-aggregate blends, regardless of RAP content, and matched the sand-cone density results. However, the gauge's moisture content readings were significantly biased by the presence of asphalt, which contains hydrogen atoms that the gauge senses as moisture. The apparent moisture increased with a higher RAP percentage, even though the actual water content did not, an error also noted in prior literature (Shabbir Hossain and Hoppe 2024). The researchers concluded that a nuclear gauge can be used to reliably monitor RAP-aggregate compaction. Still, a material-specific correction or offset must be applied to the moisture readings when asphalt-coated particles are present. This result highlights that for free-draining aggregate layers incorporating any bituminous matter (or other hydrogen sources), engineers should be cautious about the gauge's moisture number.

Nuclear gauges have proven valuable for construction quality control of open-graded drainage courses, providing direct in-situ measurements of density and moisture that help ensure the layer is properly compacted without compromising its drainage function. Key studies confirm that, with appropriate calibration and field practices, nuclear gauges can reliably guide the compaction of OGDC and similar permeable base (Garzon-Sabogal et al. 2024; Li et al. 2018; Shabbir Hossain and Hoppe 2024).

One-Point M-Cone Test: Unlike dense-graded materials, open-graded permeable base aggregates pose a special challenge for compaction assessment. These materials have very uniform, coarse gradations with high void ratios and minimal fines, which makes it challenging

to define a maximum dry density in the laboratory or to measure field density accurately using standard methods (Choi et al. 2018). Consequently, traditional density-based compaction specifications (e.g., those requiring a percentage of the Standard Proctor maximum dry density) are often not applicable or reliable for open-graded bases (Choi et al. 2018). Given these limitations, there has been a shift toward evaluating compaction via stiffness or modulus-based measurements rather than density (Choi et al. 2018). Devices such as the LWD and SSG have been recommended for assessing compaction quality by measuring the stiffness/modulus of the compacted layer (Choi et al. 2018). However, since no specific target modulus values have been established for adequate compaction, it remains challenging to interpret the results of these tests (Choi et al. 2018).

MDOT uniquely uses the One-Point M-Cone Test as a field method to determine the maximum dry density and optimum moisture content of granular base materials during construction. Whereas most agencies rely on a laboratory Proctor test and then check field density, Michigan's approach is to perform the cone test on-site. The method was initially created as a time-saving field adaptation of the Standard Proctor procedure in the 1960s. MDOT limits its use to granular soils with approximately 15% loss by washing, including 23A and 23AA, which may slightly exceed this threshold under MDOT specifications. This criterion is readily met by OGDC materials, which consist primarily of coarse aggregate. By performing the compaction test in the field on material from the exact location where it is being placed, engineers can make immediate decisions on acceptability and adjust rolling efforts or moisture as needed. Importantly, this field test is coordinated with in-place density measurements. MDOT inspectors typically take a nuclear density gauge reading of the compacted OGDC layer and then perform a one-point cone test on a sample from that spot to determine the reference maximum density for that material. The achieved field dry density (from the nuclear gauge) is then compared to the M-Cone test's maximum dry density to calculate percent compaction. This way, the M-Cone Test integrates with standard field density tests to provide real-time compaction control (Hansen and Jensen 2001).

The reliability of the M-Cone Test, particularly its repeatability for OGDC-type aggregates, has been evaluated in a few studies. Krueger (2011) conducted a comprehensive reliability evaluation of the cone test involving 11 different Michigan soils, including a representative open-graded crushed stone (MDOT designation: 4G aggregate). The standard deviation in one-point cone density for the 4G stone was around 4 pcf, compared to roughly 2–3 pcf, a typical

result for Modified Proctor tests on sands. Krueger (2011) observed that during compaction of the 4G and similar coarse mixes, the largest stones tended to concentrate toward the center of the mold, a form of segregation evident from the way the material packed under the cone. Overall, the M-Cone Test is reasonably repeatable for open-graded base materials (Krueger 2011). It is noteworthy that the cone test caused much less particle breakage in the 4G aggregate than the Proctor test, which can be attributed to the different compaction mechanisms of these tests.

Minimal particle crushing is a beneficial trait when testing OGDC, since it preserves the aggregate's intended gradation and permeability. The use of the M-Cone Test on OGDC and similar drainage aggregates offers several strengths. First, its speed and field portability enable compaction characteristics to be obtained in situ and in real-time, which is invaluable when working with materials that may vary from truckload to truckload. The test directly utilizes the as-placed aggregate, including its actual gradation and particle shape, thereby avoiding errors that may arise from sampling and transporting material to a laboratory (Krueger 2011). This is particularly important for OGDC, as even slight gradation changes (or contamination with fines) can affect compaction and permeability (Hansen and Jensen 2001). A second strength of the M-Cone Test is that its field applications in pavement foundations corroborate its practicality. The base and subbase layers in experimental slabs were compacted to moisture contents near their expected OMC, controlled by maximum densities determined by the One-Point M-Cone Test, with in-situ density verified by a nuclear gauge (Hansen and Jensen 2001).

2.4 Instrumentation for Density Measurements

Modern Intelligent Compaction (IC) systems exemplify a shift toward sensor-based geotechnical testing. IC is described as an equipment-based technology, in which vibratory rollers are outfitted with high-precision GPS, temperature sensors, and an accelerometer-based measurement system to monitor compaction in real-time (Arasteh 2017). The roller's onboard accelerometer continuously measures the machine's response as it compacts the soil. The accelerometer signal, reflecting the rebound force from the ground into the drum, is processed into an Intelligent Compaction Measurement Value (ICMV), which correlates with the stiffness or strength of the compacted material (Arasteh 2017). ICMVs can be linked to traditional properties, such as soil modulus, stiffness, and density, to provide real-time compaction feedback (Arasteh 2017). This sensor-driven approach provides 100% coverage of the

compacted area and a deeper influence zone compared to conventional tests. For instance, a roller-based ICMV covers a rectangular footprint of approximately 2 meters by 0.3 meters, with an influence depth of roughly 0.5–1.6 meters, significantly larger and deeper than the spot tests (Arasteh 2017).

The use of accelerometers on compaction equipment has enabled the measurement of new metrics for assessing soil stiffness. The vibratory roller's acceleration waveform distorts as the ground stiffens, i.e., a stiffer subgrade resists the drum, causing a brief loss of contact, bouncing, and the addition of higher-frequency components to the acceleration signal (Tamaishi et al. 2023). Conventional continuous compaction control (CCC) systems quantify this effect with indices like the Compaction Meter Value (CMV), Resonance Meter Value (RMV), or Compaction Control Value (CCV), which are calculated from the ratio of spectral components of the drum's acceleration signal (Tamaishi et al. 2023). However, challenges remain in achieving reliable correlations. The Federal Highway Administration (FHWA) notes that ICMV outputs do not always match traditional spot test results due to fundamental differences in measurement depth and footprint, as well as variability in field conditions (Arasteh 2017). Unlike a static CBR or plate load test, the roller-based measurement is dynamic and influenced by numerous factors, including the roller's vibration amplitude/frequency, speed, and the soil's moisture and gradation (Arasteh 2017). These factors can introduce noise, making absolute interpretations of ICMV difficult without calibration. Furthermore, when the soil is very stiff or the roller decouples (loses contact momentarily), the derived modulus values can become erroneous (Arasteh 2017). Thus, while accelerometer-based ICMV provides a powerful tool for continuous stiffness profiling, it often requires project-specific calibration and an understanding of its operational limits to serve as a reliable criterion for compaction acceptance.

In addition to compaction monitoring, accelerometers have been integrated into penetration tests to improve subgrade strength assessment. A notable example is the development of an instrumented dynamic cone penetrometer (DCP), which directly measures the dynamic response during penetration (Lee et al. 2019). The standard DCP provides a Dynamic Cone Penetration Index (DCPI), which is essentially the penetration per blow, this has been empirically correlated with CBR and shear strength for a long time. However, as noted earlier, the DCPI can be affected by the energy transferred during impact and the rod's alignment, potentially reducing the reliability of results for design purposes (Lee et al. 2019). They

addressed this by outfitting a DCP with a load cell and an accelerometer at the cone tip to capture the actual force and velocity time histories of each impact in real-time (Lee et al. 2019).

In a recent reliability study, the M-Cone apparatus was equipped with a high-impact accelerometer at the base of the cone to measure the acceleration pulse and energy input of each drop (Krueger 2011). The study demonstrated the use of accelerometer instrumentation to better understand the compaction process. While the M-Cone Test is a specific case, it underscores a broader point: integrating sensors, such as accelerometers or force transducers, into geotechnical test devices can significantly enhance our understanding of the energy–density–stiffness relationships and improve the reliability of field tests by accounting for dynamic effects.

2.5 Sieve Analysis Types

2.5.1 Dry Sieve Analysis

Dry sieve analysis is a fundamental laboratory method used to determine the grain size distribution (gradation) of unbound granular base (UGB) aggregates. In this test, oven-dried aggregate samples are passed through a series of standard sieves stacked in decreasing size from top to bottom to quantify the percentages of material in various size ranges. All three studies employed sieve analysis to characterize their base materials and ensure compliance with the specified gradation envelopes. For example, one study confirmed that their five graded aggregate base (GAB) materials met the AASHTO M-147 requirements for high-quality base courses (classified as A-1-a in the AASHTO system). AASHTO M-147 provides upper and lower gradation limits, expressed as percentages passing specific sieves such as 37.5 mm (1½"), 19 mm (¾"), 4.75 mm (#4), 0.425 mm (#40), and 0.075 mm (#200), to ensure a well-graded base. Notably, it limits fines (particles <0.075 mm) to around 8% at most for base layers. Haider et al. (2014) also reported that all seven quarry-sourced base aggregates in their study met the Maryland State Highway Administration (SHA) and AASHTO M-147 gradation specifications, were non-plastic, well-graded, and had as-received fines contents of approximately 6.9–10% by weight. Typically, the sieve series includes coarse screens down to fine to capture the full gradation. Cetin et al. (2014) noted that their materials were initially sieved through 38 mm, #4 (4.75 mm), and #200 (0.075 mm) sieves to determine the grain size distribution, with fines contents between roughly 8% and 12% in the source aggregates (Hatipoglu et al. 2020).

Cetin et al. (2014) took a novel approach by examining how laboratory compaction methods can change gradation. Before testing, they performed sieve analysis on each material, both before and after compaction, to quantify any particle breakdown (Cetin et al. 2014). Finally, the dry-sieve-derived gradation data highlighted the analyses of drainage behavior in these works. A narrowly graded, clean stone drains quickly but may need sufficient fines for stability, while a dense gradation with too many fines retains water. Dry sieve analysis is the tool that allows engineers to check these gradation requirements and adjust mixes accordingly. In summary, these studies demonstrate that careful gradation analysis, i.e., via dry sieving, is essential in characterizing materials (Cetin et al. 2014).

2.5.2 Wet Sieve Analysis

Wet sieve analysis (washed sieve analysis) is employed in material testing to accurately determine grain size distribution, especially the fines content (particles <0.075 mm). Cetin et al. (2014) oven-dried the aggregate samples and sieved them through a series of sieves down to 75 μm first; they reported that the fraction passing the No. 200 sieve (fines) was about 8–12% by weight for the tested quarry materials (Cetin et al. 2014). Another one, similarly measured, had as-received fines contents of approximately 6.9–10% in various graded aggregate base (GAB) samples (all non-plastic), using washed sieving to ensure these values represent all particles finer than 0.075 mm (Haider et al. 2014). Hatipoglu et al. (2020) adjusted the gradations of five different GAB materials by adding or removing fines to achieve target fines contents ranging from 2% to 14%. This process required accurate determination of the existing fines via wet sieving and the direct isolation of the fine fraction from the material to maintain the same mineralogy (Hatipoglu et al. 2020). In all cases, washed sieve analysis was crucial for preparing test specimens with known gradations and for quantifying any changes in gradation during testing. For instance, Cetin et al. (2014) conducted sieve analyses both before and after compaction of samples to evaluate aggregate breakage. This revealed a slight increase in fines, i.e., about 2% more material passing certain sieves, due to the more aggressive Modified Proctor compaction method.

Washing the aggregates through the #200 sieve ensures that all particles smaller than 0.075 mm are separated from the larger grains. Fine dust coatings and clay/silt particles can adhere to the surfaces of coarse aggregates or form agglomerates that do not fully pass through during dry sieving. Hatipoglu et al. (2020) obtained an accurate measure of the fines fraction by weight

using the wet-sieving method. This accuracy is critical because fines content is a key variable in base material performance. Haider et al. (2014) noted that state specifications (e.g., Maryland SHA) require less than 8% fines in base aggregates, a standard defined based on the wet-sieving method. Only with wet sieving can the laboratory-measured fines content be reliably compared to such limits and used in performance analysis.

Accurate determination of fines content via wet-sieve analysis enabled these studies to understand the strong effects of fines on unbound base performance. The study demonstrated that the fines content has an optimal range for mechanical behavior. Adding fines up to about 6–10% (by weight) led to an increase in base course stiffness (higher resilient modulus), as the fines were able to fill voids and improve particle packing. However, beyond this optimal stiffness, additional fines led to a sharp reduction in performance. These shifts underscore why the drainage quality of base aggregates deteriorates with increased fines content. The small particles clogged voids and impeded water flow. They concluded that to maintain satisfactory mechanical and hydraulic performance, the fines content should be limited to around 8% and an appropriate gravel-to-sand ratio should be used in the gradation (Hatipoglu et al. 2020).

2.6 Statistical Analysis

2.6.1 T-Test

Two representative studies, one examining century-old trail compaction and another focusing on the impacts of modern forestry machinery, illustrate how t-tests are applied to validate compaction effects in a statistical context. These studies emphasize the significance of t-tests in distinguishing actual compaction-induced changes from natural variability, thereby improving the interpretation of experimental results.

Brevik et al. (2002) investigated soils compacted by wagon traffic ~150 years prior, comparing on-trail (compacted) soils with adjacent off-trail (uncompacted) soils. In their experimental design, soil samples were collected at multiple depth increments (0–20 cm) and analyzed for bulk density (an indicator of compaction intensity) and soil organic carbon (SOC) content, among other variables. Statistical comparisons of the mean properties between the compacted and control soils were made using independent sample t-tests at a 5% significance level. This t-test analysis confirmed that compaction had measurably altered the soil's physical and chemical state. Bulk density in the compacted trail was significantly higher than in the off-trail

soil below the surface layer, and SOC concentrations in deeper layers (10–20 cm) were significantly lower under the compacted trail than in the undisturbed soil (Brevik et al. 2002).

In essence, the t-tests provided evidence that the higher density of the compacted soils corresponded with a depletion of organic carbon at depth, a finding that Brevik et al. interpreted as compaction forming a dense layer that restricted the downward movement of organic matter. By establishing these differences with statistical significance, the researchers could attribute changes in soil carbon distribution and fertility to the historic compaction treatment rather than to random spatial variability. The t-test thus served as a critical methodological step, validating that the observed contrasts, i.e., higher bulk density and lower subsurface SOC in the trial soils, were real effects of compaction.

Tomčík et al. (2025) examined the impact of heavy forestry machinery on forest soil conditions, with particular focus on soil CO_2 concentrations as an indicator of soil health, and used t-tests in multiple ways to evaluate compaction effects. First, one-sample t-tests were used to compute mean values and 95% confidence intervals for soil parameters within each plot. This provided a measure of inherent variability and helped verify uniform conditions before the treatment. The t-test results enabled them to observe any statistically significant differences, for example, the higher gas concentrations or moisture in the compacted soil. Over the monitoring period, the t-test comparisons revealed a clear pattern: soil compaction by machinery had a substantial and lasting impact on subsurface CO_2 levels (Tomčík et al. 2025).

In one study, the t-test results were used to attribute lower deep-soil carbon levels specifically to the presence of a compacted layer (Brevik et al. 2002). Likewise, another study relied on t-test results to confirm that forestry machine traffic caused meaningful changes in soil conditions. The fact that their t-test analyses showed significant CO_2 increases in compacted soil, while initial soil homogeneity tests showed no pre-existing differences, gave credence to the conclusion that machinery-induced compaction was responsible for the elevated CO_2 levels (Tomčík et al. 2025).

Across both studies, the use of t-test analysis was pivotal in quantifying the effects of compaction on soil parameters within a scientific confidence framework. The t-test served as a methodological cornerstone for hypothesis testing, essentially asking whether compaction causes a statistically significant change in this soil property. By comparing mean values from compacted and uncompacted conditions and evaluating their differences relative to natural

variance, the t-tests allowed researchers to confirm cause-and-effect relationships.

2.6.2 Two-Way ANOVA

Usaborisut and Ampanmanee (2015) varied three factors: soil texture (loam, silt loam, silty clay loam), moisture content, and organic matter (0% vs. 5% added). The study provided a clear example of the application of a two-way ANOVA to silty soil compaction testing, assessing the effects of these factors on compaction outcomes, namely soil bulk density and penetration resistance. The ANOVA results showed that both soil type and moisture content had statistically significant impacts on these parameters, whereas the addition of organic matter significantly affected only the bulk density. In practical terms, differences in soil texture and moisture levels resulted in notable differences in how densely the soil could be compacted and how resistant it was to penetration. However, the presence of organic matter primarily influenced the achievable density. Notably, the analysis also captured interaction effects between factors. For instance, a significant soil-moisture interaction indicated that moisture's influence on compaction outcomes depended on soil texture. The gap in bulk densities between different soils narrowed at higher moisture contents (Usaborisut and Ampanmanee 2015). Using two-way ANOVA in this way allowed the authors to rigorously confirm which factors and their combinations were truly controlling the compaction behavior of the soils and to rule out any apparent trends due to random variation.

Iliyas et al. (2024) employed a two-way ANOVA to evaluate the stabilization of clayey soil using two additives: Cement and sawdust ash (SDA). Here, the independent variables were the percentages of cement and SDA mixed into an expansive clay. The dependent responses included key geotechnical properties, notably unconfined compressive strength (UCS), hydraulic conductivity, and volumetric shrinkage strain. By using a two-factor ANOVA (without replication) on the results, they quantitatively evaluated how each stabilizer affected the soil and whether there was a combined effect when used together. The statistical analysis demonstrated that both cement content and SDA content had significant effects (at the 95% confidence level) on all measured properties. ANOVA confirmed that these improvements were statistically significant and attributable to the additives rather than random chance. The two-way ANOVA also enabled examination of the interaction between cement and ash. The results indicated a notable synergistic effect: an optimal intermediate combination of cement and SDA yielded the most significant enhancement in engineering properties. In other words,

the effectiveness of one stabilizer was partly dependent on the level of the other, a relationship that the ANOVA could detect by testing the interaction term (Iliyas et al. 2024).

Iliyas et al. (2024) emphasized that this statistical approach was crucial for validating the dual-stabilizer strategy: ANOVA quantified the improvements due to each factor and their combination, lending confidence that the observed gains, such as reduced shrinkage or increased strength, were significant and not just subjective observations. Moreover, by statistically confirming the optimal mix (cement–SDA) for improving soil properties, the study employed ANOVA as a tool for compositional optimization, a step that earlier studies had often not rigorously pursued. This illustrates how two-way ANOVA can guide engineers in identifying the most effective treatment levels and in quantifying the novelty of a stabilization method.

2.7 Department of Transportation (DOT) Procedures for Density Testing

This subsection summarizes representative procedures from six state transportation agencies: California (Caltrans), Illinois (IDOT), Ohio (ODOT), Florida (FDOT), Texas (TxDOT), and Michigan (MDOT), as listed in Table 1. These states were chosen to represent a variety of materials and QC practices for granular and open-graded drainage courses, as adopted in laboratory and field testing. Together, they highlight standard requirements and notable state-specific approaches that inform the compaction/control framework used in this study.

Table 1. Summary of State DOT Procedures and Applicability of OGDC Material

Name of the State Agency	Laboratory methods (reference)	Field methods (reference)	OGDC applicability
California (Caltrans)	CT 216 (relative compaction: lab maximum wet density via CT-216 impact procedure; oversize correction if ≥10% retained on 19-mm sieve) (Caltrans, 2023)	Sand-Cone (AASHTO T 191) for in-place wet density; RC = ρ_in-place / ρ_max × 100 with ρ_max from CT-216 (Caltrans, 2023)	Oversize-aggregate corrections apply. CT-216 impact energy is an index target; however, it may not replicate roller densification in highly open-graded layers.
Illinois (IDOT)	Standard/Modified Proctor; One-Point (AASHTO T 272) with family of curves; Relative Density (ASTM D4253/D4254) for cohesionless/open-graded aggregates (IDOT, 2020)	Nuclear gauge (AASHTO T 310) for density/moisture; Sand-Cone (AASHTO T 191) for verification (IDOT, 2020)	For OGDC, IDOT uses relative-density targets or one-point correlations; Proctor curves may be unreliable for very open gradations.
Ohio (ODOT)	One-Point Proctor on Typical Moisture–Density Curves; oversize corrections per AASHTO T 224; Test-Section Methods A, B, C when curves are not representative (ODOT, 2010)	Nuclear gauge (AASHTO T 310) with project-specific corrections; test-sections for production control (ODOT, 2010)	Method C is preferred for highly open-graded materials: performance-based control (proof-rolling, stiffness/deflection, drainage) instead of %MDD.

Florida (FDOT)	FM 1-T 099 / FM 1-T 180 (Standard/Modified Proctor; FM 1-T 180 includes Florida-specific provisions aligned with LBR); ASTM D4253/D4254 (relative density); FM 5-515 (LBR); AASHTO T 307 (Mr) (FDOT, 2024)	Nuclear gauge (AASHTO T 310); DCP for rapid in-situ strength (FDOT, 2024)	For OGDC, relative density and DCP are practical; note potential bias in nuclear moisture due to rapid drainage—use project-specific checks.
Texas (TxDOT)	TEX-113-E (Modified Proctor) for granular bases; 152-mm mold, 10-lb rammer, 18-in drop; Soil Compactor Analyzer for energy control (TxDOT, 2011)	Nuclear gauge (AASHTO T 310) with random sampling; material-specific moisture corrections for RAP, gypsum, lime, cement (TxDOT, 2024)	TEX-113-E is tailored to difficult-to-compact granular bases; provisions/corrections are applicable to open-graded drainage course materials.
Michigan (MDOT)	One-Point M-Cone Test (≤15% loss by washing): three lifts, ≥25 blows/lift; MDD/OMC from one-point chart; also Modified Proctor (AASHTO T 180) for crushed concrete/OGDC/stabilized bases (MDOT, 2024)	Nuclear gauge (e.g., Troxler 3440) with direct transmission; field density as % of lab MDD (Cone or T-180); typical acceptance ≥95% at ≤OMC; careful seating/moisture calibration for OGDC (MDOT, 2024)	Michigan uniquely uses the M-Cone (field/lab) to set reference MDD/OMC for granular/OGDC; integrates with nuclear gauge for real-time compaction control.

2.7.1 California

Laboratory Methods: Caltrans uses California Test 216 to determine the relative compaction of untreated soils, treated soils, and aggregates as the ratio of in-place wet density to laboratory maximum wet density. Laboratory preparation includes separating material on the 19 mm (¾ in.) sieve, and if at least 10 % is retained, applying oversize corrections. Compaction is performed with a 4.54 kg (10 lb) rammer dropped from 457 mm (18 in.) for 20 blows per lift over five layers, followed by five leveling blows (Caltrans 2023).

Field Methods: Caltrans uses the Sand-Cone Method (AASHTO T 191) to determine the in-place wet density by excavating a test hole, weighing the removed soil, and determining volume by backfilling with calibrated sand. Relative compaction is then calculated as shown in Eq. (1):

$$RC = \frac{D_{\text{in-place}}}{D_{\text{max}}} \times 100 \qquad \text{Eq. (1)}$$

where D_{max} is from California Test 216 (Caltrans 2023).

When establishing ρmax per CT 216, oversize-aggregate corrections apply (e.g., when ≥10% is retained on the 19-mm sieve). For highly open-graded drainage courses, note that the CT 216 impact procedure may not fully replicate field roller densification; thus, the CT 216 value should be treated as an index target (Caltrans 2023).

2.7.2 Illinois

Laboratory Methods: IDOT uses the Standard Proctor (2.5-kg [5.5-lb] rammer, 305-mm [12-in.] drop, three lifts) and the Modified Proctor (4.54-kg [10-lb] rammer, 457-mm [18-in.] drop, five lifts) to establish MDD/OMC. IDOT also permits the one-point method (AASHTO T 272) with a family of curves to estimate MDD/OMC from a single compaction point (≈20-minute test), which is helpful for variable embankment soils. For cohesionless or open-graded aggregates where Proctor curves are unreliable, relative density (ASTM D4253/D4254) is used to determine maximum and minimum index densities via vibratory table and free-fall/funnel procedures; field targets may be specified as a percentage of relative density (IDOT 2020).

Field Methods: IDOT determines in-place wet density and moisture primarily with the nuclear density gauge (AASHTO T 310) using direct transmission for density and backscatter for moisture, with sand-cone (AASHTO T 191) tests for verification (IDOT 2020).

2.7.3 Ohio

Laboratory Methods: ODOT determines MDD/OMC using a one-point Proctor plotted on Typical Moisture–Density Curves. For materials with 10–25% retained on the 19-mm (¾-in.) sieve, oversize corrections are applied in accordance with AASHTO T 224 (ODOT 2010).

Test-section approaches (Methods A, B, C). When standard moisture–density curves are not representative, ODOT uses three field methods. Method A builds a short control strip with the project materials and rollers, establishes an effective rolling pattern while monitoring in-place density (nuclear/sand-cone), and accepts production as a percentage of the control-strip target. Method B pairs limited laboratory compaction (e.g., one-point with family curves and oversize correction) with a field correlation developed on a test strip so nuclear readings can be accepted relative to the correlated laboratory index within a defined tolerance. Method C, intended for highly open-graded materials, replaces %MDD with performance verification on a test section, stable response under proof-rolling, adequate stiffness/deflection and drainage, and minimal degradation, together with a roller pattern to reproduce that performance in production. Method C is preferred for OGDC because density/OMC targets are often non-representative due to free drainage and low fines (ODOT 2010).

Field Methods: ODOT determines in-place wet density and moisture with the nuclear density gauge (AASHTO T 310), using project-specific corrections/calibration and verification as needed. ODOT procedures also address oversize-aggregate correction (per AASHTO T 224) and allow test-section approaches (Methods A–C) for highly open-graded materials (ODOT 2010).

2.7.4 Florida

Laboratory Methods: FDOT uses FM 1-T 099 (Standard Proctor) and FM 1-T 180 (Modified Proctor) but includes Florida-specific provisions like tighter moisture-increment spacing around OMC for curve development, pre-conditioning (stand/soak) times by soil group, explicit oversize-aggregate handling/recording, and FDOT sample-mass guidance, to establish

MDD/OMC. For cohesionless soils, ASTM D4253/D4254 provides maximum/minimum index densities (relative density). FDOT also employs the Limerock Bearing Ratio (FM 5-515) for base/subgrade strength and resilient modulus per AASHTO T 307 (FDOT 2024).

Field Methods: FDOT determines in-place wet density and moisture with the nuclear density gauge (AASHTO T 310) and uses the Dynamic Cone Penetrometer (DCP) for rapid in-situ strength/penetration index. For open-graded drainage courses (OGDC), relative density targets and DCP provide practical control over drainage-layer performance. It should be noted that nuclear moisture readings may be biased by rapid drainage and should be interpreted with project-specific checks (FDOT- In-Place 2024).

2.7.5 Texas

Laboratory Methods: TxDOT uses TEX-113-E (Modified Proctor) for granular bases, compacting in a 152-mm (6-in.) mold with a 4.54-kg (10-lb) rammer dropped from 457 mm (18 in.). Procedures include lift placement and blow counts consistent with Modified Proctor effort; a Soil Compactor Analyzer is used to verify uniform energy application and specimen integrity (TxDOT-113 2011).

Field Methods: TxDOT primarily uses the nuclear density gauge (AASHTO T 310) with random sampling protocols for in-place wet density and moisture, and specifies material-specific moisture corrections for reclaimed asphalt pavement (RAP), gypsum, lime, and cement (TxDOT-115 2024). TEX-113-E is tailored for difficult-to-compact granular bases and includes provisions/corrections applicable to open-graded drainage course materials.

2.7.6 Michigan

Laboratory Methods: MDOT uses the Modified Proctor test for crushed concrete and OGDC, and the stabilized granular base test: a 4.54-kg (10-lb) rammer dropped from 457 mm (18 in.) over five lifts to develop a multi-point moisture–density curve and determine MDD/OMC. The higher compaction energy provides a reasonable laboratory approximation for coarse and recycled materials (MDOT 2024).

Field Methods: MDOT determines the maximum dry density (MDD) and optimum moisture content (OMC) for granular materials with ≤15% loss by washing, including OGDC, using the One-Point M-Cone Test. A conical mold shown in Figure 1 is filled and compacted against a

hardwood block in three lifts (≥25 blows per lift), continuing until the mass increase is <10 g after 20 additional blows. Moisture is measured, and MDD/OMC are read from the one-point chart calibrated for Michigan soils, as shown in Figure 1. It can also be performed in the laboratory.

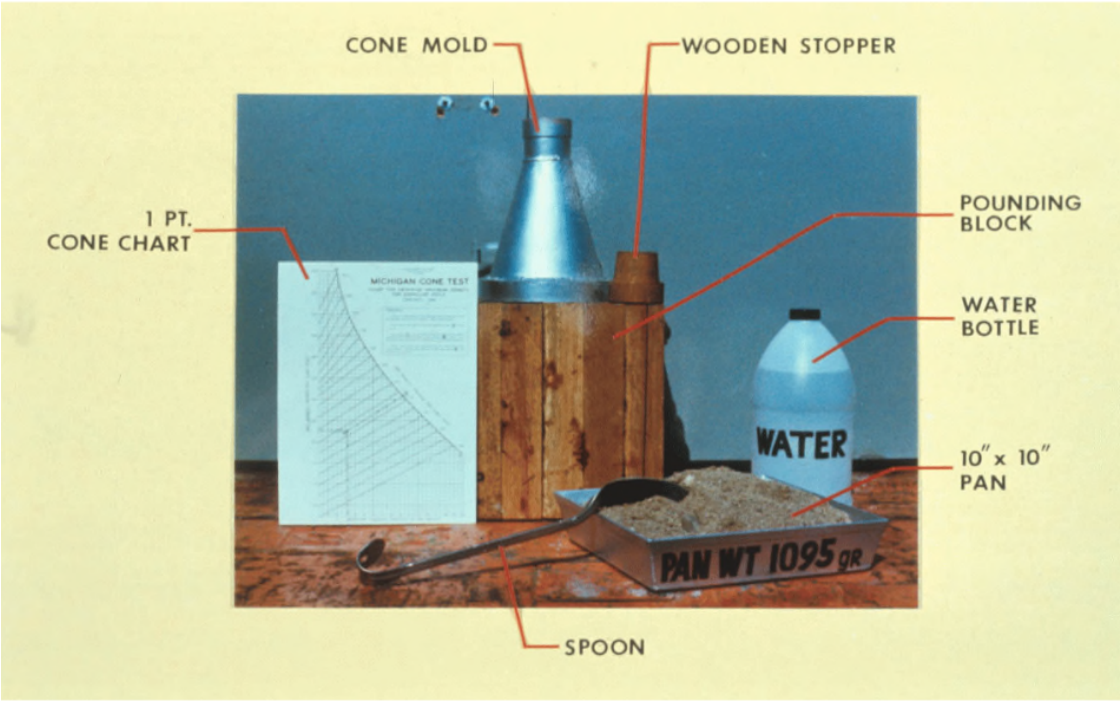


Figure 1. M-Cone Test Apparatus Comprising of M-Cone, Pounding Block, and Cone Stopper, and Chart for Interpreting Maximum Dry Density Values From M-Cone Testing

MDOT measures in-place wet density and moisture using a nuclear density gauge (e.g., Troxler 3440). Field density is expressed as a percent of the in-situ MDD (from the M-Cone or AASHTO T 180). Direct transmission is used for accuracy, with tests taken on representative, properly compacted OGDC layers. Acceptance typically requires ≥95% of lab MDD at moisture ≤ OMC. Due to the large voids in OGDC, moisture calibration and careful gauge seating/surface preparation are critical (MDOT 2024).

In MDOT practice, the selection of the compaction test is governed by soil type and fines content. Cohesive soils, fine-textured clays or clayey soils with loss by washing greater than 15%, are compacted in-situ using the One-Point T-99 test, a Michigan adaptation of AASHTO T 99 that uses the same Proctor mold, 5.5-lb (2.5-kg) rammer, and standard compaction effort but derives maximum dry density and optimum moisture content from a single compaction

point and a departmental chart (MDOT 2024). The full multi-point AASHTO T-99 and the M-Cone test are primarily reserved as referee procedures, while the One-Point T-99 serves as the routine index test for cohesive embankment and backfill materials (MDOT 2024).

Field control for cohesive soils is provided by Density In-Place (nuclear gauge) testing. The gauge measures in-place wet density and moisture, and percent compaction is computed relative to the in-situ maximum dry density from the One-Point T-99 test. Under MDOT's Controlled Density Method, each lift of cohesive embankment must achieve a specified fraction of that maximum density, and moisture at the time of compaction must not exceed approximately 3% above optimum, with tighter limits near the pavement surface. Rapid moisture checks for T-99 specimens or in-place material are obtained using the calcium carbide gas pressure ("Speedy") moisture tester, which is calibrated for both granular and cohesive soils and includes specific procedures for materials with more than 15% loss by washing. This process is performed after adjusting the in-situ moisture conditions of the material as required to determine maximum density (MDOT 2024).

While the present study focuses on granular base aggregates (4G OGDC) evaluated with M-Cone–based procedures, recognizing MDOT's separate framework for fine-grained cohesive soils, centered on the One-Point T-99, nuclear gauge density testing, and controlled-density specifications, clarifies that the findings and recommendations developed here apply specifically to the granular portion of MDOT's compaction program (MDOT 2024).

3 METHODOLOGY

This study employs a comparative mixed-methods design that integrates laboratory experiments, field validation, and computational modeling to evaluate the compaction behavior of open-graded drainage course (OGDC) aggregates. The approach encompasses (1) comparative laboratory compaction testing using multiple standardized methods, (2) field validation of compaction using in-place density measurements, and (3) statistical analysis to generalize findings. OGDC materials from several MDOT-approved sources were tested under each lab compaction method, with replication to quantify operator variability. This design enables benchmarking of MDOT's proprietary M-Cone procedure against established standards (e.g., Modified Proctor, vibratory, and gyratory) and relating laboratory maximum densities to field-achieved densities. By combining controlled lab comparisons, on-site validation, and statistical analysis, the study obtains both empirical and theoretical insights that neither approach alone could provide. In particular, laboratory methods yield repeatable benchmarks and field tests ensure real-world relevance, together providing a robust basis for evaluating OGDC compaction.

3.1 Research Design

A suite of standardized laboratory compaction tests was employed to measure and compare the maximum dry density attainable for the OGDC aggregates. Four compaction methods were selected based on their usage in practice or research: the MDOT M-Cone one-point method, the Modified Proctor (AASHTO-T180 2004), the Vibratory Table method (ASTM-D4253 2016), and compaction with a Superpave Gyratory Compactor (ASTM-D6925 2015). Each test was conducted according to its standard procedure, with appropriate adaptations for coarse aggregates, and known limitations regarding open-graded materials were noted. All specimens were prepared from representative bulk samples, with any necessary moisture conditioning as specified in the test standards. Each test was performed in multiple trials to ensure statistical reliability. Below, each method is described with its procedure, justification for inclusion, and considerations specific to OGDC compaction.

Granular materials with low fines content were compacted using MDOT's One-Point M-Cone test, which is a simplified impact compaction method. The outcome is a wet density for that compaction effort, from which a maximum dry density and corresponding moisture content are inferred using M-Cone chart. MDOT employs this one-point method in lieu of a full Proctor

test for free-draining materials (e.g., aggregate bases with ≤15% fines), as it provides a quick estimate of maximum density without requiring multiple points (MDOT, 2024). The M-Cone was included as a primary comparator because it reflects current MDOT practice for OGDC compaction and is the basis for field density specifications in Michigan. To ensure consistent compaction effort, this study instrumented the bottom of the M-Cone with an accelerometer to record the force of each cone strike and compute the actual energy imparted to the sample. This allowed quantification of compaction energy findings for the M-Cone and verification of uniformity between trials. The rationale for applying the M-Cone is that it provides a rapid, field-friendly index of maximum density for coarse-grained materials when traditional multi-point Proctor tests are time-intensive and laborious.

3.1.1 M-Cone

The one-point test remains widely used by MDOT for OGDC-type materials, and part of this study's goal was to evaluate how its results compare to those of other standard laboratory compaction methods.

3.1.2 Modified Proctor

The Modified Proctor test was performed in accordance with AASHTO T 180, providing the maximum dry density (MDD) and optimum moisture content (OMC) of each aggregate under a standardized heavy compaction effort. The Modified Proctor was included as a benchmark reference method because it is a long-established compaction standard for base materials. It provides a common basis for field compaction specification. Many agencies require base layers to be compacted to a certain percentage (often 95% or lower) of MDD obtained by Modified Proctor (Nazzal 2014). Moreover, unlike one-point tests, the Proctor test yields a compaction curve, illustrating how changes in moisture affect density. The Modified Proctor provides a thorough characterization of compaction behavior and is recognized in design and construction specifications. This study used it to provide a baseline for maximum density under heavy compaction effort, comparing it to the M-Cone's one-point result on the same material.

3.1.3 Vibratory Table

The maximum density of the coarse, cohesionless aggregates was determined using the vibratory table method (ASTM-D4253 2016). At the end of vibration, the achieved mass and

volume yield the maximum density, which is often termed the “maximum dry unit weight” for that material under zero moisture. No moisture was added in this test because the standard was intended for free-draining soils where capillary moisture is not a factor. It is particularly applicable to clean sands and gravels with little or no fines. ASTM D4253 recommends applicability for soils with a passing percentage of ≤15% through the 0.075 mm sieve. This method was included to represent the vibration-based compaction mechanism commonly used in the field for OGDC layers. The vibratory test provides a reference “maximum density” under ideal vibration conditions, which can be compared to the densities obtained from impact methods. One limitation is that the vibratory table requires specialized equipment and is time-consuming. Therefore, it is mainly used for research or to determine the relative density of sands, rather than for routine field control. Nonetheless, its inclusion in this study helps identify the maximum possible density for OGDC aggregates under ideal compaction energy, providing a valuable comparison point for the other methods.

3.1.4 Superpave Gyratory Compactor (SGC)

A Superpave Gyratory Compactor (SGC), typically used for asphalt mix design, was adapted to compact the OGDC aggregates in the laboratory. The SGC applies a combination of vertical pressure and gyratory motion (an internal angle of gyration) to a sample confined in a mold, simulating a kneading action (ASTM-D6925 2015). In terms of equipment settings, the general framework of ASTM D6925 (for asphalt mixtures) was followed. However, no asphalt binder was used. The OGDC aggregate was compacted in dry conditions to focus on grain rearrangement and breakage. The rationale for including gyratory compaction was that it provides a kneading mode of compaction more similar to field roller compaction than the purely vertical impact of the Proctor method. The gyratory method can better simulate how aggregate particles orient and lock under a combination of pressure and shear, producing cylindrical specimens that can be examined for stability. The rotating action tends to grind particles against each other. By measuring the gradation change before and after gyratory compaction, one can assess how much the aggregate breaks down under a given compaction effort.

After gyratory compaction, sieve analysis was similarly conducted to quantify any particle crushing (as detailed in the next section). There is currently no ASTM/AASHTO standard specifically for gyratory compaction of unbound aggregates. Thus, the ideal pressure, angle,

and number of gyrations to represent field conditions are not universally established; reasonable parameters were therefore chosen. If too many gyrations or excessively high pressures are used, the test could overcompact or excessively crush the aggregate, resulting in a density that may not be attainable in the field. Despite these considerations, the gyratory compactor offers a unique insight into the compaction process. By incorporating the gyratory method, one can directly compare its resulting density and aggregate breakage with those of other methods to determine if it provides an advantage in reproducing field-like conditions.

3.1.5 Specific Gravity and Absorption

Specific gravity and water absorption tests were conducted to characterize the OGDC material from various sources. Specific gravity and absorption were measured for coarse and fine fractions in accordance with ASTM C127 and ASTM C128, respectively. These measurements were used to define the effective moisture content at compaction, as shown in Eq. (2), for one-point M-Cone and Modified Proctor results. Incorporating specific gravity and absorption helped clarify the density values obtained from different tests on different OGDC sources.

$$w_{eff} = w_{OMC} - absorption \qquad \text{Eq. (2).}$$

Where w_{eff}– effective moisture content and w_{OMC}– optimum moisture content

3.1.6 Sieve Analyses: Before and After Testing

To assess the changes in gradation due to compaction, sieve analyses were performed on each aggregate sample before and after compaction. Pre-compaction gradations for each source were determined by standard dry sieving (ASTM-C136 2019) and wash sieving for fines (ASTM-C117 2004) to establish the baseline particle size distribution. After each compaction test (M-Cone, Modified Proctor, Vibratory, and Gyratory), the sample was recovered and dried (if needed), then sieved again using the same procedure. By comparing the before-and-after gradation curves, the degree of particle breakdown (degradation) caused by each compaction method was quantified. This allowed comparisons of the particle breakage between different testing methods.

Typically, OGDC is designed to be open and free-draining, so any increase in fine particles from compaction could reduce permeability and negate the drainage purpose of the layer. Moreover, changes in gradation affect density itself. If compaction breaks particles and generates smaller pieces that fill voids, the measured density will be higher. However, the material may be susceptible to clogging or settling in the future. Conducting sieve analysis before and after each compaction test method helps understand the density results and the material's long-term performance. For instance, a material source that yields very high density values due to excessive crushing may not necessarily be better for long-term performance than one that yields slightly lower density with minimal breakage.

3.1.7 Field Validation

Laboratory results were validated in the field by compacting OGDC layers and measuring their in-place density with a nuclear density gauge (ASTM-D6938 2017). Several sections of OGDC were examined using a calibrated nuclear gauge in direct transmission mode for density measurements, with moisture measured using the gauge's moisture function at multiple locations within the compacted layer. The gauge's wet density and moisture values were then used to compute the in-place dry density of the OGDC. These field-dry densities were compared with the laboratory maximum dry densities obtained from the various compaction tests. This analysis helped identify which lab test produced values closest to the field density.

3.1.8 Operator Variation: Statistical Analysis

Descriptive statistics, including mean, standard deviation, and coefficient of variation, were compiled for each material pairing. Paired t-tests were conducted to assess operator variability in maximum dry density (MDD), optimum moisture content (OMC), and delivered compaction energy for the M-Cone across all sources. A two-way ANOVA was performed to evaluate the main effects of operator and source, as well as their interaction.

In summary, the rationale for combining multiple approaches is to ensure that the study's conclusions about OGDC compaction are holistic and practically applicable. Laboratory tests alone might suggest one method yields the highest density, but without field validation, it would not be known if the density is attainable or necessary. Field tests alone may reveal a specific compaction outcome, but without the laboratory context, it can not be attributed to material properties or method differences. Statistical analysis alone finds differences, but

without understanding the “why” (which the lab mechanisms explain), it would be just numbers.

By integrating all these elements, the study provides a comprehensive understanding of what maximum densities are achievable, the methods to achieve them, how those maximum densities translate to the field, and the key factors influencing compaction, whether human, material, or method. This comprehensive insight is expected to inform the design and construction practices of the OGDC layer.

3.2 Materials/Instrumentation

3.2.1 Sources

The material sources used in this study were collected between 2024 and 2025 to ensure representation of both as-produced and field-modified OGDC aggregates used in MDOT pavement construction projects. The selection strategy was designed to capture variability in aggregate lithology, processing method, and gradation relative to the MDOT OGDC specification, while also enabling controlled blends for laboratory evaluation. Table 2 summarizes each source, its origin, collection date, handling, and any modifications.

Collected in 2024

In 2024, five primary aggregate sources were obtained directly from producer stockpiles or plant yards: Lafarge, Port Inland, Great Lake, Stone Co., and Calcite. These materials (all of which conformed to the nominal 4G OGDC gradation) were collected for laboratory evaluation of compaction behavior under the M-Cone Test, Modified Proctor, Gyratory, and Vibratory compaction procedures. Material was collected directly from active stockpiles and transported to the Michigan State University’s (MSU) testing laboratory in clean buckets. No blending or modification was performed on these 2024 sources before testing.

Blended/Collected in 2025

In 2025, additional sources were incorporated to expand the study matrix. A controlled laboratory blend, designated StGrLa2024, was produced from the wet-sieved coarse and fine fractions of Stone Co., Great Lake, and Lafarge materials collected in 2024. Fractions were proportioned to match a target OGDC gradation curve and blended under controlled conditions.

Field-collected materials included Sylvania Metro (SylMe2025), obtained in April 2025 without modification, and a tuned variant (SylMe2025_2) in which the percent passing on the No. 10, No. 20, No. 40, and No. 60 sieves was adjusted to improve conformance to the target OGDC curve approved by MDOT. Additional field sources included a slag aggregate meeting 4G OGDC gradation (Slag 4G) collected in May 2025, as well as material from the Sylvania I-275 project collected during a July 2025 field visit, during which in-place density was also measured using a nuclear gauge.

Table 2. Details of OGDC Materials Used in this Study

Source ID	Year Collected	Facility/Origin	Material Type	Location	Notes
Lafarge	2024	Quarry	4G OGDC	MI, Saginaw , Burrough's 1st St Dock	Used directly without modification
Port Inland				MI, Saginaw, Wirt Dock	
Great Lake				MI, South Rockwood, Sylvania Minerals	
Stone Co				MI, Newport	
Calcite				MI, Rogers City, Calcite quarry	
StGrLa2024	2025	Lab blend of 3 sources		Laboratory	Proportioned and mixed based on the target gradation curve

Source ID	Year Collected	Facility/Origin	Material Type	Location	Notes
SylMe2025		Metro region Project		MI, Livonia	Used directly without modification
SylMe2025_2		Lab		Laboratory	Adjusted passing on sieves #10, #20, #40, #60 to better match target gradation
Slag 4G		Slag supplier	4G OGDC (slag)	MI, Detroit	Used directly without modification
I-275		I-275 project	4G OGDC	MI, Plymouth	Used directly without modification

3.3 Testing Procedures

3.3.1 Sieve Analysis

In the research, a combined methodology was employed to determine the complete particle-size distribution of aggregate materials, incorporating both wet washing and dry sieving techniques. The amount of material finer than 75 µm (No. 200) was determined by wet washing, as per ASTM C117, followed by particle-size distribution analysis of the same sample, dried, using dry sieving, as per ASTM C136/C136M.

This sequential approach proved essential for accurate determinations of fine material (<75 µm). As specified in ASTM C117, the wet-washing procedure was performed first, and the results were incorporated into the C136 calculation and reporting framework to obtain complete gradation data (ASTM-C117 2004). This methodology aligns with the fundamental principle that material finer than the 75-µm sieve can be separated from larger particles more efficiently and thoroughly by wet sieving than through dry sieving alone (ASTM-C117 2004). The integrated approach enabled evaluation of particle degradation and fines generation by comparing gradations before and after compaction, providing critical insights into material behavior under test conditions.

Methodology strictly followed the coordinated application of two complementary ASTM standards:

- **ASTM C117**: Standard Test Method for Materials Finer than 75-µm (No. 200) Sieve in Mineral Aggregates by Washing
- **ASTM C136/C136M**: Standard Test Method for Sieve Analysis of Fine and Coarse Aggregates

The standards specifically require this sequential approach when accurate fine material determinations are needed. ASTM C136 acknowledges that "*accurate determination of material finer than the 75-µm (No. 200) sieve cannot be achieved by use of this test method alone*". It directs users to "*use Test Method C117 for determination of material finer than the 75-µm (No. 200) sieve by washing*" (ASTM-C136 2019).

Procedure A of ASTM C117, involving water-only without a wetting agent, was used as the standard approach unless otherwise specified. This procedure involves washing aggregate samples with plain water to remove clay particles, other dispersed materials, and water-soluble substances (ASTM-C117 2004). The methodology culminated in incorporating the wet washing information into the dry sieving calculations, where "*the mass finer than the 75-µm (No. 200) sieve determined by that test method was added to the mass passing the 75-µm (No. 200) sieve by dry sieving of the same sample*" (ASTM-C136 2019).

The following equipment was utilized, meeting the specific requirements of both standards:

- **Balance Systems:** Readable to 0.1 g and accurate to 0.1 g or 0.1% of test load, whichever is greater
- **Nested sieve pair**: 75 µm (No. 200) sieve below a 1.18-mm (No. 16) guard sieve
- **Washing container**: Pan or vessel sufficient to contain the sample covered with water and permit vigorous agitation without material loss
- **Mechanical sieve shaker**: Creating motion to cause particles to bounce, tumble, or turn, presenting different orientations to the sieving surface
- **Sieve series**: Nested sieves with progressively smaller openings from top to bottom
- **Oven**: Capable of maintaining a uniform temperature of 110 ± 5°C (230 ± 9°F)

Project-Specific Modifications

For the research objectives, additional equipment was incorporated:

- **Collection containers**: Labeled buckets for capturing all wash water passing the No. 200 sieve.
- **Settling apparatus**: Equipment that allows fines to settle and decant the supernatant.
- **Recovery system**: For oven-drying settled fines to serve as a pan fraction in mass balance calculations.

Wet Washing Procedure: Each test was initiated with a standardized preparation:

1. **Initial drying**: Oven-dried test samples to constant mass at 110 ± 5°C, cooled samples in a dry environment, and recorded original dry mass **B** to the nearest 0.1% of sample mass (ASTM-C117 2004).

2. **Pre-washing mass verification**: Confirmed mass stability through repeated weighing until consecutive measurements differed by less than 0.1% of total sample mass.

Washing Operation: Following Procedure A requirements strictly:

1. **Sample placement**: Placed the dry sample in the washing container and added sufficient water to fully cover the material.

2. **Agitation process**: Samples are agitated "*with sufficient vigor to result in complete separation of all particles finer than the 75-µm (No. 200) sieve from the coarser particles, and to bring the fine material into suspension*" (ASTM-C117 2004).

3. **Decanting technique**: Immediately poured wash water containing suspended and dissolved solids through a nested sieve pair with the coarser sieve on top, carefully avoiding decantation of coarser sample particles.

4. **Repeated washing**: Added a second charge of water, agitated, and decanted as before, repeating the operation until the wash water ran clear (ASTM-C117 2004).

5. **Material recovery**: Returned all material retained on nested sieves by flushing back to the washed sample container.

Post-Washing Processing:

1. **Final drying**: Oven-dried washed aggregate to constant mass at 110 ± 5°C, and determined mass **C** to the nearest 0.1% of original sample mass (ASTM-C117 2004).

2. **Mass verification**: Confirmed mass stability through repeated weighing protocols.

Project-Specific Fines Recovery: To achieve complete mass closure for the before/after compaction comparisons:

1. **Wash water capture**: Collected all wash water passing the No. 200 sieve in labeled containers.

2. **Settling process**: Allowed fines to settle completely, typically requiring 24-48 hours.

3. **Supernatant removal**: Carefully decanted clear supernatant without disturbing settled fines.

4. **Fines drying**: Oven-dried settled fines to constant mass at 110 ± 5°C.

5. **Integration**: Treated dried fines as a pan fraction in subsequent calculations to maintain mass balance integrity.

Dry Sieving Procedure: Pre-Sieving Preparation:

1. **Dryness verification**: Confirmed washed samples were completely oven-dry at 110 ± 5°C before proceeding with sieving operations (ASTM-C136 2019).

2. **Sieve assembly**: Assembled sieves from largest to smallest opening, placing the sample on the top sieve of the nested arrangement.

Sieving Operations:

1. **Mechanical sieving**: Used a mechanical shaker for a sufficient period to meet the adequacy-of-sieving criterion specified in ASTM C136.

2. **Overload prevention**: Controlled per-sieve retained mass to avoid overloading, inserting intermediate sieves when necessary to maintain effective sieving action.

3. **Adequacy verification**: Ensured final sieving met the standard requirement that "*not more than 1% by mass of material retained on any individual sieve will pass that sieve during 1 min of continuous hand sieving*" (ASTM-C136 2019).

Mass Determination and Quality Control:

1. **Individual sieve weighing**: Brushed and weighed mass retained on each sieve and pan to the nearest 0.1% of the original dry mass (ASTM-C136 2019).

2. **Mass balance verification**: Verified total post-sieve mass against original pre-wash dry mass. When differences exceeded 0.3%, the results were rejected for acceptance and subjected to repeated testing (ASTM-C136 2019).

3. **Data integration**: Added mass finer than 75 µm determined by ASTM C117 to mass passing 75 µm sieve by dry sieving, using pre-wash dry mass as basis for all percentage calculations (ASTM-C136 2019).

Calculations and Data Analysis: All percentages were calculated based on initial (pre-wash) dry mass when C117 preceded C136, following the integrated approach specified in ASTM C136.

Wet Washing Calculation: When C117 results required separate reporting, the percentage finer than 75 µm was calculated using Eq. (3):

$$A = [(B - C) / B] \times 100 \qquad \text{Eq. (3)}$$

Where:

- A = percentage of material finer than 75-µm sieve by washing
- B = original dry mass of sample (g)
- C = dry mass of sample after washing (g)

Complete gradation curves and before-and-after compaction plots for each material were produced using these equations.

Before/After Compaction Analysis: Pre-test wet-sieve gradation curves for all sources are shown in Figure 2**;** the integrated methodology enabled a comprehensive evaluation of particle degradation:

1. **Baseline gradation**: Initial particle-size distribution of uncompacted materials
2. **Post-compaction gradation**: Particle-size distribution after controlled compaction loading
3. **Degradation quantification**: Direct comparison of gradation curves to identify particle breakdown
4. **Fines generation**: Specific analysis of increased material passing the 75 µm sieve

to achieve complete particle-size characterization with documented precision and accuracy.

In addition to the standard C117–C136 sequence, a limited program of “dry-only” sieve analyses was performed to evaluate the influence of the washing step on reported gradations. For one representative post-compaction specimen from each source, in both the M-Cone and Modified Proctor series, particle-size distributions were determined using the complete wet-wash procedure (ASTM C117 followed by ASTM C136/C136M) and then repeated using ASTM C136/C136M alone, without the preceding C117 wash (ASTM-C117 2004; ASTM-C136 2019). The same nominal sample was used in each pair of tests. Differences in percent passing between the dry-only and washed gradations were computed sieve by sieve to quantify the effect of the wet-wash step.

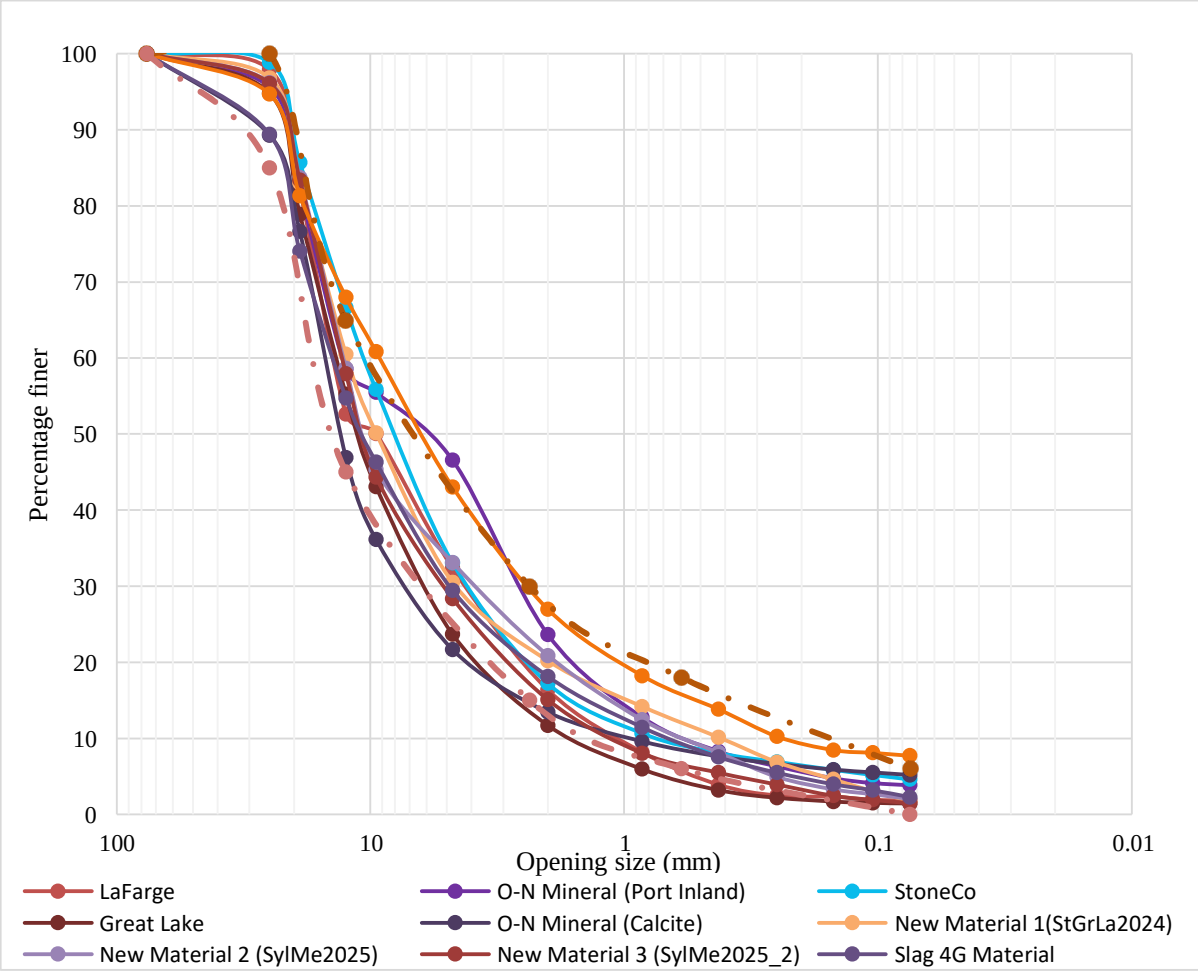


Figure 2. Wet Sieve Analysis Gradation Curves of Each OGDC Source Before Testing

Specific Gravity and Water Absorption for Fine Aggregate (ASTM C128 - Pycnometer Method):

A balance readable to 0.1 g and accurate within 0.1% of the test load; a pycnometer (e.g., 500 mL volumetric flask or jar with pycnometer top) with volume reproducible within ±0.1 cm^3 and at least 50% larger than specimen volume; a frustum cone mold and 340 g tamper for the SSD check; and an oven capable of 110 ± 5 °C (ASTM C128 2012).

Test Procedure (Gravimetric/Pycnometer)

1. Weighed 500 ± 10 g of the SSD specimen (S).

2. Partially filled the pycnometer with water, introduced the SSD specimen, filled to ~90% capacity, and agitated to eliminate air (manual rolling/inversion or gentle mechanical vibration).

3. Adjusted temperature to 23.0 ± 2.0 °C and brought the water level exactly to the calibration mark; weighed the pycnometer + specimen + water (C).

4. Removed the specimen, dried it to constant mass at 110 ± 5 °C, cooled, and weighed the oven-dry mass (A).

5. Filled the clean pycnometer with water at 23.0 ± 2.0 °C to the calibration mark and weighed (B). All masses were recorded to 0.1 g (ASTM C128 2012).

Let A = oven-dry mass (g); S = SSD mass (g); B = mass of pycnometer filled with water (g); C = mass of pycnometer with specimen and water (g).

Bulk relative density (OD) was calculated as shown in Eq. (4):

$$G_s_(OD) = A / (B + S - C) \quad \text{Eq. (4)}$$

Bulk relative density (SSD) was calculated as shown in Eq. (5):

$$G_s_(SSD) = S / (B + S - C) \quad \text{Eq. (5)}$$

Apparent relative density was calculated as shown in Eq. (6):

$$G_{s_}(app) = A \,/\, (B + A - C) \quad \text{Eq. (6)}$$

Absorption was calculated as shown in Eq. (7):

$$\text{Absorption (\%)} = 100 \times (S - A) \,/\, A \quad \text{Eq. (7)}$$

Coarse Aggregate (ASTM C127- Water-Displacement Method)

A balance accurate to 0.05% of sample mass (or 0.5 g, whichever greater) with suspension apparatus for weighing under water; a wire basket (≈ No. 6 mesh) or perforated container of adequate capacity that prevents air entrapment; a water tank for submerged weighing; sieves (4.75 mm or as needed); and an oven at 110 ± 5 °C (ASTM C127 2012).

Test Procedure

1. SSD mass in air (B): after soaking, the sample was surface-dried (rolled in absorbent cloth; wiped large particles; moving air permitted while avoiding pore drying) and weighed immediately in air to the nearest 0.5 g (or 0.05% of sample mass).

2. Submerged mass (C): the SSD sample in the basket was immersed and gently agitated to release bubbles; the apparent mass in water at 23 ± 2 °C was recorded.

3. OD mass in air (A): the sample was oven-dried to constant mass at 110 ± 5 °C, cooled (≈1–3 h), and weighed in air (ASTM C127 2012).

Let A = oven-dry mass in air (g); B = SSD mass in air (g); C = apparent mass in water (g).

Bulk relative density (OD) was calculated using Eq. (8):

$$G_{s_}(OD) = A \,/\, (B - C) \quad \text{Eq. (8)}$$

Bulk relative density (SSD) was calculated using Eq. (9):

$$G_s_(SSD) = B / (B - C) \quad \text{Eq. (9)}$$

Apparent relative density was calculated using Eq. (10):

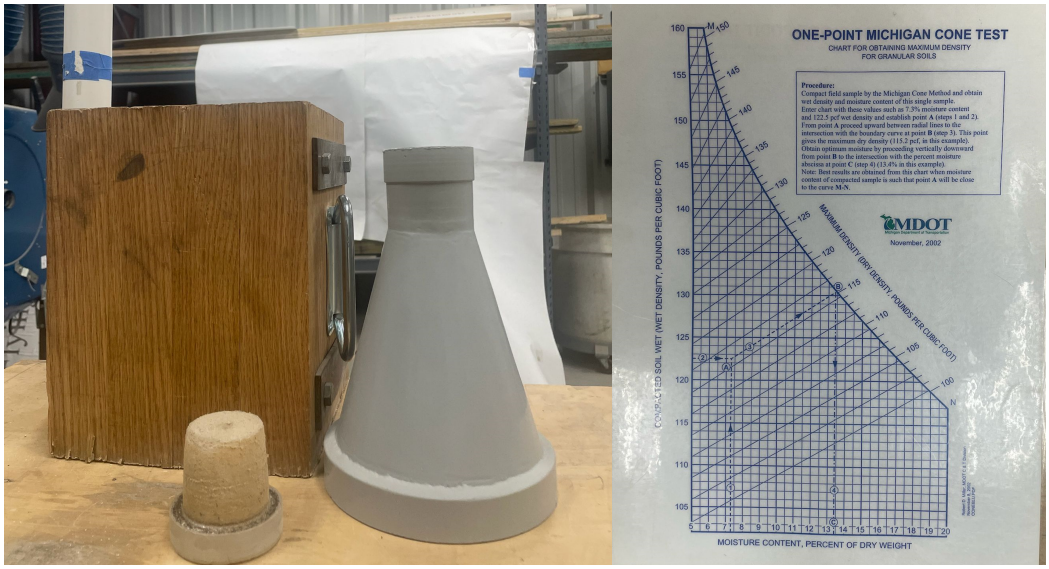
$$G_s_(app) = A / (A - C) \quad \text{Eq. (10)}$$

Absorption was calculated using Eq. (11):

$$Abs\ (\%) = 100 \times (B - A)/A \quad \text{Eq. (11)}$$

3.3.2 M-Cone Test

The apparatus included a M-Cone, an inverted, funnel-shaped mold with a solid bottom at the larger end; a hardwood pounding block with an end-grain surface to provide a stable compaction base; and a plastic stopper/straightedge for strike-off to a flush surface (Figure 3a). The balance used was readable to 1 g and used for mass determinations. Moisture content was measured using a Speedy Moisture Tester (calcium-carbide gas-pressure method). A scoop and a water bottle were used to condition the specimen's moisture. The MDOT One-Point M-Cone Chart shown in Figure 3b was applied to convert measured wet density and moisture content to maximum dry density and optimum moisture content (MDOT 2024).



(a) (b)

Figure 3. M-Cone Test (a) Apparatus Comprising Of M-Cone, Pounding Block, and Cone Stopper, (b) Chart for Interpreting Maximum Dry Density Values From M-Cone Testing

Approximately 3,500 g of material were collected from the field test location, and only particles that freely entered the cone opening were collected. The collected material retained slightly oversized gravel, capable of settling under its own weight. The moisture content was then adjusted to lie between roughly 5 percent and the expected optimum. After compaction, the final moisture content was measured using the Speedy Moisture Tester and recorded(MDOT 2024).

Test Procedure:

1. **Setup:** Placed the M-Cone upright on the hardwood block, tared the assembly if required, and confirmed stability.

2. **Compaction in Three Layers:**

    - Added soil to fill about one-third of the cone's height and compacted it by striking the cone flat against the block at least 25 times.

    - Repeated this for two-thirds height and then full height, ensuring ≥ 25 blows each layer.

- Maintained a consistent, firm vertical striking action to standardize compaction effort.

3. **Refusal and Strike-Off:** Once no further settlement occurred under the normal blows, the cone was filled, and the opening was covered by hand or with a stopper, and an additional ~10 blows were applied. Excess soil flush was then struck off with the rim using the stopper. If free water appeared, the sample was dried, and the procedure was repeated until no settlement was observed (MDOT 2024).

4. **Mass Determination:** The combined weight of the cone and the compacted soil was taken to the nearest gram and recorded.

5. **20/10 Consolidation Check:** To verify maximum consolidation, a small soil quantity was added, and 20 additional blows were applied. Then, the sample was re-struck and re-weighed. If mass increased by ≤ 10 g, consolidation was confirmed; if > 10 g, the blow/strike-off cycle was repeated until the change was ≤ 10 g (MDOT 2024).

6. **Moisture Measurement:** A representative moisture sample was obtained from the compacted soil, and its water content was measured using the Speedy Moisture Tester.

Wet soil mass was calculated by subtracting the empty cone mass from the combined mass. This mass was then converted to wet density (pcf) by dividing by the cone volume. On the One-Point M-Cone Chart, the relationship between wet density and moisture content was plotted. The chart diagonals were then followed to intersect the family of curves, and the maximum dry density (pcf) and optimum moisture content (percent) were read at the curve intersection (MDOT 2024).

The following parameters were reported in accordance with MDOT standards:

- **Test Method:** One-Point M-Cone Test
- **Maximum Density (pcf):** As read from the chart
- **Optimum Moisture Content (%):** As read from the chart

Moisture Content Determination Using the Calcium Carbide Gas Pressure Meter ("Speedy"): In the field and laboratory investigations, the calcium carbide gas pressure meter (commonly

referred to as the “Speedy” moisture tester) was employed to determine the moisture content of granular soils and processed aggregates. This method allowed for moisture readings to be obtained in under five minutes, significantly expediting the density testing workflow compared to oven-drying techniques (MDOT 2024).

The Speedy kit shown in Figure 4 consisted of a sealed pressure-gauge body, a cap assembly, a reagent scoop, two stainless-steel balls (for cohesive soils), a non-static brush, a lint-free cloth, and a precision balance. To prevent static-induced ignition, the cap was cleaned only with the provided cloth, and the meter body was cleaned only with the supplied non-conductive brush, never using any other cleaning methods. During pressure venting, the acetylene gas was directed downwind, away from the face and body, and the cap and interior body surfaces were immediately cleaned before subsequent tests (MDOT 2024).



Figure 4. Speedy Test Apparatus for In-situ Determination of Moisture Content

Sample Preparation: For all tests, samples were screened through a 6.3 mm (¼ in.) mesh to isolate the fine fraction. For gravels or processed aggregates, the material was rubbed across the screen, and the specimen was collected exclusively from the passing fraction, ensuring representative moisture results (MDOT 2024).

Test Procedure for Granular Soils:

1. Placed three level scoops of calcium carbide into the horizontal meter body.

2. Weighed a 26 g specimen, sourced from the center of the mold's middle lift, using only the screened fraction.

3. Mounted the cap and body while holding the meter horizontally, preventing premature mixing.

4. Tapped the upright meter to settle the specimen into the calcium carbide, then rotated it horizontally until the gauge needle ceased fluctuating.

5. Read the dial horizontally to the nearest 0.1 unit, then convert the wet-basis reading to oven-dry moisture content using the supplied conversion chart, interpolating to 0.1 percent.

6. Recorded moisture content in the inspection log to the nearest 0.1 percent (MDOT 2024).

This procedure enabled rapid, accurate moisture determination immediately following density tests, ensuring that moisture-sensitive compaction characteristics were adequately controlled.

M-Cone Test with Accelerometer Integration: In this study, the Michigan Department of Transportation's One-Point Cone Test procedure was adopted to evaluate granular material compaction. The standard protocol was augmented with dynamic measurements through an accelerometer. The Density Testing and Inspection Manual (MDOT 2024) was followed for all preparatory and execution steps.

Instrumentation and Accelerometer Setup: To capture the impact dynamics, the Kistler Model 8715A5000 piezoelectric accelerometer shown in Figure 5 was rigidly mounted to the base of the M-Cone. Before testing, the sensor was calibrated and connected to a Kistler LabAmp signal conditioner, which was linked to a laptop running Kistler Measurement Software. The accelerometer was sampled at 10,000 Hz, ensuring the high-resolution capture of each blow's acceleration profile. All cables were secured to prevent noise, and all system performance was validated with trial strikes on concrete before commencing soil tests.



Figure 5. Accelerometer Embedded Underneath the Base Plate of M-Cone

Test Execution and Data Recording: Each test location was prepared by leveling the surface, and then simultaneous data logging and video recording were performed. The accelerometer recorded vertical acceleration in real time, while a 4K smartphone camera, positioned adjacent to a reference pipe marked in inches, captured at 30 frames per second. This dual setup allowed frame-by-frame analysis of cone displacement. After completing each series of blows, the acceleration time-history data were exported as CSV files, and the records were backed up externally.

Energy Computation: Using the recorded acceleration $a(t)$, the instantaneous force was computed via Newton's Second Law, as shown in Eq. (12). To quantify compaction energy, total energy input was calculated as the product of force and displacement, as shown in Eq. (13):

$$F = m\,a \qquad \text{Eq. (12)}$$

$$E_{\text{total}} = F\,\Delta x, \qquad \text{Eq. (13)}$$

where Δx represents the displacement obtained through the recording of videos.

In this way, each strike energy was calculated, and then, by multiplying it by the number of strikes, the final value was obtained for each test. The acceleration was averaged at each step to calculate the effective energy across all strikes, correlating operator input consistency with the measured dry density.

Quality Assurance and Repeatability: To ensure repeatability, all tests were conducted under uniform environmental and material conditions, with two operators performing each test series. The accelerometer was recalibrated before each series, and the cone was cleaned between tests to remove fines. Post-test analysis included noise and drift checks; any trial exhibiting misalignment, excessive bounce, or spurious signals was discarded and repeated, in accordance with MDOT quality control practices.

3.3.3 Modified Proctor Compaction Test

The following equipment was utilized in accordance with AASHTO T 180 Method C specifications:

- **Compaction Mold:** A 101.6 mm (4 in.) internal-diameter cylindrical mold, equipped with a detachable collar (~50.8 mm) and base plate (AASHTO-T180 2004), was used (Figure 6).
- **Rammer:** A 4.536 ± 0.009 kg (10 lb) rammer featuring a 50.8 mm flat circular face. The rammer was designed to provide a free-fall drop of 457 ± 2 mm (18 in.) through a guide sleeve system (AASHTO-T180 2004).
- **Drying Oven:** A thermostatically controlled oven capable of maintaining temperatures of 110 ± 5°C (230 ± 9°F) for moisture content determinations was used(AASHTO-T180 2004).
- **Additional Equipment:** A hardened steel straightedge, sieves, a mixing pan, various hand tools, and a precision weighing machine were also utilized (AASHTO-T180 2004).

Sample Preparation (Method C)

Sample preparation began by gently oven-drying the field sample at temperatures not exceeding 60°C until the material became friable. Soil aggregations were carefully broken down without crushing individual particles. Subsequently, the prepared soil was sieved through

a 19.0 mm sieve, and any material retained on the sieve was discarded. For each compaction point, approximately 5 kg (12 lb) of the fraction passing the 19.0 mm sieve was selected (AASHTO-T180 2004).



Figure 6. Modified Proctor Apparatus

Compaction Procedure (Method C): A systematic five-step compaction procedure was followed:

- **Step 1 - Moisture Conditioning:** Each soil sample was thoroughly mixed with predetermined amounts of water to achieve moisture contents ranging from several points below the expected optimum to several points above. The samples were sealed and allowed to equilibrate as needed to ensure uniform moisture distribution.
- **Step 2 - Mold Assembly:** The 4-inch mold was placed on a rigid, stable base with a collar. The initial soil layer was lightly tamped to ensure it was seated correctly and to prevent fluffiness during compaction.
- **Step 3 - Layering and Compaction:** The conditioned soil was placed in five approximately equal layers within the mold. Each layer was then compacted using 25 uniformly distributed blows with a 10-lb rammer dropped from a height of 18 in. (457 mm).

- **Step 4 - Trimming and Mass Determination:** Following compaction of the fifth layer, the collar was removed, and the specimen was carefully trimmed flush with the mold top using a straightedge. The combined mass of the mold and moist soil was then measured and recorded, along with the mass of the mold alone, to calculate the compacted soil mass.
- **Step 5 - Moisture Content Determination:** The compacted specimen was extruded from the mold and sliced vertically through the center. A representative sample was then obtained from a freshly exposed face to determine the water content using the oven-dry method as specified in AASHTO T 180.

For each compaction point, the moisture content and dry density were computed using the following relationships:

Moisture Content (percent) was calculated using Eq. (14):

$$w(\%) = \frac{(A - B)}{B} \times 100 \qquad \text{Eq. (14)}$$

Where A = mass of wet soil; B = mass of dry soil.

The wet density (W_1) was calculated as the mass of the compacted soil divided by the calibrated mold volume.

Dry Density was calculated using Eq. (15)

$$W = \frac{W_1}{1 + (w/100)} \qquad \text{Eq. (15)}$$

Where W = dry density; W_1 = wet density; w = moisture content.

The dry density versus moisture content for each test series was plotted and fitted to a smooth curve through the four to five data points. From this relationship curve, the optimum moisture content (OMC) was determined to be the moisture content corresponding to the peak of the curve, and the maximum dry density (MDD) as the corresponding dry density at that moisture content (AASHTO-T180 2004).

For each test series, the following parameters were reported in accordance with AASHTO T 180:

- **Test Method:** Method C
- **Maximum Dry Density (MDD):** Reported to appropriate precision based on agency requirements
- **Optimum Moisture Content (OMC):** Reported to appropriate precision based on agency requirements
- **Rammer Face Type:** Standard 50.8 mm circular face

3.3.4 Vibratory Table Method

For the determination of maximum dry density using the vibratory table method (ASTM-D4253 2016), a comprehensive testing apparatus comprising several key components was employed. The primary component was a cylindrical mold assembly with a nominal volume of 0.500 ft^3, equipped with a guide sleeve to ensure proper containment of the specimen during testing. A base-plate and surcharge-weight system, which together applied a uniform stress of 2.0 lb/in^2 (≈13.8 kPa) to the specimen surface, was employed.

The measurement system consisted of a dial indicator with a minimum travel of 2 inches and a resolution of 0.001 inches, mounted on a stable holder to accurately monitor specimen height changes during compaction. For mass determinations, calibrated balances appropriate to the mold size and specimen mass requirements were used. Specimen preparation required a drying oven capable of maintaining 110 ± 5°C to achieve constant dry mass conditions.

The central component of the testing system was a vibrating table capable of producing a double amplitude of 0.013 ± 0.002 inches at 60 Hz (or 0.019 ± 0.003 inches at 50 Hz). Appropriate sieves for specimen selection and grading, as well as a timing device for precise control of vibration duration, were used to complement the vibrating table (Figure 7).



Figure 7. Vibratory Table Apparatus

Sample Selection and Preparation: Representative soil specimens that satisfied the Method 1 applicability criteria established in (ASTM-D4253 2016) were selected. These criteria required that specimens contain no more than 15% material passing the No. 200 sieve and that 100% of the material passes the 3-inch sieve. Additionally, the criteria required specimen masses to meet the maximum particle size, with a target mass of 34 kg for the testing procedures. Before testing, all specimens were oven-dried at 110 ± 5°C until they reached a constant mass, as specified in the standard. During the drying process, any weak particle aggregations were broken down without crushing individual particles, maintaining the soil's natural particle size distribution while eliminating moisture that could affect density measurements.

Testing Procedure (Dry Method - Method 1A): A systematic procedure outlined in ASTM D4253, Method 1A, for testing dry specimens was followed. Initially, the oven-dry specimen was thoroughly mixed to minimize segregation. Then, the material was carefully placed into the cylindrical mold using a scoop and funnel system. During filling, the mold sides were lightly tapped to settle entrapped air without causing premature densification of the specimen.

Following specimen placement, the surcharge base plate was firmly seated on the specimen surface, ensuring uniform contact with no wobbling or uneven contact that could introduce measurement errors. Then, the mold assembly was securely attached to the vibrating table, the guide sleeve was positioned, and the surcharge weight was lowered to apply the specified stress. The vibration phase constituted the critical component of the testing procedure. The specimen was vibrated for 8.00 ± 0.25 minutes at 60 ± 2 Hz (alternatively, 10.00 ± 0.25 minutes at 50 ± 2 Hz) while maintaining the calibrated double amplitude throughout. Upon completion of the vibration period, the surcharge weight and guide sleeve were removed. The base plate was then verified to have remained seated correctly.

Finally, the base plate was removed, and the mold was carefully detached from the vibrating table, with precautions taken to prevent any rim fines from falling into the compacted specimen. The mold containing the densified soil was weighed, and the dry soil mass (Ms) was computed by subtracting the previously determined mass of the empty mold. Consistent units (either SI or inch-pound) were maintained throughout the analysis. The calculation sequence involved three primary steps:

- First, the final height (H) of the specimen after densification was measured.
- Second, the specimen volume after densification was calculated using Eq. (16):

$$V = Vc - Ac \cdot H \qquad \text{Eq. (16)}$$

Where V_c represents the calibrated mold volume and A_c represents the calibrated mold cross-sectional area. This calculation accounted for the volume reduction that occurred during the densification process.

- Third, the maximum dry density for each trial was determined using Eq. (17):

$$\rho d, max = Ms / V \qquad \text{Eq. (17)}$$

Where Ms represents the dry soil mass, and V represents the calculated specimen volume after densification.

All calculations were determined using a systematic template that included spaces for recording the calibrated mold volume (V_c), calibrated mold cross-sectional area (A_c), measured height after densification (H), calculated volume (V), dry soil mass (M_s), and the resulting maximum dry density (ρd, max). This systematic approach ensured consistency and accuracy in the density determinations while facilitating quality control and verification of results(ASTM-D4253 2016).

3.3.5 OGDC Soil Compaction Using the Superpave Gyratory Compactor

For the preparation and determination of the density of OGDC soil, a comprehensive testing system centered on the Superpave Gyratory Compactor (SGC) as specified in ASTM D6925 was employed. The primary component of the testing apparatus was a Superpave gyratory compactor capable of maintaining the specified compaction pressure, angle of gyration, and rotational speed while continuously recording specimen height measurements once per gyration throughout the compaction process (ASTM-D6925 2015).

The SGC system utilized was equipped to terminate compactiont a predetermined specimen height or after reaching a specified number of gyrations, providing flexibility in testing protocols (ASTM-D6925 2015). The testing setup included steel compaction molds with matching end plates and loading ram assemblies that conformed to the geometric specifications outlined in ASTM D6925. Each mold weighed approximately 7.5 kg and was designed to withstand maximum temperatures up to 175°C during the compaction process (ASTM-D6925 2015). Supporting equipment included precision balances that met the accuracy requirements specified in the standard, along with various ancillary tools, such as paper disks for specimen preparation and trowels for material handling (Figure 8). The entire system featured integrated data-acquisition capabilities via USB for real-time monitoring and data transfer.



Figure 8. Superpave Gyratory Compactor Apparatus

Material Preparation:

Before compaction, strict thermal conditioning protocols were followed to ensure optimal specimen preparation. The aggregate components were heated to the appropriate temperatures necessary to achieve uniformity throughout the material (ASTM-D6925 2015). This heating process was critical for maintaining proper workability and ensuring representative field conditions during laboratory compaction. Both the compaction molds and end plates were preheated before specimen preparation to minimize heat loss during the transfer and compaction phases (ASTM-D6925 2015).

Mold Preparation and Compaction Procedure: The compaction procedure began with the systematic preparation of the mold assembly. A paper disk was placed in the base of the preheated mold to facilitate specimen removal and prevent adhesion to the mold surfaces (ASTM-D6925 2015). The oven-heated material was then transferred into the mold in a single lift, taking care to minimize segregation of the aggregate particles and maintain homogeneous distribution throughout the specimen volume.

Following the placement of the material, a second paper disk was positioned on the top surface of the uncompacted material to ensure uniform load distribution during compaction (ASTM-D6925 2015). The prepared mold assembly was then installed in the SGC, and the specified

compaction parameters outlined in the testing protocol were applied. During the compaction phase, continuous monitoring of the process was maintained through SGC's integrated data acquisition system. The compactor applied the predetermined compaction pressure (600 kPa), maintained the specified angle of gyration (1.16° internal angle), and operated at the standard speed of 30 gyrations per minute (ASTM-D6925 2015). Throughout this process, the system recorded specimen height measurements at each gyration. Specimens were compacted to the required number of gyrations (100, 300, and 500) as specified by the specific testing objectives.

Upon completion of the compaction cycle, specimens were allowed to cool sufficiently within the mold to prevent distortion during handling (ASTM-D6925 2015). The cooling period was critical for maintaining specimen integrity and ensuring accurate density measurements. Once adequately cooled, the specimens were extruded using the built-in specimen extruder and then cooled to room temperature on a flat, stable surface (ASTM-D6925 2015). Throughout the entire process, the recorded height-versus-gyration data were saved and printed for subsequent density calculations and volumetric analysis. Using comprehensive height data recorded by the SGC system, specimen densities were calculated at various compaction levels throughout the compaction process. The fundamental calculation involved determining the specimen volume at any given gyration level using the recorded height measurements and the known mold cross-sectional area.

For density calculations at the final gyration level, the relationship employed is provided in Eq. (18):

$$\rho = Ms / V \qquad \text{Eq. (18)}$$

Where ρ represents the specimen density, M_s represents the total mass of the compacted material, and V represents the specimen volume calculated from the final recorded height (h_{final}) and the mold's cross-sectional area.

The specimen volume was determined using Eq. (19):

$$V = A \times hfinal \qquad \text{Eq. (19)}$$

Where A represents the calibrated cross-sectional area of the compaction mold, and h_{final} represents the specimen height recorded after compaction. Density values at selected gyration levels were reported as required by the governing specification or project-specific testing plan.

3.3.6 In-Place Density and Water Content Measurement by Nuclear Gauge

Nuclear gauge testing methods were employed to determine in-place density and moisture content of soil and soil-aggregate materials in accordance with ASTM D6938. This methodology describes the procedures followed for measuring in-place density and moisture using nuclear equipment, specifically the Troxler 3440 nuclear density gauge. The density measurements were obtained using direct transmission methods, while the moisture content measurements were obtained in backscatter mode, regardless of the density measurement mode employed (ASTM-D6938 2017).

The following equipment was utilized for the study's nuclear gauge testing program:

- The Troxler 3440 nuclear density gauge with its unique standard block and gauge book (Figure 9)
- Hammer for driving the probe pin
- Drive rod and template for hole preparation
- Reference standard block for daily calibration checks
- Site preparation tools, including straightedge and leveling devices



Figure 9. Troxler 3440 Nuclear Density Gauge Setup

Safety Protocols: Strict safety protocols were followed throughout the testing program, adhering to the ALARA (As Low As Reasonably Achievable) principle by minimizing exposure time, maintaining a safe distance from the source, and using appropriate shielding. The gauge was transported in its padded box, in accordance with proper lockdown procedures, and a safe distance was maintained between untrained personnel and the testing area. All radioactive sources were kept at least 9 m (30 ft) away from the gauge during operation to prevent interference with measurements (ASTM-D6938 2017).

Daily Standardization Procedures: Standardization procedures were performed daily at the beginning of each testing day to correct for the long-term aging effects of radioactive sources and ensure measurement accuracy (ASTM-D6938 2017). The standard block was placed on sound earth, at least 10 ft from large objects or standing water, and the gauge was seated with the scalar end toward the block's metal end plate.

Standard count measurements lasting 240 seconds were conducted, and the resulting moisture and density standard counts were compared to the acceptable ranges specified in the gauge book. The moisture standard ranges remained valid for 1 year, while the density ranges varied monthly due to the radioactive source's half-life. When standardization counts fell outside acceptable limits, the equipment was repositioned, and the procedure was repeated. If persistent issues requiring contact with authorized personnel for gauge evaluation were present, the procedure for addressing the issue was followed in accordance with the guidance of authorized personnel. Standardization counts were evaluated daily using the criteria established in ASTM D6938. For density measurements, standardization counts were verified to have fallen within ±1% of the average of the four preceding standardization counts. For moisture measurements, the procedure requires standardized counts to fall within ±2% of the preceding average (ASTM-D6938 2017). When these initial criteria were not met, the exponential decay equations were applied, accounting for the source half-life, to determine acceptable ranges.

Selected test locations using visual inspection techniques, focusing on areas that were likely to exhibit the least compaction, in accordance with the spot-check philosophy. Test locations were positioned at least 600 mm (24.0 in.) away from any objects that could potentially modify the gauge response (ASTM-D6938 2017). Each test site was prepared by removing all loose and disturbed material to expose the true surface of the material being tested. The test area was graded and scraped to achieve a smooth surface that maximized contact between the gauge and the material. The depth of the maximum voids beneath the gauge was verified not to exceed 3 mm (1/8 in.) for each test, and any voids were filled with native material that did not contain gravel (ASTM-D6938 2017).

Access holes were prepared using the template, hammer, and drive rod system. The holes were driven perpendicular to the prepared surface to depths of 2, 4, 6, or 8 inches as required by the testing program. The grooves were aligned carefully, noting that when the 8-inch groove was flush with the template handle, the actual penetration was approximately 2 inches deeper, allowing disturbed material to fall clear. During hole preparation, one foot was maintained on the template while driving and extracting the rod by twisting straight out without wiggling to prevent hole distortion. Three sides around the template were scribed before removal to ensure proper gauge positioning.

The gauge was then positioned within the scribed lines, and the source rod was inserted to the designated test depth, ensuring the trigger was appropriately seated in the notch. The left side of the gauge was hand-tapped to seat the body tightly against the borehole, ensuring firm, gap-free contact between the probe and the borehole wall along the source-to-detector gamma path(ASTM-D6938 2017). Each test was initiated by pressing Start/Enter to begin the one-minute count period, then the user stepped back 8-10 steps during the measurement to minimize radiation exposure. The direct transmission method provided density measurements that averaged the bottom of the probe to the gauge surface (ASTM-D6938 2017).

Data Recording and Analysis: The following parameters were recorded for each test:

- D = dry density (pcf)
- WD = wet density (pcf)
- M = water content (pcf) and %M = moisture percentage
- DC = density count and MC = moisture count (accessed via Shift → 1)

Representative samples were obtained from each test area to determine Maximum Dry Density (MDD) using approved laboratory methods from the Proctor family or approved field-laboratory procedures. The MDD values were entered into the gauge memory system, and the percent compaction was calculated using the relationship:

%PR (percent compaction) = (In-place Dry Density / Maximum Dry Density) × 100

Data Management and Reporting: Comprehensive field records were maintained, including test numbers, location coordinates, visual material descriptions, lift numbers or elevations, operator identification, gauge specifications, test modes and depths, standardization data, and any applied corrections (ASTM-D6938 2017). All measurements were recorded to appropriate significant figures: wet and dry density to the nearest 1 kg/m³ (0.1 pcf) and water content to the nearest 0.1%. In MDOT construction practice, the nuclear density gauge is used as a point test applied at a prescribed minimum frequency across each lift. For granular foundation layers, including subbase and aggregate base, the Density Testing and Inspection Manual specifies that in-place density be verified by nuclear gauge at minimum frequencies on the order of one test per 500 ft of project length for a 24-ft-wide section, with additional tests required where

results are borderline or where construction conditions suggest nonuniform compaction (MDOT 2024).

4 RESULTS

4.1 Specific Gravity and Water Absorption

Specific gravity and water absorption (%Abs) were measured for each source in accordance with ASTM C127/C128 and are summarized in Table 3. These properties provided context for the density outcomes and moisture requirements.

Table 3. Summary of Specific Gravity and Water Absorption Test Results

	Retain on Sieve No. 4				Pass sieve No. 4			
Source	**Specific gravity (OD)**	**Specific gravity (SSD)**	**Apparent specific gravity**	**Absorption (%)**	**Specific gravity (OD)**	**Specific gravity (SSD)**	**Apparent specific gravity**	**Absorption (%)**
Lafarge	2.75	2.78	2.83	1.0	2.81	2.85	2.92	1.40
Port Inland	2.62	2.65	2.71	1.2	2.68	2.74	2.86	2.26
Great Lake	2.53	2.61	2.76	3.3	2.64	2.74	2.93	3.76
Stone Co	2.56	2.64	2.78	3.1	2.64	2.75	2.97	4.16
Calcite	2.51	2.55	2.63	1.8	2.55	2.66	2.87	4.34

Source	Retain on Sieve No. 4				Pass sieve No. 4			
	Specific gravity (OD)	Specific gravity (SSD)	Apparent specific gravity	Absorption (%)	Specific gravity (OD)	Specific gravity (SSD)	Apparent specific gravity	Absorption (%)
StGlLa	2.52	2.60	2.72	2.8	2.79	2.88	3.06	3.16
Syl_2025	2.52	2.61	2.76	3.4	2.85	2.89	2.98	1.50
Syl_2025_2	2.53	2.61	2.75	3.2	2.73	2.79	2.91	2.35
Slag	2.30	2.38	2.48	3.2	2.45	2.56	2.73	4.14
I-275	2.51	2.60	2.75	3.5	2.77	2.81	2.87	1.22

4.2 Density Results

4.2.1 M-Cone

The Brief overview table with details about M-Cone Testing - sources, number of operators, replicates, and any other details for quick reference is shown in Table 4. M-Cone test results were used to derive the maximum dry density (MDD) using the MDOT one-point cone procedure and chart referenced in Table 5. The method was used to obtain MDD for the OGDC material from each source considered in this study. Densities were reported as MDD (g/cm^3), rounded to two decimal places; the optimum moisture content (OMC) was reported as a percentage.

Table 4. Details of M-Cone Testing

Sno.	Sources	Operators	Total Replicates	Remarks
1	Lafarge	2	6	Accelerometer was used on all of these tests
2	Port Inland	2	6	Accelerometer was used on all of these tests
3	Great Lake	2	7	Additional test was conducted based on the input from the project technical panel
4	Stone Co	2	6	Accelerometer was used on all of these tests
5	Calcite	2	6	Accelerometer was used on all of these tests
6	StGrLa	1	3	No accelerometer used on all of these tests
7	SylMe2025	1	6	Additional test was conducted based on the input from the project technical panel
8	SylMe2025_2	1	3	No accelerometer used on all of these tests
9	Slag	1	3	No accelerometer used on all of these tests
10	I-275	1	3	No accelerometer used on all of these tests

Two operators conducted M-Cone tests on five aggregate sources using the instrumented setup that included an accelerometer to record impact energy. A single operator tested the remaining materials without the accelerometer. For each source, specimens were compacted in accordance with the M-Cone test procedure, and the resulting dry densities and moisture content were converted to MDD and OMC using the M-Cone one-point chart.

Across all materials, MDD ranged from 1.81 to 2.41 g/cm³, with a mean of 2.20 g/cm³ and a standard deviation of 0.151 g/cm³. Table 5 summarizes cone-derived densities by source. For the five sources tested by both operators with the accelerometer, both a two-way ANOVA and a T-test indicated no meaningful operator effect on cone-derived density/MDD. The main effect of the operator was not significant, and the interaction between the operator and source was also not significant.

The Statistical Maximum, Minimum, Average, and Standard Deviation from the One-Point M-Cone Tests were determined and summarized in Table 6. Relative to laboratory references, M-Cone MDD values were compared with those from other methods in Table 14.

Table 5. M-Cone Test Results from Various Sources

Testing Date	Source/Operator	Set	MDD (pcf)	MDD (g/cm^3)	Actual Moisture Content in the Field (%)	OMC (%)
11/20/2024	Lafarge [1]	1	145.5	2.33	5.2	6.4
11/21/2024		2	145.2	2.33	5.6	6.4
11/22/2024		3	144	2.31	5.4	6.6
11/20/2024	Lafarge [2]	1	143.9	2.31	5.8	6.6
11/21/2024		2	143.3	2.30	5.2	6.7
11/22/2024		3	145.3	2.33	5.8	6.4
11/27/2024	Port Inland [1]	1	136.7	2.19	5.2	7.8
12/3/2024		2	135.9	2.18	5.1	7.9

Testing Date	Source/Operator	Set	MDD (pcf)	MDD (g/cm³)	Actual Moisture Content in the Field (%)	OMC (%)
12/5/2024		3	137.5	2.20	5.1	7.6
11/27/2024		1	140.1	2.24	5.6	7.2
12/3/2024	Port Inland [2]	2	132.9	2.13	5.2	8.6
12/5/2024		3	133.7	2.14	5.2	8.4
12/6/2024		1	137	2.19	5.4	7.7
12/10/2024	Great Lake [1]	2	134	2.15	5.2	8.3
12/11/2024		3	136.4	2.18	5.5	7.8
12/6/2024	Great Lake [2]	1	136.6	2.19	5.2	7.8
12/10/2024		2	137	2.19	5.2	7.7

Testing Date	Source/Operator	Set	MDD (pcf)	MDD (g/cm³)	Actual Moisture Content in the Field (%)	OMC (%)
12/11/2024		3	136.6	2.19	5.4	7.8
7/18/2025		4	136.7	2.19	5.6	7.8
12/11/2024		1	148.3	2.38	5.1	6.1
12/11/2024	Stone Co [1]	2	146	2.34	5.4	6.2
12/12/2024		3	145.5	2.33	5.1	6.4
12/11/2024		1	148.2	2.37	5.3	6.1
12/11/2024	Stone Co [2]	2	149.5	2.39	5.2	5.9
12/12/2024		3	150.2	2.41	5.1	5.9
11/25/2025		4	146.8	2.35	5.2	6.2

Testing Date	Source/Operator	Set	MDD (pcf)	MDD (g/cm³)	Actual Moisture Content in the Field (%)	OMC (%)
12/12/2024	Calcite [1]	1	145.6	2.33	5.5	6.4
12/13/2024		2	148.7	2.38	5.1	6
12/13/2024		3	149.9	2.40	5.6	5.9
12/12/2024	Calcite [2]	1	150.3	2.41	5.1	5.9
12/13/2024		2	147.1	2.36	5.4	6.2
12/13/2024		3	150.4	2.41	5.2	5.9
11/25/2025		4	147.4	2.36	5.1	6.2
5/7/2025	StGrLa [2]	1	136.1	2.18	5.5	7.9
5/7/2025		2	136.7	2.19	5.4	7.8

Testing Date	Source/Operator	Set	MDD (pcf)	MDD (g/cm³)	Actual Moisture Content in the Field (%)	OMC (%)
5/7/2025		3	137.1	2.20	5.2	7.7
5/9/2025		1	127.8	2.05	6.0	9.7
5/9/2025		2	128.2	2.05	5.8	9.6
5/9/2025	SylMe2025	3	129.5	2.07	5.4	9.3
5/23/2025	[2]	4	129.5	2.07	6.2	9.3
6/17/2025		5	130.3	2.09	7.9	9.1
7/18/2025		6	131.4	2.10	6.3	8.9
5/12/2025	SylMe2025_2	1	122.2	1.96	7.1	11.2
5/12/2025	[2]	2	121.2	1.94	6.7	11.5

Testing Date	Source/Operator	Set	MDD (pcf)	MDD (g/cm³)	Actual Moisture Content in the Field (%)	OMC (%)
5/12/2025		3	125.5	2.01	5.8	10.3
6/10/2025		1	113	1.81	5.1	13.9
6/10/2025	Slag [2]	2	117	1.87	7.6	12.8
6/10/2025		3	118	1.89	7.7	12.5
7/11/2025		1	136.7	2.19	5.9	7.8
7/11/2025	I - 275 [2]	2	136.1	2.18	5.8	7.9
7/11/2025		3	136.4	2.18	5.2	7.8

[1] Operator 1

[2] Operator 2

Table 6. Summary of Statistical Results from One-Point M-Cone Test

Units	Max MDD	Min MDD	Mean	Standard Deviation
pcf	150.4	113	137.4	9.509
g/cm^3	2.41	1.81	2.20	0.151

4.2.2 Modified Proctor

Modified Proctor compaction tests were performed in accordance with the AASHTO procedure (AASHTO T 180, Method C). Densities were reported as MDD (g/cm³), rounded to two decimal places; the optimum moisture content (OMC) was reported as a percentage. For each material, compaction curves were developed over a range of moisture contents to identify the maximum dry density (MDD) and corresponding optimum moisture content (OMC).

Specimens were prepared and compacted according to Method C using the specified hammer, drop height, and number of layers. For each source, at least four moisture levels were tested to characterize the whole shape of the compaction curve, recognizing that some materials may exhibit secondary peaks. For some sources, a fifth moisture level was added to improve curve resolution because four points were insufficient to clearly define the peak. A single operator performed all tests. Across all materials, the resulting MDD values spanned from 1.91 to 2.41 g/cm³, with a mean of 2.17 and a standard deviation of 0.122 g/cm³. Table 7 summarizes modified proctor densities by source. The Modified Proctor test's statistical results, including Maximum MDD, Minimum MDD, average MDD, and the standard deviation, were summarized in Table 8. Relative to laboratory references, the modified proctor MDD values were compared with those of other methods in Table 14.

Table 7. Modified Proctor Test Results from Various Sources

Testing Date	Source	Set	MDD (pcf)	MDD (g/cm³)	OMC (%)
9/28/2024		1	150.5	2.41	5.1
9/28/2024	Lafarge	2	144.2	2.31	4.5
9/28/2024		3	148.3	2.38	5.3
9/30/2024		1	139.5	2.23	5.2
9/30/2024	Port Inland	2	139.3	2.23	5.9
9/30/2024		3	137.3	2.20	5.9
10/2/2024		1	139.7	2.24	8.2
10/2/2024	Great Lake	2	141.5	2.27	8.5

Testing Date	Source	Set	MDD (pcf)	MDD (g/cm³)	OMC (%)
10/2/2024		3	140.7	2.25	8.3
10/4/2024		1	135.7	2.17	9
10/4/2024		2	134.7	2.16	8.5
10/4/2024	Stone Co	3	136.8	2.19	8.4
17/7/2025		4	138.0	2.21	8.5
10/7/2024		1	139.4	2.23	7.4
10/7/2024		2	138.8	2.22	7.8
10/7/2024	Calcite	3	137.9	2.21	7.8
17/7/2025		4	140.0	2.24	7.7

Testing Date	Source	Set	MDD (pcf)	MDD (g/cm³)	OMC (%)
5/13/2025		1	139.0	2.23	9.4
5/13/2025	StGrLa	2	138.4	2.22	9.1
5/13/2025		3	139.2	2.23	8.4
5/14/2025		1	130.0	2.08	10.3
5/14/2025	SylMe2025	2	132.1	2.12	10.6
5/14/2025		3	131.2	2.10	10.2
5/15/2025		1	126.0	2.02	8.7
5/15/2025	SylMe2025_2	2	125.9	2.02	9.6
5/15/2025		3	125.5	2.01	10.5

Testing Date	Source	Set	MDD (pcf)	MDD (g/cm³)	OMC (%)
6/13/2025		1	119.2	1.91	9.4
6/13/2025	Slag	2	119.5	1.91	10.6
6/13/2025		3	120.0	1.92	10
7/15/2025		1	138.0	2.21	7.8
7/15/2025	I - 275	2	139.0	2.23	8.6
7/15/2025		3	138.7	2.22	8.4

Table 8. Summary of Statistical Results from Modified Proctor Test

Units	Max MDD	Min MDD	Mean MDD	Standard Deviation
pcf	150.5	119.2	135.748	7.627
g/cm³	2.41	1.91	2.174	0.122

4.2.3 Gyratory

Gyratory compaction was performed according to the ASTM procedure (ASTM D6925). Densities were reported as average dry density (ADD) (g/cm³), rounded to two decimal places. For each material, specimens were compacted to target gyration counts of 100, 300, and 500 under the specified normal pressure, internal angle, and rotation rate. Height versus gyration data was recorded. Final dry density was calculated from the mass-to-volume ratio. For sources tested at all three gyration levels, the final ADD was taken as the mean of the three specimens compacted to 500 gyrations, which produced the highest densities.

For each source, specimens were compacted at a normal pressure of 603 kPa, an internal angle of 1.16°, and a standard mold configuration. The targets were N = 100, 300, and 500 gyrations. The initial moisture condition was oven dry. Across all materials, the final ADD at 500 gyrations ranged from 1.84 g/cm³ to 2.29 g/cm³, with a mean of 2.12 g/cm³ and a standard deviation of 0.13 g/cm³. The summary table by source was provided in Table 9. The Gyratory method's statistical results, including Maximum MDD, Minimum MDD, average MDD, and the standard deviation, were summarized in Table 10. The gyratory test ADD values were compared with those of other methods in Table 14.

Table 9. Gyratory Test Results from Various Sources

Testing Date	Source/Operator	Set	ADD (pcf)	ADD (g/cm³)
9/17/2024		1	139.2	2.23
9/17/2024	Lafarge	2	142.3	2.28
9/17/2024		3	143.0	2.29
9/17/2024		1	132.9	2.13
9/17/2024	Port Inland	2	131.9	2.11
9/17/2024		3	133.2	2.13
9/17/2024	Great	1	133.5	2.14
9/17/2024	Lake	2	135.1	2.16

Testing Date	Source/Operator	Set	ADD (pcf)	ADD (g/cm³)
9/17/2024		3	134.9	2.16
9/17/2024		1	142.7	2.29
9/17/2024	Stone Co	2	140.2	2.25
9/17/2024		3	142.3	2.28
9/26/2024		1	121.6	1.95
9/26/2024	Calcite	2	121.0	1.94
9/26/2024		3	123.8	1.98
7/8/2025	StGrLa	1	132.7	2.13
7/8/2025	SylMe2025	1	126.5	2.03

Testing Date	Source/Operator	Set	ADD (pcf)	ADD (g/cm³)
7/8/2025	SylMe2025_2	1	120.3	1.93
7/8/2025	Slag	1	114.9	1.84
7/20/2025	I – 275	1	133.7	2.14

Table 10. Summary of Statistical Results from Gyratory Compaction Test

Units	Max MDD	Min MDD	Mean	Standard Deviation
pcf	143.0	114.9	132.3	8.4
g/cm³	2.29	1.84	2.12	0.13

4.2.4 Vibratory

Vibratory Table tests were performed according to the ASTM procedure (ASTM D4253). Densities were reported as average dry density (ADD) (g/cm³), rounded to two decimal places. Specimens for each source were placed in the mold according to D4253, with the specified surcharge, vibratory frequency, and duration. Material handling steps (filling method, leveling, and surcharge seating) were followed as per the ASTM procedure. For each source, three replicates were performed with surcharge; a single operator conducted all tests for five sources. These Vibratory Table test results are displayed in Table 11. Across all materials, the vibratory table ADD ranged from 1.94 g/cm³ to 2.48 g/cm³, with a mean of 2.23 g/cm³ and a standard deviation of 0.16 g/cm³. Summary of statistical results are given in Table 12.

As expected for a vibration-based densification, both M-Cone and Modified Proctor results exceeded vibratory table densities. Consistent with D4253, testing was performed under near-dry conditions; any residual moisture was assumed to be negligible. No systematic relationship between minor moisture variations and ADD was detected, in line with the standard's emphasis on dry density. The vibratory table test ADD values were compared with those of other methods in Table 14.

Table 11. Vibratory Table Test Results from Various Sources.

Testing Date	Source / Operator	Set	ADD (pcf)	ADD (g/cm³)
9/10/2024		1	143.6	2.30
9/10/2024	Lafarge	2	146.7	2.35
9/10/2024		3	139.8	2.24
9/10/2024		1	126.7	2.03
9/10/2024	Port Inland	2	121.1	1.94
9/10/2024		3	136.7	2.19
9/20/2024	Great Lake	1	121.1	1.94
9/20/2024		2	139.2	2.23

Testing Date	Source / Operator	Set	ADD (pcf)	ADD (g/cm³)
9/20/2024		3	146.7	2.35
9/20/2024		1	141.7	2.27
9/20/2024	Stone Co	2	149.2	2.39
9/20/2024		3	136.1	2.18
9/20/2024		1	154.8	2.48
9/20/2024	Calcite	2	146.7	2.35
9/20/2024		3	139.2	2.23

Table 12. Summary of Statistical Results from Vibratory Table Test

Units	Max MDD	Min MDD	Mean	Standard Deviation
pcf	154.8	121.1	139.3	9.9
g/cm^3	2.48	1.94	2.23	0.16

4.2.5 Nuclear Gauge

Nuclear gauge measurements were performed as per the ASTM procedure (ASTM D6938). Field readings were recorded as wet density and moisture, from which dry density was computed; densities were reported in g/cm³ (two decimals) and humidity in percent. Field points were taken on compacted lifts prepared from a single source in accordance with the project's standard placement and compaction sequence. For each location, the gauge was seated on a prepared test spot with surface correction as required, and repeat counts were obtained. Where feasible, companion material samples were collected to verify moisture content. Locations, lift IDs, and project details were summarized in Table 13.

Compared to Modified Proctor MDD (138.5 pcf), field dry densities averaged 96.86% ± 0.56% of MDD, with a mean (field − MDD) of − 0.070 g/cm³, standard deviation (SD) 0.012 g/cm³; n = 2). Relative to M-Cone MDD (136.4 pcf), the mean bias was −0.036 g/cm³ (SD 0.012 g/cm³), corresponding to 98.35% ± 0.57% of MDD**.**

Table 13. Summary of Nuclear Gauge Information and Test Results

DATE	CONTROL SECTION ID	JOB NUMBER	ROUTE NUMBER or STREET	GAUGE NUMBER
07/03/2025	82162	208481	M-14	60374

TEST			DETERMINATION OF IN-PLACE DENSITY								LOCATION OF TEST				
ORIGINAL	RECHECK	TEST DEPTH inch	COUNTS (MC)	COUNTS (DC)	DRY DENSITY PCF	WET DENSITY PCF	MOISTURE PCF	MOISTURE %	MAX DENSITY PCF	PERCENT OF COMPACTION	STATION	DISTANCE FROM ft		DEPTH BELOW PLAN GRADE ft	ITEM OF WORK
												LEFT	RIGHT		
1	2	3	4	5	6	7	8	9	10	11	12	13	14	15	16
1		8	98	1019	133.6	141.3	7.7	5.8	137.5	97.1	67+70		1	0.8	OGDC
2		8	93	1003	134.7	141.9	7.3	5.4	137.5	97.9	71+80		14	0.8	OGDC

Table 14. Dry Density Results for Four Laboratory Compaction Methods

	Avg MDD (pcf)		Avg DD (pcf)	
Source/Operator	**M-Cone**	**Modified Proctor**	**Vibratory Table**	**Gyratory Compaction**
Lafarge [2]	144.2	147.6	143.4	141.5
Lafarge [1]	144.9	-	-	-
Port Inland [2]	135.5	138.7	128.2	132.7
Port Inland [1]	136.7	-	-	-
Great Lake [2]	136.7	140.6	135.7	134.5
Great Lake [1]	135.8	-	-	-
Stone Co [2]	149.3	135.7	142.3	141.7
Stone Co [1]	146.6	-	-	-
Calcite [2]	149.3	138.7	146.9	122.1
Calcite [1]	148	-	-	-

	Avg MDD (pcf)		Avg DD (pcf)	
Source/Operator	**M-Cone**	**Modified Proctor**	**Vibratory Table**	**Gyratory Compaction**
StGrLa2024 [2]	136.6	138.9	-	132.7
SylMe2025 [2]	129.1	131.1	-	126.5
SylMe2025_2 [2]	123	125.8	-	120.3
Slag [2]	116	119.6	-	114.9
I-275 [2]	136.4	138.6	-	133.7

[1] Operator 1

[2] Operator 2

4.3 Sieve Analysis

Sieve analyses were performed as described in the procedure (Procedure A: water wash). Percent passing was reported to the nearest 0.1% for fine sieves; cumulative percent-passing curves were plotted on semi-log axes. For all materials, pre-compaction and post-compaction sampling were used to summarize changes in percent passing and assess crushing and fines generation. For each source, washed gradations were obtained after oven drying, washing through the No. 200 sieve, oven drying the retained fractions, and recovering settled fines from the wash buckets (counted as pan material). Specification conformance to the project OGDC 4G envelope was evaluated for each source.

Aggregate gradations generally met the OGDC 4G specification band; six sources were entirely within the envelope (Figure 10). Box plots of the change in percentage passing between before and after the test indicated particle degradation and the generation of fines. For each material, the difference in percent passing between post-compaction and pre-compaction conditions was computed. All replicates were included in the distributions. To quantify the influence of the wet-wash step itself, paired “dry-only” and washed gradations were obtained for one representative specimen from each source in the M-Cone and Modified Proctor test series. In these supplementary tests, the dry-only gradations were determined using ASTM C136/C136M without the preceding ASTM C117 wash, while the washed gradations followed the full C117–C136 sequence as per the ASTM procedure (ASTM-C117 2004; ASTM-C136 2019). Table 15 summarizes these differences by sieve and source for one set. These comparisons document how much of the reported gradation, particularly in the fraction finer than the 75-µm (No. 200) sieve, reflects the wet-wash procedure required by ASTM C117 rather than dry sieving alone.

Table 15. Comparison of Dry and Wet Percent Passing No. 200 for Representative Specimens by Source and Method

Source	Method	% passing No. 200 (wet)	% passing No. 200 (dry)	ΔP (dry − wet)
Lafarge	M-Cone	0.71	0.85	0.14
Port Inland	M-Cone	0.19	1.20	1.01
Great Lake	M-Cone	0.51	1.34	0.83
Stone Co	M-Cone	0.37	1.11	0.74
Calcite	M-Cone	0.40	1.01	0.60
StGrLa2024	M-Cone	0.19	0.79	0.60
SylMe2025	M-Cone	0.10	0.80	0.70

Source	Method	% passing No. 200 (wet)	% passing No. 200 (dry)	ΔP (dry − wet)
SylMe2025_2	M-Cone	0.35	0.85	0.50
Slag	M-Cone	0.16	1.37	1.21
I-275	M-Cone	0.40	1.81	1.42
Lafarge	Modified Proctor	0.05	0.36	0.31
Port Inland	Modified Proctor	0.16	0.38	0.23
Great Lake	Modified Proctor	0.19	0.59	0.40
Stone Co	Modified Proctor	0.23	0.59	0.37
Calcite	Modified Proctor	0.35	0.72	0.38

Source	Method	% passing No. 200 (wet)	% passing No. 200 (dry)	ΔP (dry − wet)
StGrLa2024	Modified Proctor	0.22	0.28	0.06
SylMe2025	Modified Proctor	0.35	0.70	0.35
SylMe2025_2	Modified Proctor	0.25	0.47	0.22
Slag	Modified Proctor	0.29	0.39	0.11
I-275	Modified Proctor	0.43	0.51	0.08

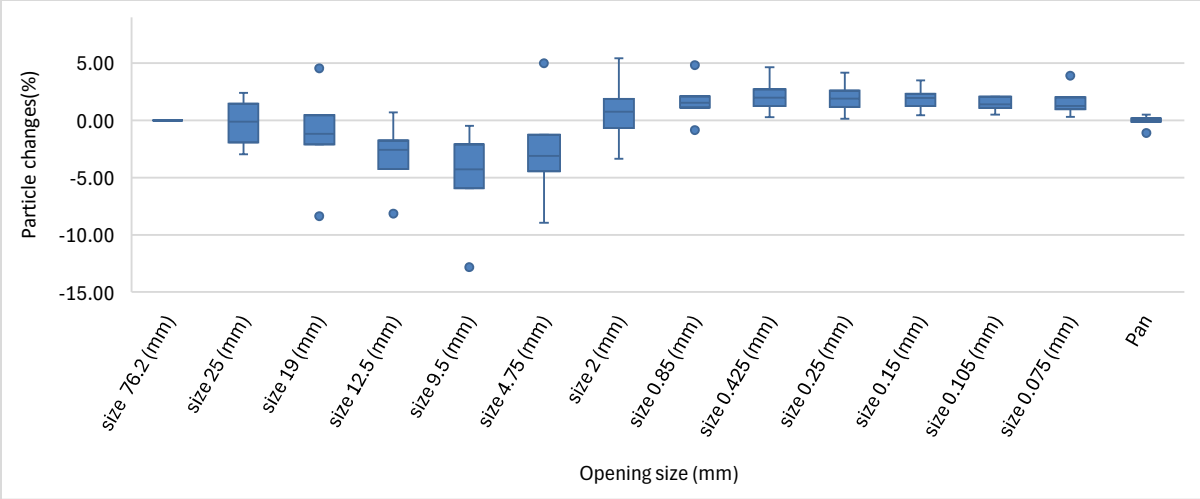


Figure 10. Box Plot of the Percentage Difference in Wet Sieve Analysis Results Between the After-Compaction and Before-Compaction Tests using M-Cone Test for All Sources

4.4 Energy Values

Impact energy during M-Cone compaction was quantified using the instrumented setup (accelerometer mounted to the bottom of the cone). Energy per blow, E (J), was calculated from the measured acceleration time histories using the work–energy integration method; the total input energy per test, E_{total} (J), was the sum of all valid blows. Statistical comparisons used $\alpha = 0.05$. Two operators performed instrumented cone tests on five sources; the remaining materials were tested without instrumentation. For the instrumented set, E was recorded for each validated blow, with quality control on saturation, clipping, timing gaps, and the 20/10 rule consolidation criterion.

Across instrumented trials, E_{total} per specimen ranged from 34.75080354×10^{6}J to 12.63652103×10^{6} J. Tables 16 summarize total energy by source and operator. For the five sources tested by both operators with instrumentation, a two-way ANOVA and a T-test (factors: source and operator) on E_{total} showed no significant effect of the operator, and the interaction between the operator and source was also not significant.

Table 16. Impact Energy and Compaction Results from Various Sources

Source	Testing Date	Set Num.	Operator	Total Energy Before the 20/10 Rule (J)	Total Energy After the 20/10 Rule (J)	Maximum Density(g/cm^3)
Lafarge	11/20/2024	Set 1	Operator 1	15.22087518×10^6	24.32893495×10^6	2.33
			Operator 2	12.59021211×10^6	19.22237559×10^6	2.31
	11/21/2024	Set 2	Operator 1	16.96048403×10^6	23.72052662×10^6	2.33
			Operator 2	12.13862555×10^6	17.5204277×10^6	2.30
	11/22/2024	Set 3	Operator 1	11.67267499×10^6	17.59308973×10^6	2.31
			Operator 2	13.98739856×10^6	24.69837945×10^6	2.33
Port Inland	11/27/2024	Set 1	Operator 1	14.49337786×10^6	24.74645026×10^6	2.19
			Operator 2	16.76756395×10^6	25.64573075×10^6	2.24

Source	Testing Date	Set Num.	Operator	Total Energy Before the 20/10 Rule (J)	Total Energy After the 20/10 Rule (J)	Maximum Density(g/cm³)
Great lake	12/3/2024	Set 2	Operator 1	17.30395025×10^{6}	23.46003448×10^{6}	2.18
			Operator 2	11.62196546×10^{6}	17.00124327×10^{6}	2.13
	12/5/2024	Set 3	Operator 1	12.06001145×10^{6}	23.86893851×10^{6}	2.20
			Operator 2	15.15724467×10^{6}	19.17371088×10^{6}	2.14
	12/6/2024	Set 1	Operator 1	20.53342205×10^{6}	28.96126622×10^{6}	2.19
			Operator 2	12.45728911×10^{6}	17.54311567×10^{6}	2.19
	12/10/2024	Set 2	Operator 1	95.69255062×10^{6}	12.63652103×10^{6}	2.15
			Operator 2	19.00085352×10^{6}	28.9942256×10^{6}	2.19

Source	Testing Date	Set Num.	Operator	Total Energy Before the 20/10 Rule (J)	Total Energy After the 20/10 Rule (J)	Maximum Density(g/cm³)
	12/11/2024	Set 3	Operator 1	12.58817439×10^{6}	18.87634108×10^{6}	2.18
			Operator 2	12.51076764×10^{6}	19.73288018×10^{6}	2.19
Stone Co	12/11/2024	Set 1	Operator 1	13.52114413×10^{6}	21.21992544×10^{6}	2.38
			Operator 2	14.25720332×10^{6}	19.7096282×10^{6}	2.37
	12/11/2024	Set 2	Operator 1	13.28592395×10^{6}	16.36919063×10^{6}	2.34
			Operator 2	16.20667648×10^{6}	23.23154483×10^{6}	2.39
	12/12/2024	Set 3	Operator 1	14.20046902×10^{6}	16.8218426×10^{6}	2.33
			Operator 2	21.40284345×10^{6}	22.56303788×10^{6}	2.41

Source	Testing Date	Set Num.	Operator	Total Energy Before the 20/10 Rule (J)	Total Energy After the 20/10 Rule (J)	Maximum Density(g/cm³)
Calcite	12/12/2024	Set 1	Operator 1	24.08379592×10^{6}	27.61181498×10^{6}	2.33
			Operator 2	21.2835863×10^{6}	33.58068952×10^{6}	2.41
	12/13/2024	Set 2	Operator 1	21.12743362×10^{6}	28.57480585×10^{6}	2.38
			Operator 2	19.64336121×10^{6}	26.77470099×10^{6}	2.36
	12/13/2024	Set 3	Operator 1	22.77067702×10^{6}	34.75080354×10^{6}	2.40
			Operator 2	20.58620637×10^{6}	27.61187824×10^{6}	2.41

4.5 Statistical Analysis

4.5.1 T-Test

A t-test is a statistical hypothesis test used to determine whether a sample provides sufficient evidence to reject a null hypothesis about a population mean. It was applicable when the population standard deviation was unknown, and the sample was assumed to have been drawn from a normally distributed population (Navidi 2020). The test compared the observed sample mean with a hypothesized population mean, accounting for sample variability, to evaluate whether any observed difference was likely due to random variation or reflected an actual difference in the population parameter (Navidi 2020).

The null hypothesis (H_0) typically asserts that there was "no effect," "no change," or "no difference." In the case of a paired t-test, H_0 stated that the mean difference between paired observations was zero. Under this assumption, any variation in the differences was attributed to random variation rather than a systematic cause. The alternative hypothesis (H_1) was the logical complement to H_0 and, for a two-tailed test, specified that the mean difference was not equal to zero, indicating a consistent and systematic difference between the two sets of measurements. The difference was not equal to zero ($\boldsymbol{\mu D = 0}$), indicating a consistent and systematic difference between the two sets of measurements (Navidi 2020).

A **two-tailed paired *t*-test** was used when differences in either direction (positive or negative) were of interest. In this case, both significant positive and large negative deviations from zero provide evidence against H_0 (Navidi 2020)

The paired *t*-test procedure involved the following steps:

Calculate the differences: For each pair, compute $D_i = X_{i1} - X_{i2}$, where (X_{i1}) and (X_{i2}) were the paired measurements.

Determine the sample statistics: Calculated the mean difference $\overline{D}$ and the sample standard deviation of the differences s_D.

Compute the test statistic: calculate the test statistic (t) using the relationship in Eq. (20)

$$t = \frac{\overline{D} - \mu_0}{s_D/\sqrt{n}} \quad \text{Eq. (20)}$$

where n is the number of pairs, and μ_0 is the hypothesized mean difference. **Determine the P-value:** Using the Student's *t* distribution with $n - 1$ degrees of freedom.

Make a decision: If |t| exceeds the critical *t* value for the chosen significance level α, or if the P-value is less than α, reject H_0; otherwise, fail to reject H_0 (Navidi 2020).

In this study, each soil sample (defined by source and set) was tested by two operators, Operator 1 and Operator 2, to measure Maximum Dry Density (MDD) and Optimum Moisture Content (OMC). This produced paired observations, consisting of two measurements taken on the same sample, one from each operator. This would have increased error variance and decreased statistical power. The paired t-test, in its turn, directly analyzed the within-sample differences:

- In case of MDD: $d_{i,\text{MDD}} = \text{MDD}_{i,\text{Operator 1}} - \text{MDD}_{i,\text{Operator 2}}$
- In the case of OMC: $d_{i,\text{OMC}} = \text{OMC}_{i,\text{Operator 1}} - \text{OMC}_{i,\text{Operator 2}}$

By focusing on d_i, the paired t-test controls for sample-to-sample variability in soil properties and isolates the effect of operator differences.

The hypotheses for each parameter (MDD and OMC) are:

- Null Hypothesis (H_0): $\mu d = 0$ (there is no operator variability)
- Alternative Hypothesis (H_1): $\mu d \neq 0$ (there is operator variability)

The dataset contains paired MDD and OMC measurements for multiple material sources and sets. The differences were computed as d_i = Operator 1 – Operator 2 for each sample and parameter. The results of the paired T-test are shown in Table 17.

Table 17. Paired T-Test Results for Maximum Dry Density and Optimum Moisture Content Analysis

Parameter	n	$\bar{d}$	s_d	t	p	**Decision (α=0.05)**
MDD (pcf)	15	-0.593	2.752	-0.835	0.418	Fail to reject H_0
OMC (%)	15	0.027	0.435	0.237	0.816	Fail to reject H_0
Energy (ft-lbf)	15	235820.508	5674911.162	0.160941533	0.874438779	Fail to reject H_0

For both MDD and OMC, $p > 0.05$, so H_0 is not rejected. Statistically, there is no evidence that the two operators differ systematically in their measurements. Any observed differences are consistent with the random variation inherent in the testing process. From a practical engineering standpoint, this result supports the conclusion that operator variability is not a significant factor in this dataset.

4.5.2 ANOVA

Two-way Analysis of Variance (ANOVA) with replication is a statistical method used to examine how two categorical factors, and their interaction, affect a continuous response variable. This method is beneficial in factorial experiments where each combination of factor levels has multiple observations. The approach enables the analyst to test the Main effects of each factor, the interaction effects between the factors, and the Random error, each independently estimated from separate replications (Navidi 2020).

In this research, Factor A was defined as *Operator* (Operator 1, Operator 2), and Factor B as *Material Source* (Lafarge, Port Inland, Great Lake, Stone Co., Calcite). Replication was achieved by using multiple test sets for each Operator × Source combination, allowing precise estimation of the error term and assessment of interactions. Key concepts used in the two-way ANOVA include the factor, a categorical variable that may influence the response (e.g., Operator); the level, a specific category within a factor (e.g., Operator 1); the response variable, the measured outcome affected by combinations of factor levels, such as maximum dry density (MDD), optimum moisture content (OMC) or energy value; and replication, repeated observations within each cell that provide an independent estimate of within-cell (random) error variance and support valid tests of main and interaction effects (Navidi 2020).

Hypothesis Statement for Two-Way ANOVA with Replication: In the context of this factorial experiment, a two-way analysis of variance (ANOVA) with replication was used to evaluate the effects of two categorical factors, Operator and Material Source, on the response variables, Maximum Dry Density (MDD) and Optimum Moisture Content (OMC). Three distinct hypothesis tests were conducted: one for each main effect (Operator and Source), and one for their interaction. These tests determined whether the mean responses differed significantly across levels of each factor or whether their combined interaction contributed meaningfully to response variability.

Factor A: Operator Effect

To formalize the hypothesis tests, the operator effect (Factor A) is evaluated with H_0^A: $\mu_1 = \mu_2 = \cdots = \mu_a$ (all operator means are equal) versus H_1^A: not all μ_i are equal; rejecting H_0^A indicates statistically significant differences among operators.

Factor B: Source Effect

The source effect (Factor B) is tested with H_0^B: $\mu_1 = \mu_2 = \cdots = \mu_b$ (all material sources yield the same mean) versus H_1^B: not all μ_j are equal; rejection implies the material source significantly influences the compaction results.

Interaction Effect (Operator × Source)

The interaction (Operator × Source) is assessed with H_0^{AB}: $\mu_{ij} - \mu_{i\cdot} - \mu_{\cdot j} + \mu_{\cdot\cdot} = 0$ (No interaction between factors) versus H_1^{AB}: At least one combination differs beyond main effects; rejecting H_0^{AB} implies the operator effect depends on the material source.

Grand Mean (GM):

The mean of all observations across all operators and sources were calculated using the relationship in Eq.21.

$$\bar{x} = \frac{1}{abn}\sum_{i=1}^{a}\sum_{j=1}^{b}\sum_{k=1}^{n} x_{ijk} \qquad \text{Eq. (21)}$$

Where:

a: number of levels in Factor A (operators), b: number of levels in Factor B (sources), n: number of replicates per cell, and x_{ijk} : value for operator i, source j, replicate k

Row Means (Operator-wise): The row means were calculated using Eq. (22)

$$x_{i\cdot\cdot} = \frac{1}{bn}\sum_{j=1}^{b}\sum_{k=1}^{n} x_{ijk}$$ Eq. (22)

Column Means (Source-wise): The column means were calculated using Eq. (23)

$$x_{\cdot j\cdot} = \frac{1}{an}\sum_{i=1}^{a}\sum_{k=1}^{n} x_{ijk}$$ Eq. (23)

Cell Means (Operator × Source): The cell means were calculated using Eq. (24)

$$x_{ij\cdot} = \frac{1}{n}\sum_{k=1}^{n} x_{ijk}$$ Eq. (24)

Calculate the Sums of Squares

Total Sum of Squares (SS_T)

It represents the total variability of the data from the grand mean; this value was calculated using Eq. (25):

$$SS_{\mathrm{T}} = \sum_{i=1}^{a}\sum_{j=1}^{b}\sum_{k=1}^{n}\left(x_{ijk} - \bar{x}_{\ldots}\right)^2$$ Eq. (25)

Sum of Squares for Factor A (SS_A – Operator)

It measures variation between operator means, this value was calculated using Eq. (26):

$$SS_A = bn\sum_{i=1}^{a}(x_i - \bar{x}_{\ldots})^2$$ Eq. (26)

Sum of Squares for Factor B (SS_B – Source)

It measures variation between source means, this value was calculated using Eq. (27):

$$SS_B = an\sum_{j=1}^{b}\left(x_j - \bar{x}_{...}\right)^2 \quad \text{Eq. (27)}$$

Sum of Squares for Interaction (SS_{AB} – Operator × Source)

It captures how the effect of one factor depends on the level of the other, this value was calculated using Eq. (28):

$$SS_{AB} = n\sum_{i=1}^{a}\sum_{j=1}^{b}\left(x_{ij} - x_i - x_j + \bar{x}_{...}\right)^2 \quad \text{Eq. (28)}$$

Sum of Squares for Error (SS_E – Within-cell variation)

It represents the random error or unexplained variation, this value was calculated using Eq. (29):

$$SS_E = \sum_{i=1}^{a}\sum_{j=1}^{b}\sum_{k=1}^{n}\left(x_{ijk} - x_{ij}\right)^2 \quad \text{Eq. (29)}$$

It can be observed in Eq. (30) that the total sum of squares, SS_T, is equal to the sum of the others. This is the analysis of variance identity for two-way ANOVA

$$SS_T = SS_A + SS_B + SS_{AB} + SS_E \quad \text{Eq. (30)}$$

Calculate Degrees of Freedom

Degrees of freedom (df) for the two-way ANOVA with replication are allocated as follows: Factor A (Operator) has $(a-1)df_A$, Factor B (Source) has $(b-1)df_B$, and the interaction $(A \times B)$has $(a-1)(b-1)df_{AB}$. The error term carries $ab(n-1)df_E$, and the total degrees

of freedom equal($abn - 1$). Here, a is the number of operators, $b$is the number of sources, and $n$is the number of replications per cell.

Compute Mean Squares and F-Ratios

Divide each sum of squares by its corresponding degrees of freedom as shown in Eq. (31):

$$MS_A = \frac{SS_A}{df_A}, \qquad MS_B = \frac{SS_B}{df_B}, \qquad MS_{AB} = \frac{SS_{AB}}{df_{AB}}, \qquad MSE = \frac{SS_E}{df_E} \qquad \text{Eq. (31)}$$

Where SS_A, SS_B, SS_{AB}, SS_Esum of squares due to Operator, Source, Interaction, and Error, respectively, and $df_A = (a-1)$, $df_B = (b-1)$, $df_{AB} = (a-1)(b-1)$, $df_E = ab(n-1)$

Now compute F-ratios using Eq. (32):

Each F-ratio compares the MS of a factor to the MS of the error term (residuals), to test if the variation due to that factor is significantly greater than random variation.

$$F_O = \frac{MS_A}{MSE} \quad F_S = \frac{MS_B}{MSE} \quad F_I = \frac{MS_{AB}}{MSE} \qquad \text{Eq. (32)}$$

F_O: Tests if there's a significant difference between operator means, F_S: Tests if there's a significant difference between source means, and F_I: Tests whether there is an interaction between operator and source.

If the computed F-value exceeds the critical value from the F-distribution (or p-value < 0.05), the null hypothesis for that factor is rejected (Navidi 2020). The Conditions and Conclusions of the two-way ANOVA are summarized in Table 18.

Table 18. Two-Way ANOVA Condition and Conclusion

Condition	Conclusion
$F > F\alpha$	Reject H_0: The factor has a significant effect
$p < 0.05$	Reject H_0: The result is statistically significant
$orF \leq F\alpha \ \ or \ \ p \geq 0.05$	Fail to reject H_0: No evidence of significant effect

The experiment includes two factors: Operator (2 levels) and Material Source (5 levels),

Multiple replicates (sets) exist for each Operator × Source combination. The goal was to test the main effects and interaction (Operator × Source). The two-way ANOVA with replication was the statistically correct method. It allowed for proper partitioning of variability, and isolated true treatment effects from random noise, which was critical for evaluating systematic operator and source differences in compaction data (Navidi 2020). The ANOVA Test Results for MDD, OMC, and Energy are summarized in Tables 19, 20, and 21, respectively.

Table 19. ANOVA Test Results for MDD

MDD	P- value		F- value	F - critical	Null Decision	Significance
Operator (F_O)	0.38	> 0.05	0.82	4.35	Fail to reject null	Not significant
Source (F_S)	1.7E-11	< 0.05	70.41	2.87	Reject null	Statistically significant
Interaction (F_I)	0.37	> 0.05	1.13	2.87	Fail to reject null	Not significant

Table 20. ANOVA Test Results for OMC

OMC	P- value		F- value	F - critical	Null Decision	Significance
Operator (F_O)	0.81	> 0.05	0.06	4.35	Fail to reject null	Not significant
Source (F_S)	8.74E-11	< 0.05	58.94	2.87	Reject null	Statistically significant
Interaction (F_I)	0.49	> 0.05	0.88	2.87	Fail to reject null	Not significant

Table 21. ANOVA Test Results for Energy

Energy	P- value		F- value	F - critical	Null Decision	Significance
Operator ($\mathbf{F_O}$)	0.85635304	> 0.05	0.03	4.35	Fail to reject null	Not significant
Source ($\mathbf{F_S}$)	0.01275302	< 0.05	4.18	2.87	Reject null	Statistically significant
Interaction ($\mathbf{F_I}$)	0.80125884	> 0.05	0.41	2.87	Fail to reject null	Not significant

The results of the two-way ANOVA indicated that there were no statistically significant differences in compaction outcomes between the two operators, indicating that the effect of source on MDD is consistent across both operators and does not depend on who performed the test. In contrast, a statistically significant main effect was observed for material sources, with the five sources (Lafarge, Port Inland, Great Lake, Stone Co., and Calcite) exhibiting distinct influences on the measured maximum dry density (MDD or OMC).

5 DISCUSSION

This chapter discusses the key findings of the compaction testing study on open-graded drainage course (OGDC) aggregates. The discussion is organized into three main areas: (1) operator variability in the M-Cone test, (2) comparison of maximum dry density (MDD) values from the Modified Proctor and M-Cone tests, and (3) evidence of particle crushing during compaction. In each area, the study's results are compared with relevant literature. The chapter then reflects on practical implications for Michigan DOT procedures and acknowledges the study's limitations.

5.1 Operator Variability in the M-Cone Test

In this study, two different operators (Operators A and B) were used to perform one-point M-Cone tests on multiple OGDC aggregate sources approved by MDOT (with several replicate trials per source). The resulting maximum dry densities (MDDs) between operators for the same source were statistically indistinguishable. A direct comparison of MDD results showed that any differences between Operators A and B were within the margin of experimental error, on the order of 0.01–0.02 g/cm³ (well under 1% relative variation). Formal hypothesis tests confirmed this observation: a t-test found no significant difference between the two operators' MDD averages, and a two-way ANOVA (with factors "operator" and "material source") showed no significant main effect of operator on the compaction outcome (at $\alpha = 0.05$). In other words, when the M-Cone procedure was followed consistently, different operators obtained equivalent compaction results for the same material source. The consistency can be attributed to the careful concentration of both operators conducting this test in the laboratory. Indeed, the statistical analysis revealed that the material source, rather than the operator, was the dominant factor influencing MDD in the experiments. The observed variability in material density across different OGDC sources was attributable to inherent aggregate characteristics of each source (e.g., gradation, particle shape, specific gravity, water absorption, and others). This finding underscores that with proper training and technique, the M-Cone test's manual elements did not introduce statistically significant variability within the conditions evaluated. These findings should be interpreted within the context of the controlled laboratory conditions and the trained personnel involved in this study. They should not be generalized to all field testing conditions.

In addition to the density measurements, the study employed accelerometer-based instrumentation on the M-Cone apparatus to quantify the actual compaction energy delivered in each test. An accelerometer was mounted at the base of the cone to record the acceleration impulse of each strike, enabling calculation of the energy per blow and total energy imparted to the specimen. This instrumentation was intended to objectively verify the compaction effort of both operators. The accelerometer data showed that each operator indeed delivered a very similar total energy to the samples. Across all instrumented trials, the total input energy per test was on the order of 1.3×10^7–3.5×10^7 J (i.e., tens of megajoules), and critically, a two-way ANOVA found no significant difference in energy input between the two operators for the five sources tested with instrumentation by two operators. There was also no operator–source interaction for energy, meaning that neither operator consistently imparted more energy on any particular material. In practical terms, both technicians applied similar compaction effort. Notably, the instrumentation also indicated that the energy per blow and the number of blows required were uniform across repeated trials on the same material. This suggests that the one-point test (as governed by the 20/10 seating criterion) is reproducible. Thus, the accelerometer-based measurements validate that the M-Cone test's design and procedure effectively constrain the compaction process to a repeatable energy input for a given aggregate, thereby explaining the nearly identical density outcomes between operators. It should also be noted that the accelerometer measurements in this study were limited to quantifying compaction energy consistency. Other procedural factors associated with operator variability, such as material placement, handling, and adherence to testing procedures, were not independently evaluated.

Overall, these findings demonstrate that the M-Cone test is a repeatable compaction method for open-graded aggregates when conducted by trained operators in the laboratory. From a practical standpoint, this means that agencies can have confidence that M-Cone test results can be consistent across different field personnel and testing settings. This level of consistency is especially noteworthy, given the inherently heterogeneous nature of open-graded aggregates. Despite greater particle-size variation and a more variable void structure in OGDC, the M-Cone method yielded consistent compaction endpoints across operators in this study. The implication for field practice is that the M-Cone test can be used confidently as a standard quality-control tool for OGDC base layers, provided technicians are adequately trained and follow the standard method (e.g., the pounding technique and the correct number of blows per lift), and that outcomes are reproducible. The study's accelerometer data provided additional

assurance that the strikes in the M-Cone test effectively delivered a controlled, repeatable compaction energy.

5.2 Comparison of MDD Results: M-Cone vs. Modified Proctor

Overall, the one-point M-Cone compaction test produced maximum dry densities (MDD) that almost matched those from the standard Modified Proctor (AASHTO T-180) test for all open-graded drainage course (OGDC) aggregates tested in this study, except for two sources. The M-Cone MDD values spanned approximately 1.81–2.41 g/cm³ (about 113–150 pcf), virtually overlapping with the Modified Proctor MDD range of 1.91–2.41 g/cm³ (120–150 pcf). On average, the M-Cone yielded very similar maximum dry densities (mean ~2.20 g/cm³) with Proctor MDD typically equal to or slightly lower (mean ~2.17 g/cm³) for these coarse aggregates, except for two sources. In most cases, the Modified Proctor yielded a slightly higher MDD (on the order of 1-3 percent greater than M-Cone), which is the expected trend given the Proctor's greater overall compaction effort applied in multiple layers. However, two notable exceptions were observed where this trend was reversed.

Two aggregate sources, identified here as Stone Co. and Calcite, exhibited M-Cone MDD values that were 5–8% higher than their Modified Proctor MDDs. In practical terms, these materials achieved dry densities roughly 0.15–0.18 g/cm³ greater under the M-Cone test than under the Proctor. This outcome contradicts the trend observed in other sources. To understand this anomaly, it is crucial to examine the material properties of Stone Co. and Calcite and how those properties influence the outcomes from the two compaction methods.

Both Stone Co. and Calcite aggregates share a key characteristic, unusually high water absorption, particularly in the fine portion (material passing US Sieve No. 4) of the material (on the order of 4% by weight). In standard compaction tests, water absorption can mask the effective moisture content that is actually available during compaction. Here, effective moisture content is defined as the moisture content available for lubrication and compaction after accounting for water absorbed by the aggregate. In other words, effective moisture content is the free moisture that actively surrounds particles, equal to the total moisture content minus the material's absorption capacity.

For Stone Co. and Calcite, a large fraction of the water added was soaked into the aggregates themselves rather than remaining free in the inter-particle voids. Under the Modified Proctor

test, these materials had an optimum moisture content (OMC) of 7–9% (total water by dry weight), corresponding to a free moisture level of roughly 3–5% after accounting for their ~4% absorption. In contrast, when the same materials were compacted with the one-point M-Cone method, the procedure effectively found their peak density at a much drier state – only about 1.6–2.2% effective moisture. In other words, during the M-Cone compaction of Stone Co. and Calcite, the majority of water might have been absorbed by the aggregate, leaving a smaller amount of free water between particles. The M-Cone test essentially compacted these samples in a near-dry condition, whereas the Proctor test compacted them at a somewhat wetter state, with a few percent of free moisture present to act as a lubricant.

Under typical conditions, one would expect that such a low effective moisture content would hinder compaction. Insufficient free water usually means high particle friction and poor lubrication, resulting in a lower achievable density. This is why every soil or aggregate has an optimum moisture content for compaction. At first glance, it seems contradictory that the drier M-Cone condition produced a higher density than the wetter Proctor condition for Stone Co. and Calcite. However, this trend can be explained by differences in the compaction energy intensity and mechanism between the two tests, combined with the unique behavior of high-absorption aggregates. The Modified Proctor method applies a higher total energy, but it is delivered in a layered fashion, with a standard hammer dropped repeatedly on each lift in a relatively large mold. Each Proctor hammer blow imparts a moderate impact distributed over the layer's surface area, and the presence of more free water (3–5% in these cases) helps particles slide during compaction but also occupies space in the sample. Table 22 compares %Abs, derived w_{eff}, and the paired MDD results for each source.

Table 22. A Comparison of Density, Moisture Content and Effective Moisture Content of Various OGDC Sources for Different Tests

Source/ Operator	Absorption	Modified Proctor MDD (pcf)	Modified Proctor OMC (%)	Avg MDD M-Cone* (pcf)	M-Cone Avg Field Moisture * (%)	Modified Proctor w_{MPeff} (%)	Avg M-Cone w_{MCeff} (%)	Diff $w_{\mathrm{MP}eff} - w_{MCeff}$ (%)
Lafarge	1.4	147.6	5	144.2	6.6	3.6	5.2	-1.6
Port Inland	2.26	138.7	5.7	135.6	5.3	3.4	3.0	0.4
Great Lake	3.76	140.6	8.3	136.7	7.8	4.6	4	0.6
Stone Co	4.16	136.3	8.6	149.3	6	4.4	1.8	2.6
Calcite	4.34	139	7.7	149.3	6	3.3	1.7	1.6
StGrLa	3.16	138.9	9	136.6	7.8	5.8	4.6	1.2
SylMe2025	1.5	131.1	10.4	129.5	9.3	8.9	7.8	1.1

Source/ Operator	Absorption	Modified Proctor MDD (pcf)	Modified Proctor OMC (%)	Avg MDD M-Cone* (pcf)	M-Cone Avg Field Moisture * (%)	Modified Proctor w_{MPeff} (%)	Avg M-Cone w_{MCeff} (%)	Diff $w_{\mathrm{MP}eff} - w_{MCeff}$ (%)
SylMe2025_2	2.35	125.8	9.6	123	11	7.3	8.7	-1.4
Slag	4.14	119.6	10	116	13.1	5.9	8.9	-3
I - 275	1.22	138.6	8.3	136.4	7.8	7	6.6	0.4

Note: M-Cone averages are based on the original three Operator 2 test replicates used for the paired comparison dataset.

In contrast, the M-Cone test compacts material by repeatedly striking the cone and its contents against a rigid base, producing an impact-driven densification mechanism that differs from the layered hammer compaction used in the Modified Proctor test. Differences in compaction response between the two methods are therefore more appropriately attributed to variations in compaction procedure, confinement conditions, moisture distribution, and energy transfer characteristics. In highly absorptive aggregates such as Stone Co. and Calcite, the lower effective moisture content during M-Cone compaction may have reduced the cushioning effect of free water and allowed greater particle interlock during densification, contributing to the higher dry densities observed.

From a compaction theory standpoint, this outcome aligns with known principles, even though it defies the initial expectation based on the total energy imparted by the two compaction methods under focus. It is well established that increasing compaction effort on a given material will tend to raise the maximum dry density and reduce the optimum moisture content. In the context of Stone Co. and Calcite, the M-Cone's method, by virtue of its concentrated energy delivery, effectively exerted a higher compaction effort on the sample (per unit of material, at the point of impact) than the Modified Proctor hammer, shifting the compaction curve to a new optimum point: one at a lower moisture content and higher dry density. The Modified Proctor, although it requires a greater total energy input, has a lower energy intensity per blow and relies more on moisture to achieve particle reorientation. Thus, the Proctor test on these materials found an optimum at a higher moisture where lubrication was available, but that very moisture limited the maximum dry density (since water takes up volume and adds less density than solid aggregate, and also acts as a cushioning). The M-Cone test, in essentially a drier (low effective moisture content) and high-impact condition, achieved a state of packing with more solids and less water, resulting in a higher dry density. What appeared to be a contradiction is thus explained by the interplay of material absorption and compaction energy concentration. The M-Cone delivered sufficient impact to compact an almost-dry aggregate.

In contrast, the Modified Proctor required additional water to compensate for the lower per-blow energy, which, in turn, limited the density that could be achieved. This phenomenon was not observed in the other aggregates because their compaction conditions differed significantly. For most other sources, either the absorption capacity was lower, or the added water was not fully absorbed, leaving sufficient free moisture during compaction to facilitate particle rearrangement without exceeding the optimal moisture range. In those cases, the additional

water did not create a surplus that interfered with compaction; instead, it supported efficient densification under the Proctor's layered energy input. As a result, the Proctor test yielded MDDs that were similar to or slightly higher than those of the M-Cone. Only in the specific case of Stone Co. and Calcite, where high absorption and very low effective moisture coincided, did the added water in the Proctor test act more as an energy-dissipating medium than as a compaction aid, thereby limiting achievable density. This outcome was not general but material-specific, arising from the particular interaction between aggregate absorption, free water availability, and compaction method.

It is important to emphasize that this anomalous behavior was specific to the material. Not all high-absorption aggregates showed a higher M-Cone density; in fact, most other materials followed the conventional pattern (M-Cone MDD matching or slightly below Modified Proctor MDD). For example, a slag aggregate in the study also had a comparably high water absorption (approximately 4.1%), yet did not exhibit a higher density under the M-Cone test. Instead, the slag's M-Cone result was in line with or slightly lower than its Modified Proctor density. The difference lies in the effective moisture content and compaction response of the slag compared with those of the Stone Co. and Calcite materials. In the Modified Proctor tests, the slag required a higher total water content to reach its optimum moisture content (~10% by dry weight), but unlike the Calcite and Stone Co aggregates, a substantial portion of that water remained free rather than being absorbed. Consequently, the slag had a much higher effective moisture content at compaction (on the order of 6% free moisture, compared with near zero in the Calcite and Stone Co aggregates under similar conditions).

Under the one-point M-Cone test, the slag also retained a moderate effective moisture level during compaction, indicating it was not compacted in an ultra-dry state. With sufficient free moisture present, the slag's behavior was "normal" – the M-Cone did not gain an unusual advantage, and its maximum density fell slightly below the Proctor value (as would be expected due to the Modified Proctor's greater total compaction effort). This contrast reinforces that the M-Cone density surpluses observed for Stone Co. and Calcite were not solely due to high absorption, but to the specific combination of high absorption and low effective moisture at the time of compaction. In cases where even a highly absorptive aggregate still has adequate free water during compaction (as with the slag), the M-Cone did not exceed the MDD values from Modified Proctor.

5.3 Particle Crushing During Compaction

The open gradation and hardness of OGDC aggregates raised questions about particle degradation under compaction. This study directly examined the phenomenon by performing pre-compaction and post-compaction sieve analyses on the samples. The results showed particle crushing (degradation) during compaction. In every compaction test method (including the M-Cone), an increase in the percentage of fines was observed after compaction, indicating that the gradation shifted slightly toward having a higher amount of smaller-sized particles. Box plot comparisons of gradation before vs. after compaction showed that all materials generated some additional finer particles (passing smaller sieves) due to compaction. This was true even though the OGDC aggregates had very low initial fines; the mechanical action of compaction caused a portion of the larger grains to abrade or fracture, resulting in particles that fell into the finer size ranges. These findings confirm that particle breakage is a real phenomenon during the compaction of open-graded aggregates, and that achieving a high density often comes at the expense of particle integrity.

This study did not directly compare breakage between methods quantitatively, but the general observations are consistent. The fines generated in the M-Cone tests were relatively small relative to the modest gradation shifts, which were mainly within the OGDC specification envelope, suggesting that breakage was limited. The worst-case method for particle crushing would likely be the Modified Proctor or Gyratory Compactor, which exerts higher total energy and, in the Proctor's case, uses a metal rammer that can pulverize weaker particles. By contrast, the M-Cone's design may concentrate force in the center and encourage particle reorientation rather than extensive fracture. Minimal particle crushing is beneficial for OGDC, as it preserves the intended gradation and high permeability. Thus, the M-Cone's gentler compaction mechanism could be seen as an advantage in maintaining drainage capacity, provided it still achieves the necessary density. The study results show that while some breakdown is unavoidable (even under the cone method), it is not excessive as to drastically alter the gradation. Nonetheless, the implication for field compaction is that higher compaction effort might grind the aggregate, potentially reducing void space and permeability over time.

6 CONCLUSIONS

Overall, this study confirms that the M-Cone procedure, conducted in laboratory conditions, is a reliable test for evaluating the density of Open-Graded Drainage Course (OGDC) materials. By integrating accelerometer data and statistical analysis, the research demonstrated consistent results between trained operators under controlled laboratory conditions. While the M-Cone aligns closely with traditional Modified Proctor standards, the study identified that aggregates with high water absorption require specialized attention to effective moisture content to avoid density deviations. Furthermore, the M-Cone was found to achieve necessary stability with less aggregate degradation than other laboratory methods, effectively preserving the drainage capacity of the base layer. Some of the salient findings from the study are provided as follows:

- The study confirms that the one-point M-Cone test, when properly executed under laboratory conditions, consistently yields maximum dry densities (MDD) comparable to those obtained with the Modified Proctor test.

- Across the aggregate sources tested, M-Cone MDD values (1.81 to 2.41 g/cm^3) closely aligned with Modified Proctor values (1.91 to 2.41 g/cm^3), validating MDOT's use of the one-point field test to establish reliable compaction benchmarks.

- Statistical analyses, including paired t-tests and two-way ANOVA, indicated no statistically significant operator variability in the M-Cone results for the OGDC sources evaluated within the controlled laboratory conditions of this study. This finding was further supported by exploratory accelerometer data, which showed that the compaction energy delivered during testing remained generally consistent across the two operators.

- While results were generally comparable across methods, two specific aggregate sources, Stone Co. and Calcite, achieved M-Cone densities 5–8% higher than their Modified Proctor counterparts. This deviation is attributed to the high-water absorption of these materials (approximately 4%) and to the difference between the Modified Proctor effective moisture and the M-Cone effective moisture (≥1.5%).

- Sieve analyses conducted before and after compaction confirmed that all testing methods result in some degree of particle degradation. This crushing was found to be moderate in M-Cone tests but significantly more pronounced in Modified Proctor and

Gyratory procedures.

- The results suggest that the M-Cone, paired with an understanding of material-specific absorption characteristics, provides an evidence-based approach to achieving the necessary balance between structural support and long-term drainage performance.

7 RECOMMENDATIONS

Building on the findings discussed, this study proposes the following recommendations on density testing of OGDC aggregate:

- MDOT may consider including the moisture absorption of each aggregate source as part of the M-Cone Testing procedure. This helps shift moisture control in the field from a fixed total target to an "effective moisture" target that accounts for the material's internal water demand.

- Use the relationship between Modified Proctor and M-Cone effective moisture content as a procedural check:

    - When the water absorption is less than 4% or $w_{MPeff} - w_{MCeff} < 1.5\%$: The standard M-Cone procedure is considered reliable, and testing can proceed as normal.

    - When the water absorption is greater than 4% or $w_{MPeff} - w_{MCeff} \geq 1.5\%$: The material needs further evaluation to ensure accurate density targets.

- For aggregates having water absorption greater than 4% or $w_{MPeff} - w_{MCeff} \geq 1.5\%$, a targeted evaluation is needed to determine whether modifications to the M-Cone moisture interpretation procedure or supplemental Modified Proctor evaluation are appropriate. This assessment can be correlated with both laboratory and field conditions to ensure the density targets are realistic and attainable.

- When evaluating compaction methods for high-water-absorption materials, MDOT may need to verify their impact on permeability. The goal is to ensure that achieving higher densities, which the M-Cone tends to do with these specific materials, does not result in excessive aggregate breakage that would clog the drainage layer.

- MDOT might also consider developing one-point Modified Proctor charts specifically for high-water-absorption aggregates to help prevent field engineers from chasing unrealistic density or moisture targets.

REFERENCES

AASHTO-T180. 2004. *Standard Method of Test for*.

ACSE. 2025. *2025 INFRASTRUCTURE REPORT CARD*.

Arasteh, M. 2017. *TECHNICAL BRIEF INTELLIGENT COMPACTION MEASUREMENT VALUES (ICMV) A ROAD MAP*.

ASTM C127. 2012. "Test Method for Relative Density (Specific Gravity) and Absorption of Coarse Aggregate." West Conshohocken, PA: ASTM International.

ASTM C128. 2012. *Standard Test Method for Density, Relative Density (Specific Gravity), and Absorption of Fine Aggregate 1*.

ASTM-C117. 2004. *Standard Test Method for Materials Finer than 75-µm (No. 200) Sieve in Mineral Aggregates by Washing 1*.

ASTM-C136. 2019. "Test Method for Sieve Analysis of Fine and Coarse Aggregates." West Conshohocken, PA: ASTM International.

ASTM-D4253. 2016. "Test Methods for Maximum Index Density and Unit Weight of Soils Using a Vibratory Table." West Conshohocken, PA: ASTM International.

ASTM-D6925. 2015. "Test Method for Preparation and Determination of the Relative Density of Asphalt Mix Specimens by Means of the Superpave Gyratory Compactor." West Conshohocken, PA: ASTM International.

ASTM-D6938. 2017. "Test Methods for In-Place Density and Water Content of Soil and Soil-Aggregate by Nuclear Methods (Shallow Depth)." West Conshohocken, PA: ASTM International.

Aydilek, A. H., I. Haider, Z. Kaya, A. Cetin, and M. Hatipoglu. 2015. *STATE HIGHWAY ADMINISTRATION RESEARCH REPORT DEVELOPMENT OF DESIGN GUIDELINES FOR PROPER SELECTION OF GRADED AGGREGATE BASE IN MARYLAND STATE HIGHWAYS*.

Baladi, G. 1998. *RR-761 - Reconstruction of Rigid Pavements Using Asphalt Pavement Alternatives*.

Brevik, E., T. Fenton, and L. Moran. 2002. *Effect of soil compaction on organic carbon amounts and distribution, South-Central Iowa*.

Caltrans. 2023. *California Test 216 STATE OF CALIFORNIA-CALIFORNIA STATE TRANSPORTATION AGENCY DEPARTMENT OF TRANSPORTATION METHOD OF TEST FOR RELATIVE COMPACTION OF UNTREATED AND TREATED SOILS AND AGGREGATES*.

Cetin, A., Z. Kaya, B. Cetin, and A. H. Aydilek. 2014. “Influence of laboratory compaction method on mechanical and hydraulic characteristics of unbound granular base materials.” *Road Materials and Pavement Design*, 15 (1): 220–235. https://doi.org/10.1080/14680629.2013.869505.

Chen, Y., Q. Yu, W. Li, Y. Xiao, T. Yang, Z. Li, X. Zhi, and P. Deng. 2022. “Experimental Study on Vibratory Compaction Behavior of Tunneling Rock Wastes Used as Unbound Permeable Aggregate Base Materials.” *Materials*, 15 (22). MDPI. https://doi.org/10.3390/ma15228016.

Choi, Y., D. Ahn, Y. Lee, and J. Ahn. 2020. “Compaction quality monitoring of open-graded aggregates by light weight deflectometer and soil stiffness gauge.” *Sustainability (Switzerland)*, 12 (6). MDPI. https://doi.org/10.3390/su12062521.

Choi, Y. J., D. Ahn, T. H. Nguyen, and J. Ahn. 2018. “Assessment of field compaction of aggregate base materials for permeable pavements based on plate load tests.” *Sustainability (Switzerland)*, 10 (10). MDPI. https://doi.org/10.3390/su10103817.

Drnevich, V., A. Evans, and A. Prochaska. 2007. *FHWA/IN/JTRP-2007/12 Final Report A STUDY OF EFFECTIVE SOIL COMPACTION CONTROL OF GRANULAR SOILS*.

Fattah, M. Y., S. G. Mohammed, M. Y. Fattah, M. B. A. Al-Jabbar, and M. S. Student. 2019. “COMPARISON BETWEEN COMPACTION OF SUBBASE MATERIAL BY PROCTOR TESTS AND SUPERPAVE GYRATORY COMPACTOR.” *Article in Global Journal of Engineering Science and Research Management*. https://doi.org/10.5281/zenodo.3250717.

FDOT- In-Place Density of Soils and Soil Aggregates. 2024. *Florida Method of Test for In-Place Density of Soils and Soil Aggregates by Nuclear Methods*.

FDOT, S. and F. H. 2024. “Soils and Foundations Handbook 2024.”

FHWA. 2025. *BUDGET ESTIMATES FISCAL YEAR 2026 FEDERAL HIGHWAY ADMINISTRATION SUBMITTED FOR THE USE OF THE COMMITTEES ON APPROPRIATIONS*.

Garzon-Sabogal, L., A. Getchell, P. J. Becker, P. L. Bourdeau, and M. Santagata. 2024. *Control Guidelines for Aggregate Drainage Layers and Evaluation of In-Situ Permeability Testing Methods for Aggregates*. West Lafayette, Indiana.

Gladious, J., P. S. Paul, and M. Mukhopadhyay. 2025. “Machine learning based prediction of geotechnical parameters affecting slope stability in open-pit iron ore mines in high precipitation zone.” *Sci Rep*, 15 (1). Nature Research. https://doi.org/10.1038/s41598-025-99026-4.

Haider, I., Z. Kaya, A. Cetin, M. Hatipoglu, B. Cetin, and A. H. Aydilek. 2014. “Drainage and Mechanical Behavior of Highway Base Materials.” *Journal of Irrigation and Drainage Engineering*, 140 (6). American Society of Civil Engineers (ASCE). https://doi.org/10.1061/(asce)ir.1943-4774.0000708.

Hansen, W., and E. A. Jensen. 2001. *Transverse Crack Propagation of JPCP as Related to PCC Toughness*.

Hatipoglu, M., B. Cetin, and A. H. Aydilek. 2020. “Effects of Fines Content on Hydraulic and Mechanical Performance of Unbound Granular Base Aggregates.” *Journal of Transportation Engineering, Part B: Pavements*, 146 (1): 04019036. American Society of Civil Engineers (ASCE). https://doi.org/10.1061/jpeodx.0000141.

IDOT. 2020. *Geotechnical Manual State of Illinois*.

Iliyas, S., A. Idris, I. H. Umar, H. Lin, A. Muhammad, and L. Xie. 2024. “Experiment and Analysis of Variance for Stabilizing Fine-Grained Soils with Cement and Sawdust Ash as Liner Materials.” *Materials*, 17 (10). Multidisciplinary Digital Publishing Institute (MDPI). https://doi.org/10.3390/ma17102397.

Jennifer E. Nicks, Michael T. Adams, Nicholas Culbreth, and Thomas Gebrenegus. 2023. *FHWA-HRT-23-046: Variability in the Engineering Properties of Open-Graded Aggregate Backfills: A Large-Scale Direct Shear Round-Robin Study*.

Krueger, K. M. 2011. “M-Cone test : a reliability study.” Houghton, Michigan: Michigan Technological University.

Lee, J. S., S. Y. Kim, W. T. Hong, and Y. H. Byun. 2019. “Assessing subgrade strength using an instrumented dynamic cone penetrometer.” *Soils and Foundations*, 59 (4): 930–941. Elsevier B.V. https://doi.org/10.1016/j.sandf.2019.03.005.

Li, J., J. D. White, and K. R. P. Vennapusa. 2018. *Improving the Foundation Layers for Concrete Pavements: Field Assessment of Variability in Pavement Foundation Properties Technical Report*.

Linden, R. N., J. P. Mahoney, and N. C. Jackson. 1989. *Effect of Compaction on Asphalt Concrete Performance*.

Marathe, S., and A. Sheshadri. 2025. “Machine-Learning-Based Prediction of California Bearing Ratio (CBR) for Lateritic–Lithomargic Pavement Subgrades through the Major Index Properties.” *Indian Geotechnical Journal*. Springer. https://doi.org/10.1007/s40098-025-01297-1.

Markow, M. J. 1989. *TRANSPORTATION RESEARCH RECORD 1276*.

MDOT. 2009. *Performance Evaluation of JRCP with Stabilized Open-Graded Drainage Course 5. Report Date*.

MDOT. 2024. *CONSTRUCTION FIELD SERVICES DIVISION DENSITY TESTING AND INSPECTION MANUAL 2024 EDITION*.

Navidi, W. Cyrus. 2020. *Statistics for engineers and scientists*. McGraw-Hill Education.

Nazzal, M. D. 2014. *Non-nuclear methods for compaction control of unbound materials*. Transportation Research Board.

Nicks Jennifer. 2018. *HRT-18-048: Impact of Initial Density on Strength-Deformation Characteristics of Open-Graded Aggregates*.

Nieves. 2013. *DESCRIPTION OF IC FOR SOIL/BASE CONSTRUCTION*.

Novak, Jr. 1983. "SPR-1211-Report."

ODOT. 2010. *STATE OF OHIO DEPARTMENT OF TRANSPORTATION SUPPLEMENT 1015 COMPACTION TESTING OF UNBOUND MATERIALS*.

Ping, W. V, P. E. Guiyan, X. M. Leonard, and Z. Yang. 2003. *FINAL REPORT Evaluation of Laboratory Compaction Techniques for Simulating Field Soil Compaction (Phase II)*.

Schaefer, V. R., D. J. White, H. Ceylan, L. J. Stevens, V. R. ; Schaefer, D. J. ; White, and H. ; Ceylan. 2008. *Design Guide for Improved Quality of Roadway Subgrades and Subbases*.

Shabbir Hossain, M., and E. J. Hoppe. 2024. *Use of Nuclear Gauge for Construction Quality Control of Unbound Base Course Containing Reclaimed Asphalt*.

Smith, Roger., Thomas. Freeman, and Olga. Pendleton. 1993. *Pavement maintenance effectiveness*. Strategic Highway Research Program, National Research Council.

Tamaishi, J. C., K. Fukuda, K. Nakashima, R. Maeda, K. Matsumoto, and R. Kurazume. 2023. *Evaluation of ground stiffness using multiple accelerometers on the ground during compaction by vibratory rollers*.

Thapa, I., and S. Ghani. 2025. "Explainable AI-enhanced machine learning for CBR prediction in stabilized and unstabilized subgrade soils." *Appl Soft Comput*, 178. Elsevier Ltd. https://doi.org/10.1016/j.asoc.2025.113275.

Tomčík, D., J. Merganič, V. Juško, M. Ferenčík, M. Allman, Z. Dudáková, M. Vlčková, K. Merganičová, and J. Výbošťok. 2025. "Assessing the Impact of Forest Machinery Passage on Soil CO2 Concentration." *Forests*, 16 (6). Multidisciplinary Digital Publishing Institute (MDPI). https://doi.org/10.3390/f16061025.

Tran, N., L. Ga, P. Turner, and J. Shambley. 2016. *NCAT Report 16-02 ENHANCED COMPACTION TO IMPROVE DURABILITY AND EXTEND PAVEMENT SERVICE LIFE: A LITERATURE REVIEW*.

TxDOT-113. 2011. *LABORATORY COMPACTION CHARACTERISTICS AND MOISTURE-DENSITY RELATIONSHIP OF BASE MATERIALS TXDOT DESIGNATION: TEX-113-E Test Procedure for LABORATORY COMPACTION CHARACTERISTICS AND MOISTURE-DENSITY RELATIONSHIP OF BASE MATERIALS*.

TxDOT-115. 2024. *MEASURING IN-PLACE DENSITY AND MOISTURE CONTENT OF SOILS AND BASE MATERIALS TXDOT DESIGNATION: TEX-115-E Test Procedure for MEASURING IN-PLACE DENSITY AND MOISTURE CONTENT OF SOILS AND BASE MATERIALS*.

Usaborisut, P., and J. Ampanmanee. 2015. "Compaction properties of silty soils in relation to soil texture, moisture content and organic matter." *American Journal of Agricultural and*

Biological Science, 10 (4): 178–185. Science Publications. https://doi.org/10.3844/ajabssp.2015.178.185.

Xiao, Y., M. Wang, X. Wang, J. Ren, W. Wang, and X. Chen. 2021. "Evaluating gyratory compaction characteristics of unbound permeable aggregate base materials from meso-scale particle movement measured by smart sensing technology." *Materials*, 14 (15). MDPI AG. https://doi.org/10.3390/ma14154287.

Zaltuom, A. M. 2018. "A Review Study of The Effect of Air Voids on Asphalt Pavement Life." 618–625. AIJR Publisher.

APPENDIX- A

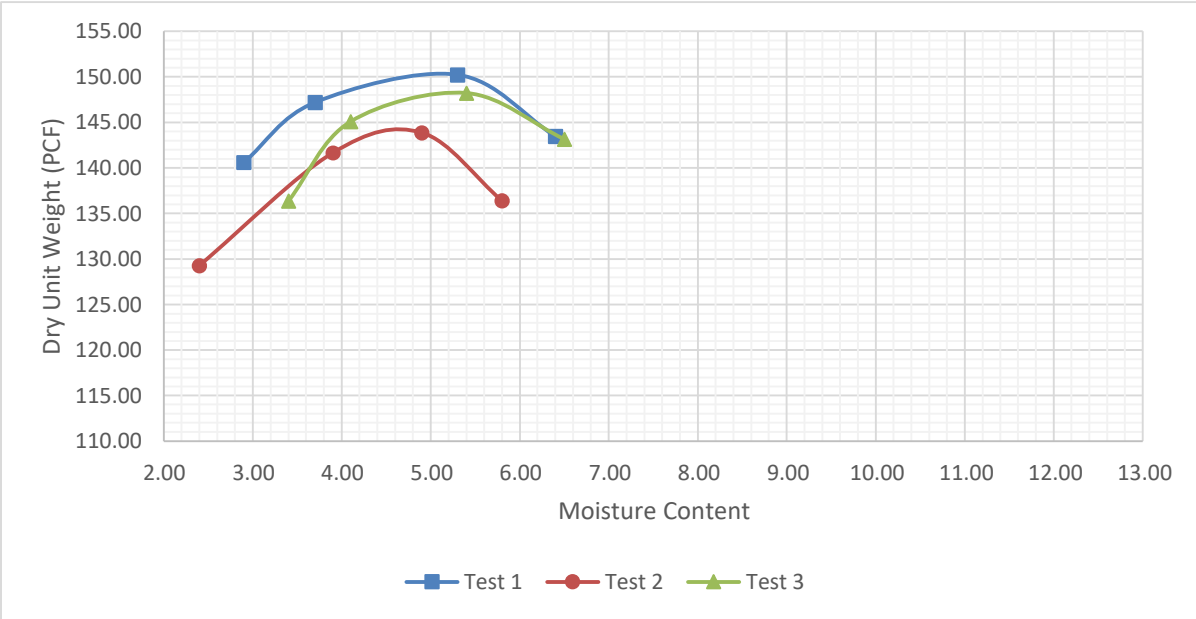


Figure 11A. Modified Proctor Test: Maximum Dry Unit Weight-Optimum Moisture Content Plot for Lafarge

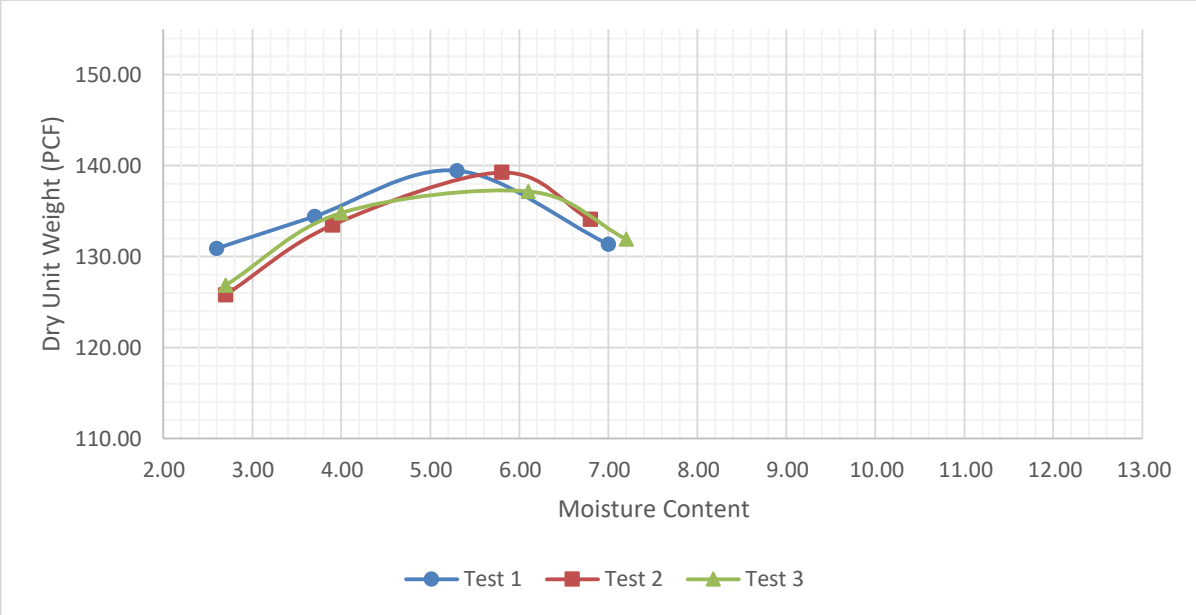


Figure 12A. Modified Proctor Test: Maximum Dry Unit Weight-Optimum Moisture Content Plot for Port Inland

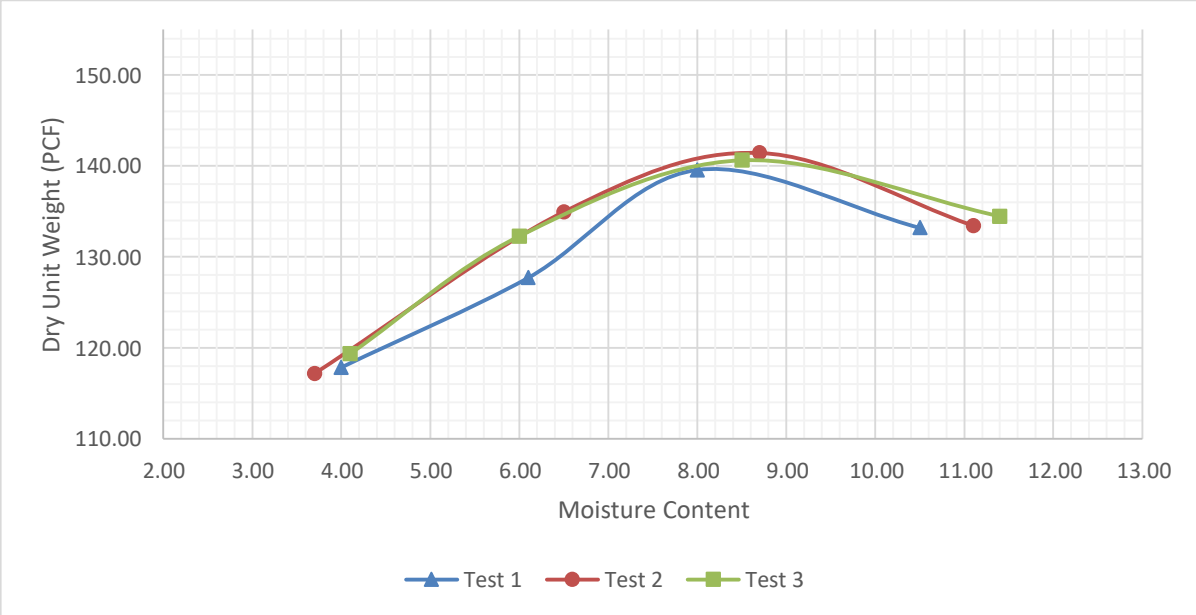


Figure 13A. Modified Proctor Test: Maximum Dry Unit Weight-Optimum Moisture Content Plot for Great Lake

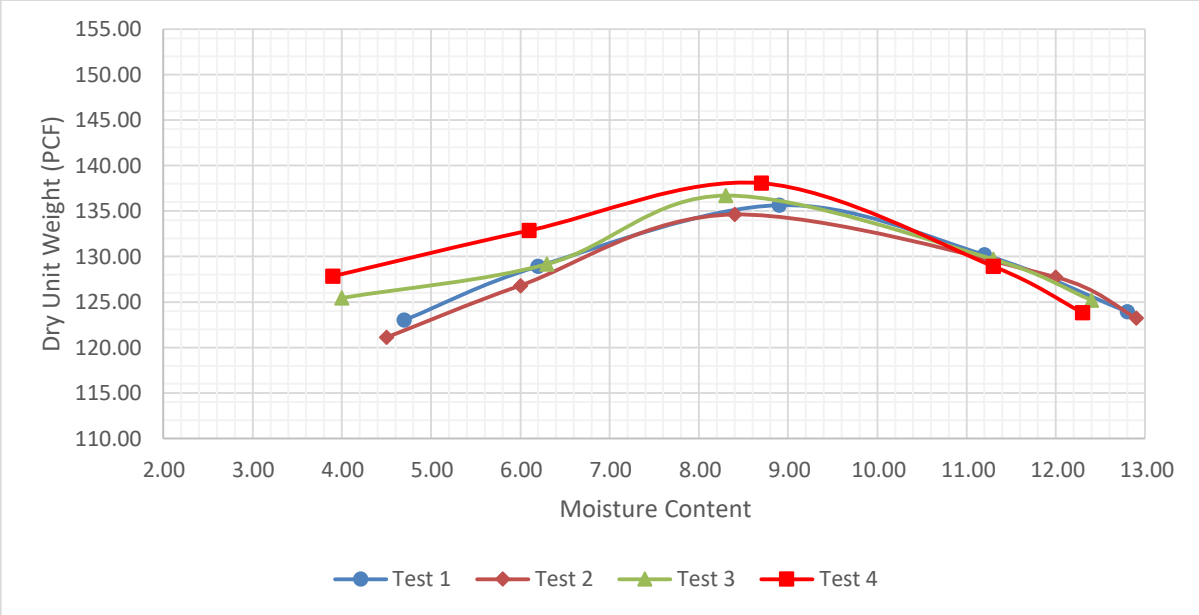


Figure 14A. Modified Proctor Test: Maximum Dry Unit Weight-Optimum Moisture Content Plot for Stone Co

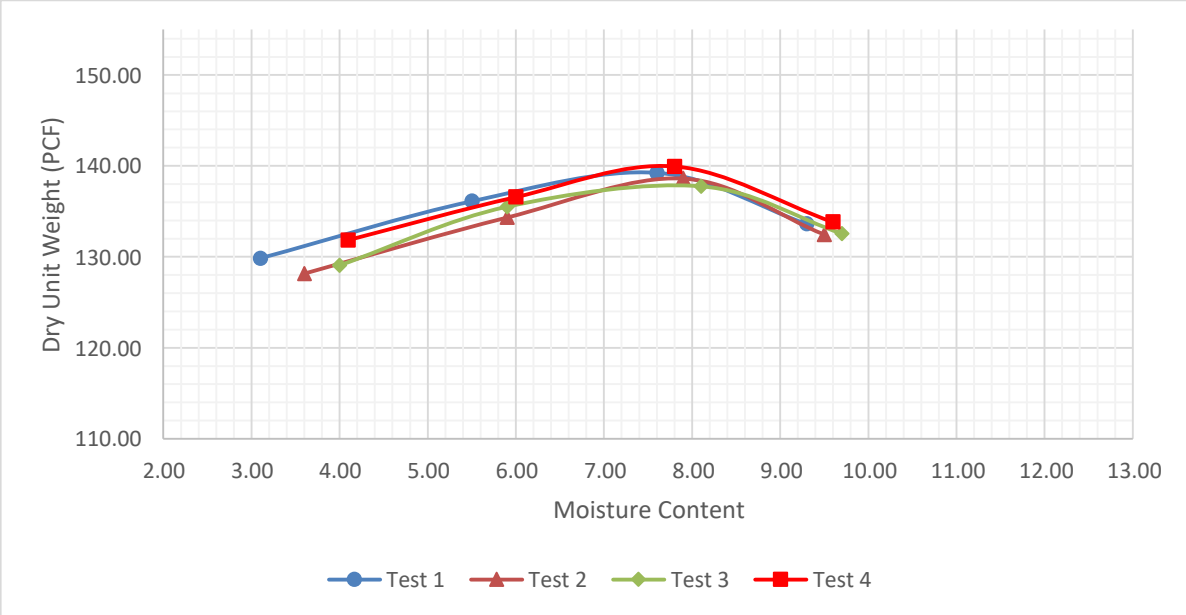


Figure 15A. Modified Proctor Test: Maximum Dry Unit Weight-Optimum Moisture Content Plot for Calcite

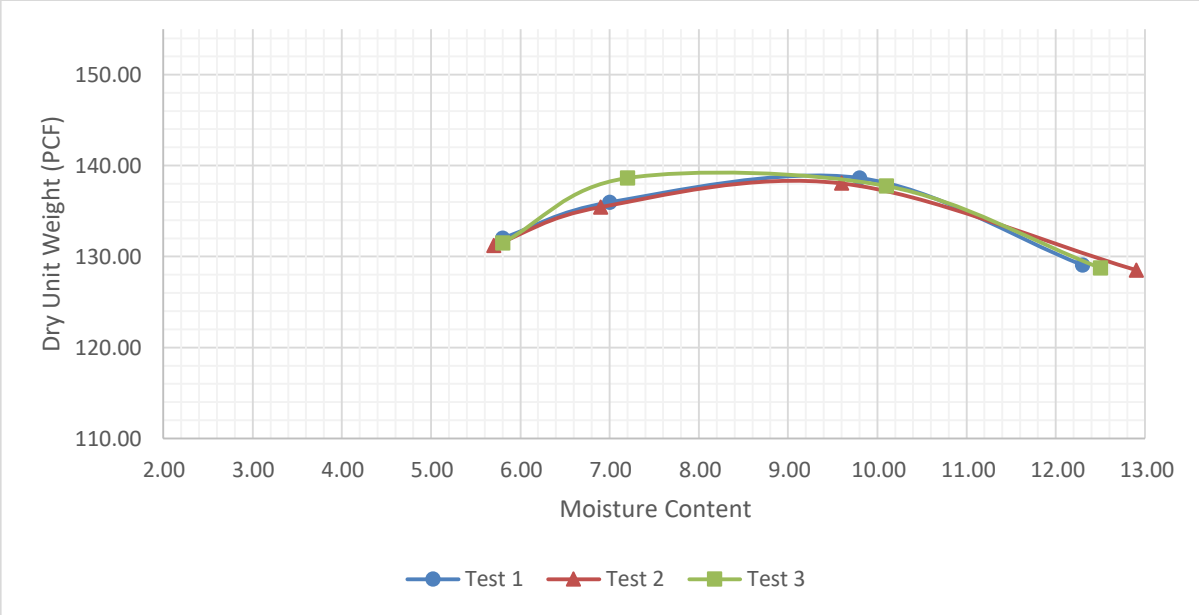


Figure 16A. Modified Proctor Test: Maximum Dry Unit Weight-Optimum Moisture Content Plot for StGrLa2024

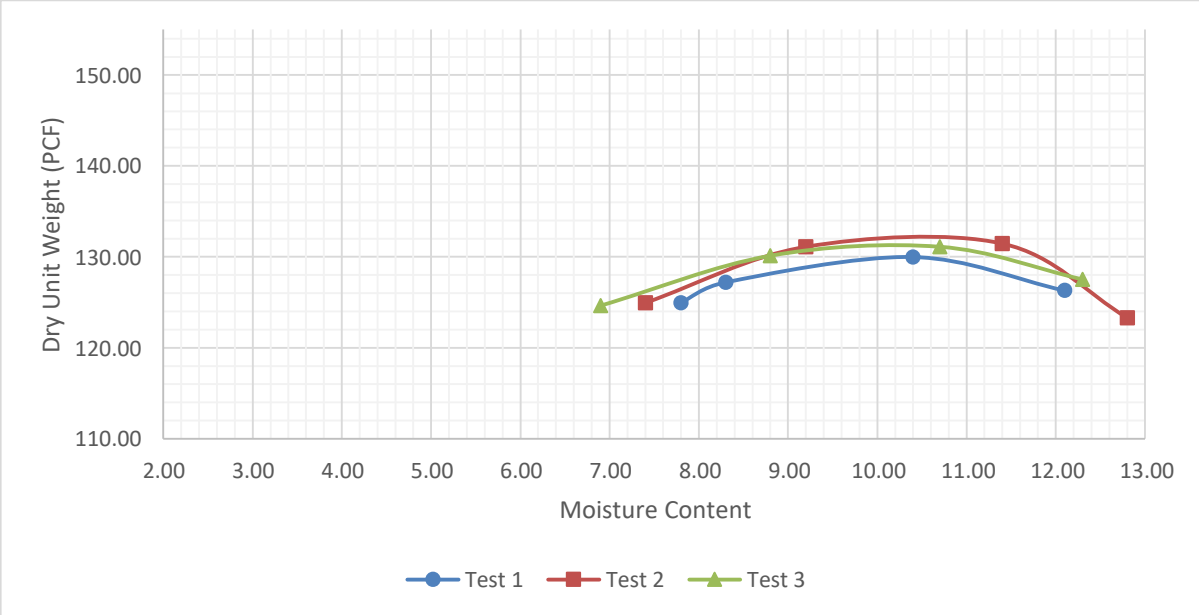


Figure 17A. Modified Proctor Test: Maximum Dry Unit Weight-Optimum Moisture Content Plot for SylMe2025

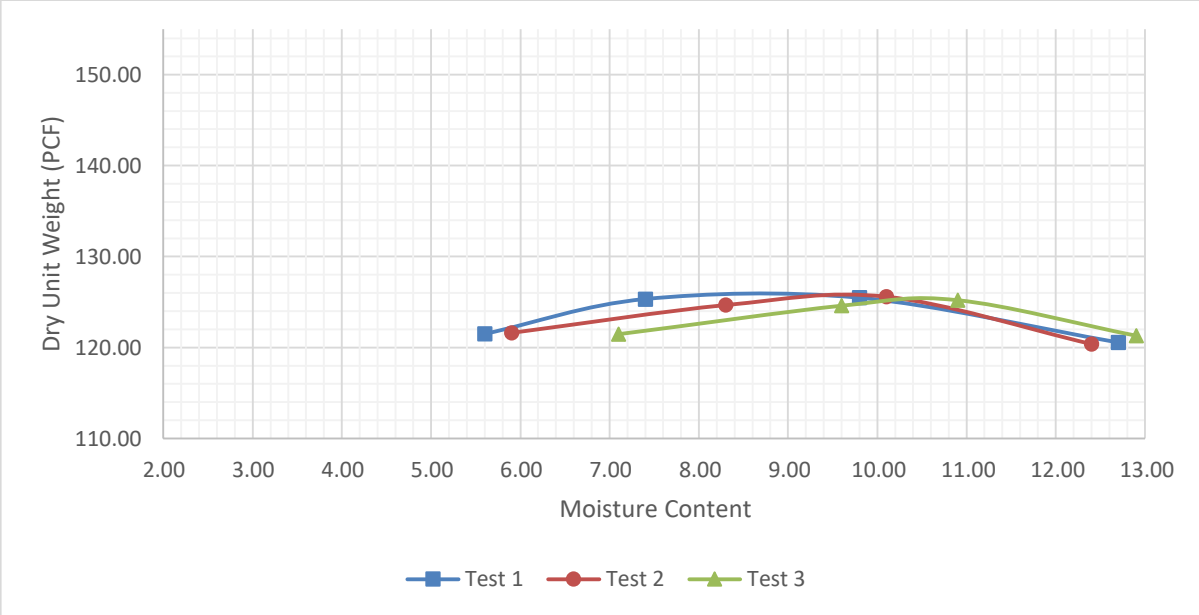


Figure 18A. Modified Proctor Test: Maximum Dry Unit Weight-Optimum Moisture Content Plot for SylMe2025_2

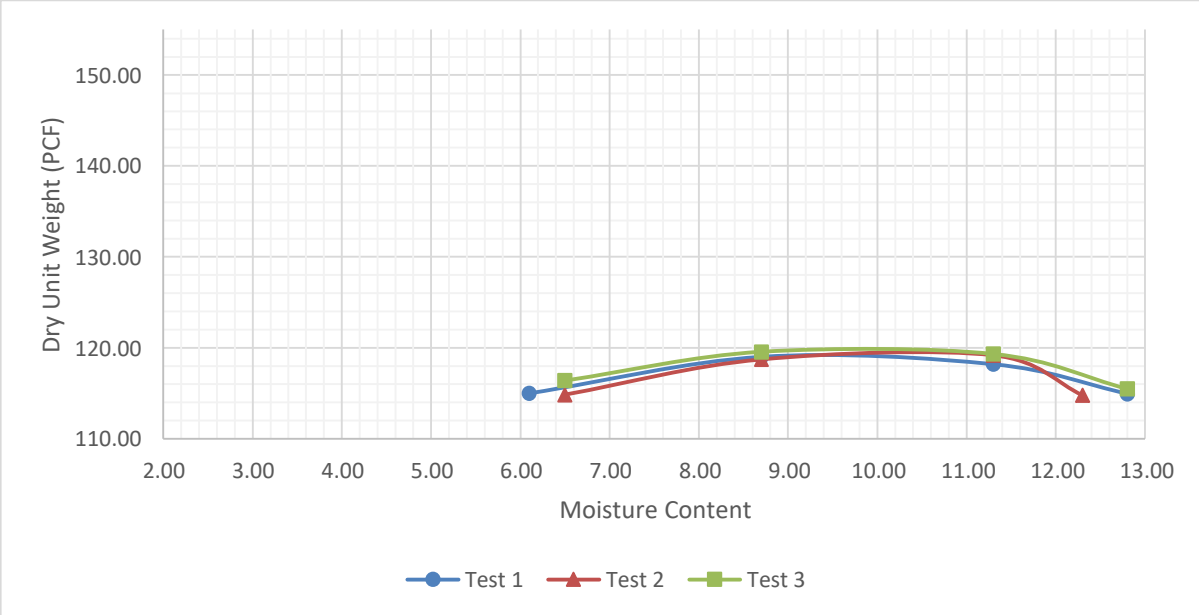


Figure 19A. Modified Proctor Test: Maximum Dry Unit Weight-Optimum Moisture Content Plot for Slag

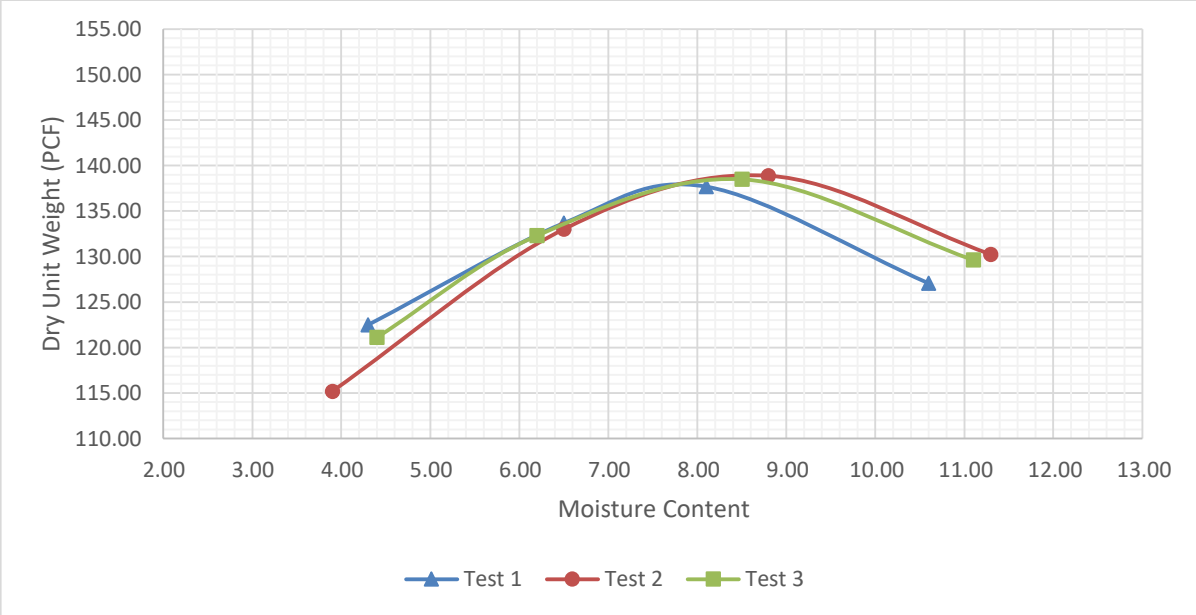


Figure 20A. Modified Proctor Test: Maximum Dry Unit Weight-Optimum Moisture Content Plot for I-275